

University of Szeged
Faculty of Pharmacy
Institute of Pharmaceutical Analysis

**Liquid chromatographic enantiomer separation
of amino acid analogs with chiral stationary phases
utilizing superficially porous particles**

Ph.D. thesis
Dániel Tanács

Supervisor:
Dr. István Ilisz

2023

List of publications, presentations, and posters

Publications related to the thesis

Publications related to the thesis

- i. **D. Tanács**, R. Berkecz, A. Misicka, D. Tymecka, F. Fülöp, D.W. Armstrong, I. Ilisz, A. Péter: Enantioseparation of β -amino acids by liquid chromatography using core-shell chiral stationary phases based on teicoplanin and teicoplanin aglycone
Journal of Chromatography A. 1653 (2021) 462383.
<https://doi.org/10.1016/j.chroma.2021.462383>.
if.: 4.601
- ii. **D. Tanács**, R. Berkecz, S. Shahmohammadi, E. Forró, D.W. Armstrong, A. Péter, I. Ilisz: Macrocyclic glycopeptides- and derivatized cyclofructan-based chiral stationary phases for the enantioseparation of fluorinated β -phenylalanine analogs
Journal of Pharmaceutical and Biomedical Analysis. 219 (2022) 114912.
<https://doi.org/10.1016/j.jpba.2022.114912>.
if.: 3.571
- iii. **D. Tanács**, R. Berkecz, D.W. Armstrong, A. Péter, I. Ilisz: Enantioseparation of α -substituted proline analogs with macrocyclic glycopeptide-based chiral stationary phases immobilized on superficially porous particles of silica applying liquid chromatography with ultraviolet and mass spectrometric detection
Journal of Chromatography A. 1697 (2023) 463997.
<https://doi.org/10.1016/j.chroma.2023.463997>.
if.: 4.601

Sum if.: 12.773

Other publications

- iv. T. Orosz, A. Bajtai, T. Minh Le, **D. Tanács**, Z. Szakonyi, F. Fülöp, A. Péter, I. Ilisz: Chiral high-performance liquid and supercritical fluid chromatographic enantioseparations of limonene-based bicyclic aminoalcohols and aminodiols on polysaccharide-based chiral stationary phases
Biomedical Chromatography. 33 (2019) e4517.
<https://doi.org/10.1002/bmc.4517>.
if.: 1.911
- v. **D. Tanács**, T. Orosz, Z. Szakonyi, T.M. Le, F. Fülöp, W. Lindner, I. Ilisz, A. Péter: High-performance liquid chromatographic enantioseparation of isopulegol-based β -amino lactone and β -amino amide analogs on polysaccharide-based chiral stationary phases focusing on the change of the enantiomer elution order
Journal of Chromatography A. 1621 (2020) 461054.
<https://doi.org/10.1016/j.chroma.2020.461054>.
if.: 4.601
- vi. A. Bajtai, **D. Tanács**, R. Berkecz, E. Forró, F. Fülöp, W. Lindner, A. Péter, I. Ilisz: High-performance liquid chromatographic evaluation of strong cation exchanger-based chiral stationary phases focusing on stationary phase characteristics and mobile phase effects employing enantiomers of tetrahydro- β -carboline and 1,2,3,4-tetrahydroisoquinoline analogs
Journal of Chromatography A. 1644 (2021) 462121.
<https://doi.org/10.1016/j.chroma.2021.462121>.
if.: 4.601
- vii. **D. Tanács**, T. Orosz, I. Ilisz, A. Péter, W. Lindner: Unexpected effects of mobile phase solvents and additives on retention and resolution of N-acyl-D,L-leucine applying *Cinchonane*-based chiral ion exchangers
Journal of Chromatography A. 1648 (2021) 462212.
<https://doi.org/10.1016/j.chroma.2021.462212>.
if.: 4.601

- viii. **D. Tanács**, A. Bajtai, R. Berkecz, E. Forró, F. Fülöp, W. Lindner, A. Péter, I. Ilisz: *Cinchona*-alkaloid-based zwitterionic chiral stationary phases as potential tools for high-performance liquid chromatographic enantioseparation of cationic compounds of pharmaceutical relevance
Journal of Separation Science. 44 (2021) 2735–2743.
<https://doi.org/10.1002/jssc.202100264>.
if.: 3.614
- ix. R. Berkecz, **D. Tanács**, A. Péter, I. Ilisz: Enantioselective liquid chromatographic separations using macrocyclic glycopeptide-based chiral selectors
Molecules. 26 (2021) 3380.
<https://doi.org/10.3390/molecules26113380>.
if.: 4.927
- Total if.: 37.028**

Posters and presentations

- x. **Dániel Tanács**, Ferenc Fülöp, Antal Péter, István Ilisz: Ultrahigh-performance liquid chromatographic enantioseparation of some β^2 -amino acids
26th International Symposium on Analytical and Environmental Problems, 23-24. November 2020., Szeged; Presentation
- xi. **Tanács Dániel**, Berkecz Róbert, Aleksandra Misicka, Dagmara Tymecka, Fülöp Ferenc, Daniel W. Armstrong, Péter Antal, Ilisz István: β^2 -Aminosavak enantioszelektív elválasztása teikoplanin és teikoplanin-aglikon szelektorrall rendelkező héjszerkezetű királis állófázisok segítségével
METT 25, a Magyar Elválasztástudományi Társaság 25 éves jubileumi konferenciája, 18-21. October 2021., Egerszalók; Poster
- xii. **Dániel Tanács**, Róbert Berkecz, Antal Péter, István Ilisz: Enantioselective separations with high- and ultrahigh-performance chiral liquid chromatography stationary phases
27th International Symposium on Analytical and Environmental Problems, 22-23. November 2021., Szeged; Presentation

- xiii. **Dániel Tanács**, Róbert Berkecz, Sayeh Shahmohammadi, Enikő Forró, Daniel W. Armstrong, Antal Péter, István Ilisz: Liquid chromatographic enantioseparation of fluorinated β -phenylalanine analogs utilizing superficially porous particles
33rd International Symposium on Chromatography, 18-22. September 2022., Budapest; Poster
- xiv. **Dániel Tanács**, Róbert Berkecz, Antal Péter, István Ilisz: Enantioselective separations of proline analogs with macrocyclic glycopeptide-based chiral stationary phases
28th International Symposium on Analytical and Environmental Problems, 14-15. November 2022., Szeged; Presentation

Abbreviations and symbols

t_R	retention time
t_0	dead/void volume
k	retention factor, $k = (t_R - t_0)/t_0$
α	selectivity, $\alpha = k_2/k_1$
R_S	resolution, $R_S = 2 \times [(t_{R2} - t_{R1})/(w_1 + w_2)]$, w = peak width at the base of the peak
H	height equivalent of a theoretical plate (HETP)
u	linear flow rate
CSP	chiral stationary phase
PI(M)	polar ionic (mode)
PO	polar organic
NP	normal-phase
RP	reversed-phase
QN	quinine
QD	quinidine
CF6	cyclofructan-6
MeOH	methanol
MeCN	acetonitrile
H ₂ O	water
TEA	triethylamine
AcOH	acetic acid
TFA	trifluoroacetic acid
FA	formic acid
NH ₄ HCOO	ammonium formate
NH ₄ OAc	ammonium acetate
B2-	β^2 -amino acids
BPA-	β -phenylalanines
Pr-	proline analogs

Table of Contents

List of publications, presentations, and posters.....	ii
Abbreviations and symbols.....	vi
1. Introduction and aims.....	1
2. Literature overview	3
2.1. Chirality	3
2.2. Enantioselective chromatography	3
2.3. Chiral stationary phases.....	3
2.3.1. Macrocyclic antibiotics	5
2.3.1.1. Vancomycin.....	6
2.3.1.2. Teicoplanin and teicoplanin aglycone	7
2.3.2. Quinine and quinidine	8
2.3.3. Cyclofructans.....	9
2.4. Thermodynamic considerations of chiral separations	10
2.5. Kinetic considerations, the van Deemter equation	11
2.6. Core-shell particles as stationary phases	13
2.7. Amino acids.....	15
3. Experimental.....	17
3.1. Chromatography system.....	17
3.2. Applied columns.....	17
3.3. Chemicals	17
3.4. Investigated analytes	17
4. Results and discussion.....	19
4.1. Effect of mobile phase composition	19
4.1.1. β^2 -Amino acids	19
4.1.2. Fluorinated β -phenylalanines	21
4.1.3. α -Substituted proline analogs	24

4.2. Effects of nature of mobile phase additives	26
4.2.1. β^2 -Amino acids	26
4.2.2. α -Substituted proline analogs	27
4.3. Effect of counter ion concentration, application of the stoichiometric displacement model.....	28
4.3.1. β^2 -Amino acids	28
4.3.2. Fluorinated β -phenylalanines	29
4.3.3. α -Substituted proline analogs	30
4.4. Structure–retention relationships.....	31
4.4.1. β^2 -Amino acids	31
4.4.2. Fluorinated β -phenylalanines	33
4.4.3. α -Substituted proline analogs	36
4.5. Influence of the temperature.....	39
4.5.1. β^2 -Amino acids	39
4.5.2. Fluorinated β -phenylalanines	40
4.5.3. α -Substituted proline analogs	42
4.6. Kinetic studies	43
4.6.1. β^2 -Amino acids	44
4.6.2. Fluorinated β -phenylalanines	46
4.6.3. α -Substituted proline analogs	47
5. Summary	49
References	51
Acknowledgments.....	A1
Appendix	A2
Publications related to the thesis.....	A13

1. Introduction and aims

Chirality is a type of molecular asymmetry that is important in biological systems. Numerous molecules are chiral, e.g., amino acids (except glycine), peptides, proteins, enzymes, and saccharides. A living organism possesses chiral interaction sites, and the enantiomers of chiral molecules may have different biological activities. They can have different utilization, distribution, metabolism, etc. Consequently, it is necessary to investigate the effects of the enantiomers both separately and in racemic mixtures [1,2]. In most cases, just one of the enantiomers has favorable activity, referred to as eutomers. The other enantiomer can have either no effect, an unwanted side effect, or toxic activity, referred to as distomers. For example, (*S*)-ofloxacin exhibits high antimicrobial activity (eutomer), and it is marketed in pure enantiomeric form as levofloxacin, while (*R*)-ofloxacin can show neurotoxic activity (distomer) [3]. While the pharmaceutical industry pays outstanding attention to chiral compounds, it is important to realize that they are also present as food additives, agricultural chemicals, or fragrance materials.

The separation of enantiomers is more challenging than the separation of achiral compounds. In these separations, we have to account for the chiral effects next to the achiral ones. For the separation of chiral compounds, chromatographic techniques are the most popular. The separation of the enantiomers of chiral compounds started with indirect methods, in which chiral derivatization reagents were used to produce diastereomers [4]. In this way, the formed diastereomers were separable in achiral systems. However, the enantiomeric purity of the reagents is critical, and when the pure chiral compound is needed, these diastereomer products must be further treated. Racemization and kinetic resolution during the derivatization process are further drawbacks. Due to these limitations, this technique is rarely used for analytical purposes nowadays. Direct chromatographic methods use chiral mobile phase additives or chiral stationary phases. The chiral mobile phase additives form complexes with the enantiomers and they can be separated with achiral columns [5]. These additives can be easily removed.

The aim of this Ph.D. work was to study the enantiomeric separation of amino acid analogs by applying chiral stationary phases immobilized on superficially porous particles. The investigated amino acid analogs have different chemical properties, but the structural analogies provide a good basis for interpreting the observed correlations between structure and retention properties. The primary goal of these studies is to explore

and evaluate the relationships between the molecular structure of the selector and the chromatographic properties of the sample compounds. The main objectives are:

1. interpretation of the effect of the structure on chiral recognition,
2. evaluation of the effect of the eluent composition and the quality and quantity of various additives on the separation,
3. studying the effect of temperature on chromatographic parameters, determining thermodynamic parameters, thermodynamic characterization of separation processes,
4. kinetic characterization of enantioselective separation processes.

2. Literature overview

2.1. Chirality

Chirality is a significant structural property, and it is present in every biological system. Many different molecules are chiral. For example, most of the amino acids are chiral, which also affect the enzymes made of these amino acids. The enantiomers, in some cases, can exhibit distinct effects making chirality one of the main focus points in the development of potential pharmaceuticals in the pharmaceutical industry.

2.2. Enantioselective chromatography

Direct enantioselective chromatography is a widely used technique primarily applying chiral stationary phases (CSPs). It is a straightforward approach that can be optimized for a wide range of analytes, because of the wide range of selectors and columns available [6–8]. The selectors are chiral molecules that have various functional groups. Employing CSPs has several advantages in comparison to other chiral separation techniques. The chiral purity is not critical, like in an indirect method, and it is possible to separate the enantiomers of molecules that do not have a reactive functional group that could be used for derivatization. The enantiomers of a chiral molecule possess mostly the same physical properties, e.g., light absorption, and, consequently, their spectra will be the same, making the identification and quantitation easier. The recovery of the separated pure enantiomers is easy, making these CSPs usable in preparative processes.

The instrumentation is the same used in a non-chiral system; the only difference is the column. This also means that the change from a non-chiral to a chiral method is relatively easy from a hardware view. The same type of detectors (e.g., detectors based on light absorption, fluorescence, refraction, scattering, or mass spectrometry) can also be used. However, the circular dichroism detector is widely used in chiral separations.

2.3. Chiral stationary phases

The rapid development of chiral stationary phases started in the 1980s. At first, developing new and more effective selectors was the main target, then optimizing the particles and particle size. Now the main focus is increasing efficiency and reducing analysis times.

The separation of enantiomers on a CSP is based on the different strengths of interactions of the enantiomers with the selector. The most widely accepted model to

explain stereoselectivity was developed by *Easson* and *Stedman* in 1933 [9], and the first chiral separation was published by *Henderson* and *Rule* in 1938 [10]. *Dalgliesh* interpreted the three-point interaction model for the separation of amino acids by thin-layer chromatography (**Figure 1**) [11]. This model was later extended by *Pirkle* and *Pochapsky* [12] and *Davankov* [13]. In addition to the attractions, they included the steric (repulsion) effects remarking that one of the necessary interactions must be stereoselective. This model is still used to understand and explain chiral separations [14]. Some studies claimed that this is only a geometric model and not a necessary condition for chiral discrimination [15,16]. However, *Kasat et al.* found that their results are consistent with the three-point model [17]. They used chromatography with attenuated total reflection infrared spectroscopy and amylose *tris*(3,5-dimethylphenylcarbamate) as a selector.

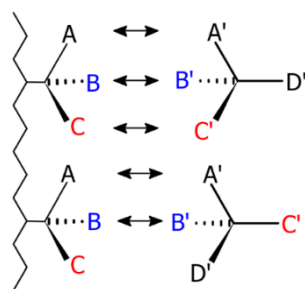


Figure 1. Three-point interaction model

There are several possible interactions between the analytes and the selectors:

- hydrophilic
- hydrophobic
- ionic
- H-bonding
- π - π
- steric

The CSPs can be grouped by the origin of their selectors, such as natural, half-synthetic, and synthetic. However, they are grouped mainly by the nature of the selector. Some of these are:

- oligosaccharides (cyclofructans, cyclodextrins)
- polysaccharides (cellulose-based, amylose-based)
- amino acids, peptides, proteins

- ion-exchangers
- macrocyclic molecules (crown ethers, antibiotics)
- molecularly imprinted compounds

Results presented in my Ph.D. thesis are based on the application of macrocyclic glycopeptides (teicoplanin, modified teicoplanin, teicoplanin aglycone, vancomycin), cyclofructane, and quinine; consequently, the most important characteristics of these CSPs will be discussed below.

2.3.1. *Macrocyclic antibiotics*

CSPs based on macrocyclic antibiotics were first introduced by *Armstrong* and co-workers in 1994 [18,19]. The first three antibiotics they experimented with were vancomycin, rifamycin B, and thiostrepton. Since then, there have been several other antibiotics utilized as CSP, such as teicoplanin [20], teicoplanin aglycone, ristocetin A [21], and avoparcin [22]. The first commercially available columns, called Chirobiotic™, were made by Astec. Nowadays, it is the trademark of Sigma-Aldrich. Due to their favorable characteristics, these selectors have become popular in recent years.

The family of macrocyclic antibiotics involves several hundreds of highly diverse structures, but only a small number of them are used as chiral selectors. Structurally, they can be specified by their cyclic heptapeptide scaffold that has aromatic fragments, surrounded by polar and ionizable groups, and carries carbohydrate moieties. These molecules have a molar mass range between 600 and 2200 g/mol. They contain acidic, basic, and neutral functional groups, capable of forming H-bridges, π - π interactions, hydrophobic-hydrophobic interactions, etc. Their complex yet well-defined structure makes them suitable for separating a wide range of enantiomers [23].

These selectors can be chemically bound to silica gel providing broad chemical compatibility. Thus, the column can be used in different operation modes like polar ionic (PI), polar organic (PO), normal-phase (NP), reversed-phase (RP), or supercritical fluid chromatography (SFC). However, it is important to know that changing the operation mode can lead to significantly different enantioselectivities, which, in some cases, are drawbacks but can make great opportunities in others.

Their great chiral recognition ability comes mainly from two structural characteristics, namely their macrocycles and ionic property. Nevertheless, further possible interactions are also significant. Since they have a well-defined structure, the time needed for method development can be reduced by knowing the structure of the

analyte. Complementary properties can also be observed. It comes from their structural analogies and it means that if one selector cannot separate or can just partially separate enantiomers, some other macrocyclic antibiotics can achieve baseline separation. One interesting aspect of these antibiotics is that since they are macrocyclic molecules, they can form inclusion complexes under RP conditions, similar to cyclodextrins.

Based on the structure, macrocyclic antibiotics can be classified into different groups. The ones used as CSPs nowadays can be classified into three: ansamycins, glycopeptides, and polypeptides.

Table 1. Classification of some macrocyclic antibiotics applicable as a CSP

Macrocyclic antibiotics		
Ansamycins Rifampicin(s) Rifamycin(s)	Glycopeptides Teicoplanin and its analogs Vancomycin	Polypeptides Thiostrepton

The most important and most often used antibiotics as CSPs are vancomycin, teicoplanin, teicoplanin aglycone, ristocetin A, and avoparcin, which are all glycopeptides.

2.3.1.1. *Vancomycin*

Kornfield discovered vancomycin from a dirt sample and found that it was produced by *Streptomyces orientalis* [24]. That time they named it "compound 05865" and found it effective against gram-positive and some anaerobic organisms. Resistance was induced *in vitro* experiments against this molecule in staphylococci. After 20 serial passages, resistance to compound 05865 was only 4–8-fold, while it was around 100,000-fold against penicillin [25]. It was named vancomycin later, before it was made available for clinical trials. There have been more than 100 macrocyclic antibiotics discovered.

Vancomycin has a molecular mass of 1449 g/mol. It has three macrocycles and 18 chiral centers (**Figure 2**). It also has a polar character; however, its basket-like structure can form hydrophobic–hydrophobic and π – π interactions. It has two sugar units, which contribute to enantioselectivity considerably [26]. There are primary and secondary amino groups (most of them forming amido groups) and carboxylic groups, which are

involved in ionic interactions. It has nine hydroxy groups that can form H-bonds, and two aromatic rings bear chlorine substituents with a π -acidic character.

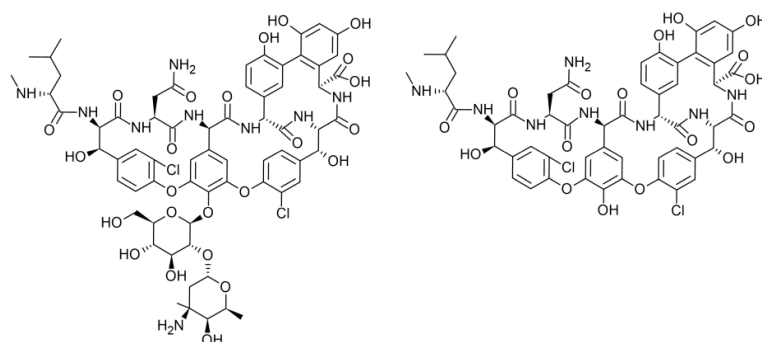


Figure 2. Structure of vancomycin (left) and vancomycin aglycone (right)

The so-called aglycone unit is obtained by removing the sugar moieties from these glycopeptides (**Figure 2**). This modification changes the enantioselectivity, sometimes decreasing it, while an increase may be found in others [27]. Vancomycin aglycone is not as widely used as vancomycin or teicoplanin aglycone.

2.3.1.2. *Teicoplanin and teicoplanin aglycone*

Teicoplanin is produced by *Actinoplanes teichomyceticus*, and it is a mixture of five compounds of similar structures [28]. The main component is the A₂₋₂ (**Figure 3**), and its structure will be discussed further in this work. It is active against aerobic and anaerobic gram-positive bacteria [29]. The A₂₋₂ is the selector of Chirobiotic T and T2.

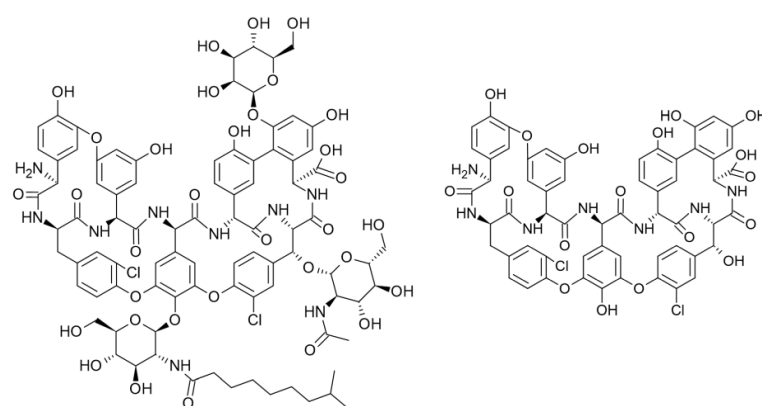


Figure 3. Structure of teicoplanin A₂₋₂ (left) and teicoplanin aglycone (right)

It has a molecular mass of 1877 g/mol and has four macrocycles with 23 chiral centers. The basket-like structure behaves in a manner similar to that of vancomycin;

however, it has one more macrocyclic unit. It can also form hydrophobic–hydrophobic and π – π interactions. This basket contains seven aromatic rings, two have chlorine substituent, and three have a hydroxy group. It has a free carboxyl group ($pK \sim 2.5$), a primary amino group ($pK \sim 9.2$), and eight amido groups. The two ionic groups can make strong ionic interactions, and the molecule also has three sugar units (two D-glucosamines and one D-mannose). They can contribute to chiral recognition in different ways, such as blocking access to the basket, inhibiting interactions, or making possible new ones [26].

Removing the sugar moieties gives teicoplanin aglycone, a widely used chiral selector.

2.3.2. Quinine and quinidine

Quinine and quinidine are native *Cinchona* alkaloids naturally present in the cinchona tree (*Cinchona ledgeriana*). They were first isolated by *Pelletier* in 1820 [30], and later *Strecker* determined their molecular formula [31]. Their first chromatographic use occurred in the 1950s. Later *Izumoto* [32,33] and *Pettersson* [34,35] used them in ion-pair chromatography. *Rosini et al.* were the first to immobilize *Cinchona* alkaloids on silica to make chiral stationary phases [36].

Quinine- (QN) and quinidine-based (QD) CSPs are widely used nowadays. QN and QD are pseudoenantiomers, which means that structurally they are diastereomers, but in chiral separations, they often behave as enantiomers, showing reversed enantiomeric order. *Cinchona* alkaloids have multiple chiral centers, QN and QD differ in the configuration of carbon 8 and 9 (QN: 8*S*,9*R*, QD: 8*R*,9*S*).

They are immobilized through the C=C double bond at C-1 and can be further functionalized at other groups. In 1996, *Lindner et al.* presented their results in the functionalization of QN and QD with *tert*-butyl carbamate and they were able to make a weak anion-exchanger CSP [37] (**Figure 4**). It was later commercialized as Chiralpak® QN-AX and QD-AX. These selectors were further developed and were modified with *trans*-2-aminocyclohexanesulfonic acid through a carbamoyl group at the C-9 position. With this modification, a strong cation exchanging moiety is present in the selector, making a zwitterionic CSP. These selectors are named Chiralpak® ZWIX(+) and ZWIX(–).

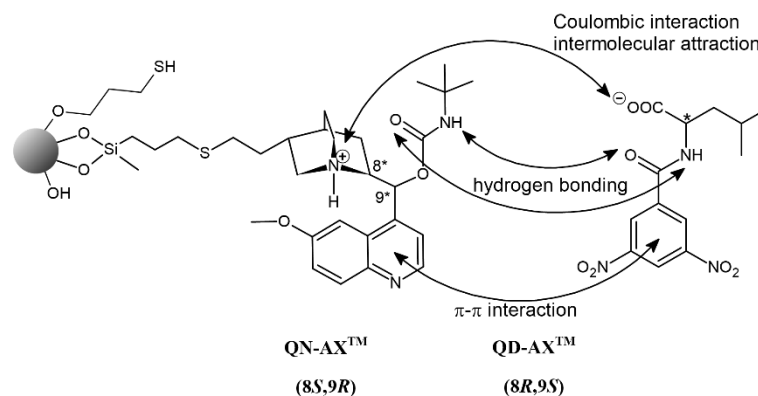


Figure 4. The structure and possible interactions of quinine- and quinidine-based CSPs

2.3.3. Cyclofructans

Cyclofructans were discovered by *Kawamura* and *Uchiyama* in 1989 [38]. They found a strain of *Bacillus circulans* (OKUMZ 31B) with an enzyme that converts inulin into cyclinulo-oligosaccharides, mainly cyclinulo-hexaose. Later, *Kushibe et al.* found a different strain of *Bacillus circulans* (MCI-2554) and developed a more efficient cyclofructan production [39]. Their first use as chiral selectors was in 2009 [40].

Cyclofructans are cyclic oligosaccharides made of β -2,1-linked fructofuranose units. Therefore, they can be distinguished by the number of fructofuranose units. The first widely used molecule was cyclofructan-6 (or cyclinulo-hexaose, CF6), which is available in good purity [41] (**Figure 5**). There are also CF7 and CF8, which were less accessible but they have become more available in recent years.

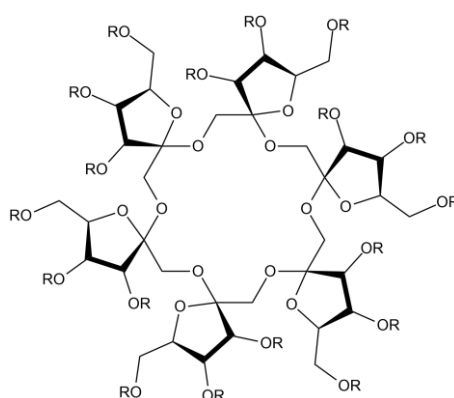


Figure 5. The structure of cyclofructan-6 (CF-6)

R: modifier groups

CF6 forms a macrocycle, which is similar to a crown ether. Its two sides (center and outside surface) have different hydrophobicity, because most hydroxy groups face

outside or towards a nearby fructofuranose unit. The latter hydroxy groups form H-bondings, stabilizing the basket-like structure. Compared to crown ethers, CF6 has no central hydrophobic cavity, making the inclusion complex formation difficult [42]. Therefore, native CF6 has limited chiral activity [43]. With derivatization (through their hydroxy groups), a wide range of enantiomeric separations became possible with cyclofructans [40].

Cyclofructans as chiral selectors are used primarily in PIM in liquid chromatography [44]. They exhibit enantiomeric separation in organic solvents, even without polar modifiers, because their amino groups are not needed to be protonated [45]. This makes them also a great supercritical fluid chromatography selector. They are also used in gas chromatography and capillary electrophoresis.

2.4. Thermodynamic considerations of chiral separations

It is widely observed that chiral separations show a more significant dependence on the temperature than achiral separations. With increasing temperature, the viscosity of the eluent decreases and, consequently, the rate of diffusion between the two phases increases [46]. It is a kinetic effect; however, the achiral separations are also affected in this way, that is, the main difference must be in the thermodynamics.

The standard Gibbs energy of equilibrium processes can be specified with the following equation:

$$-\Delta G^0 = RT \ln K \quad (1)$$

where R is the universal gas constant, T is the absolute temperature in Kelvin, and K is the equilibrium constant.

Using the *Gibbs–Helmholtz* equation,

$$\Delta G^0 = \Delta H - T\Delta S^0 \quad (2)$$

where ΔH^0 is the standard change of enthalpy, and ΔS^0 is the standard change of entropy. We can express $\ln K$ with the following equation:

$$\ln K = -\frac{\Delta H^0}{RT} + \frac{\Delta S^0}{R} \quad (3)$$

The retention factor (k) can be expressed by multiplying the equilibrium constant and phase ratio:

$$k = K\phi = K \frac{V_s}{V_m} \quad (4)$$

where ϕ is the phase ratio, V_s is the volume of the stationary phase, and V_m is the volume of the mobile phase.

With **equations 3** and **4**, we can get the van't Hoff equation, which interprets the dependence of $\ln k$ vs. $1/T$:

$$\ln k = -\frac{\Delta H^0}{RT} + \frac{\Delta S^0}{R} + \ln \phi \quad (5)$$

In this equation, the $\ln \phi$ is unknown in numerous cases, and its correct measurement is difficult [47–50]. However, it can be eliminated with the difference of two standard free energy:

$$\Delta(\Delta G^0)_{2,1} = \Delta G^0_2 - \Delta G^0_1 = \ln \frac{k_2}{k_1} \quad (6)$$

The fraction of the retention factors gives us the selectivity, expressed in the following equation:

$$\ln \frac{k_2}{k_1} = \ln \alpha \quad (7)$$

Using **equation 7** with the van't Hoff **equation 5**, the following equation can be written:

$$\ln \alpha = -\frac{\Delta(\Delta H)^0}{RT} + \frac{\Delta(\Delta S)^0}{R} \quad (8)$$

This equation describes the dependence of $\ln \alpha$ vs. the reciprocal of temperature ($1/T$), and its slope provides $\Delta(\Delta H^0)$, and the intercept gives $\Delta(\Delta S^0)$.

2.5. Kinetic considerations, the van Deemter equation

For the description of the performance of a column, the height equivalent of a theoretical plate (HETP) is a parameter used generally. A plate is a "theoretical unit" of a column in which the mass transfer kinetics are in equilibrium between the stationary phase and mobile phase. Since the 1920s, many models have been developed to describe the mass transfer kinetics and to predict the kinetic performance of chromatographic columns. *Lapidus* and *Amundson* published their work on a mathematical solution of the general mass balance equation of chromatographic columns in 1952 [51]. This model

included the axial dispersion and adsorption–desorption kinetics between the two phases. *van Deemter et al.* in 1956 published a simplified equation of *Lapidus* and *Amundson*'s work, which has the exact solution, when the band profile is narrow and the column efficiency is appropriate [52].

$$HETP = A + B/u + C \times u \quad (9)$$

This equation is the dependency of HETP (H) on the linear flow rate (u), which has three coefficients, A , B , and C (**Figure 6**).

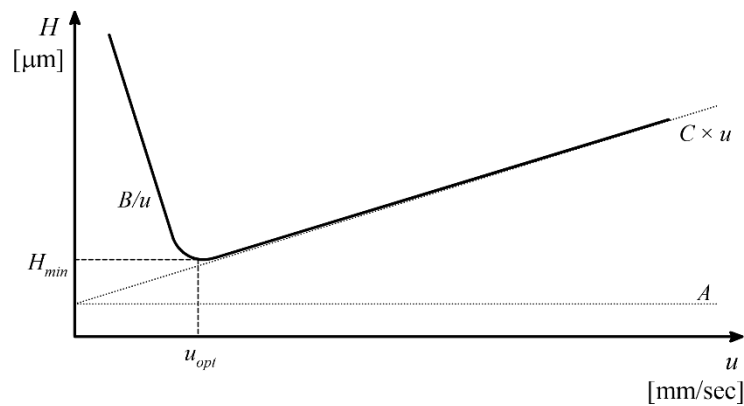


Figure 6. The general representation of the van't Hoff equation

The A term is the eddy dispersion caused by the different paths of the molecules throughout the column. Because of this, some molecules will take longer to reach the end of the column/the detector and cause band broadening. It is independent of the flow rate, but it can be reduced by packing the column with particles that have excellent homogeneity in shape and size.

The B term interprets axial (longitudinal) diffusion of the component(s) to be separated in the mobile phase. It is proportional to the time of components staying in the mobile phase. This longitudinal diffusion primarily takes place in the mobile phase. However, in some cases, it is not negligible in the stationary phase either. Longitudinal diffusion can be reduced by increasing the flow rate.

The C term is related to the transfer of solute between the phases. The molecules are sorbed in the stationary phase and it takes time to return to the mobile phase and, in this way, it falls behind. This effect is proportional to the flow rate.

The B term decreases with increasing flow rate, but the C term changes in the opposite manner. Because of this, we have to find the optimal flow rate to get the lowest plate heights.

2.6. Core-shell particles as stationary phases

Silica microspheres are the most frequently used packing materials for packed HPLC columns. Monolithic columns are also used in various places, mainly for fast separations, because of their low backpressures. The reason for this is their highly interconnected pores that have high permeability. They can be effectively used to separate large biomolecules [53], but they are not as widely used as the packed columns. One of the main reasons for that is the difficulty of good reproducibility. They can differ from batch to batch, making it difficult to reproduce the same pore structure.

The packed columns are still dominating the market, because of their favorable properties. These microspheres can be prepared from polymers and ceramics, but silica microspheres are still used most widely. At first, nonporous particles were applied, and porous ones became available later. Both of these are still used, having both advantages and disadvantages. In the case of nonporous particles, separation takes place on the surface of the particles. It causes low band broadening due to the short path through the column and the fast mass transfer kinetics. However, the selectivity and resolution are relatively low for the same reasons. The use of fully porous particles tried to solve these shortcomings. Because they have pores inside the spheres, there is a more significant surface area for adsorption, which increases the selectivity and resolution. However, this also increases the time the molecules stay in the column, slowing mass transfer and increasing band broadening (the effect related to the *C* term, discussed earlier).

It is possible to make a column more effective (in terms of theoretical plates) by decreasing the diameter of the filling particles and increasing the surface area, but this also comes with increased backpressures [54]. The backpressures quadruple if the particle size is halved ($\Delta p \sim 1/d^2$) [55]. The decrease in the particle size also increases the retention times. This can be compensated by increasing the flow rate, which further increases the pressure. Most new columns use sub-3 μm particles, but sub-2 μm porous particles represent the state-of-the-art. The UHPLC instruments were developed to use these columns effectively.

The newest particles used as packing materials are the core-shell particles (also called fused-core, solid core, and superficially porous particles). There is an increasing interest in these core-shell particles, because of their effectiveness and relatively low backpressures at high flow rates [56]. A core-shell particle has two parts: a solid core with a porous shell around, where the shell contains the selector molecules. The porosity of the shell provides a relatively high surface area. There are several commercially

available ones, like Cortecs (Waters), Kinetex (Phenomenex), and Accucore (Thermo Fischer Science). The 2.7 μm core-shell particles, having a 1.7 μm core and a 0.5 μm thick porous shell, are widely used. They have an operating backpressure similar to the 3 μm , fully porous particles but they show the efficiency of sub-2 μm particles in many cases [57]. There are several other core-shell particle sizes with varying separation parameters [58,59].

The effectiveness of core-shell particles can be interpreted by examining the three terms in the van Deemter equation (**equation 9**). At high flow rates, the *A* and *C* terms are more significant than the *B* term. Both of them are mainly affected by the size of the packing material. With the smaller particle size, both the mass transfer resistance, and the *C* term will be lower. In addition, the smaller and more uniform particles result in a lower *A* term. The core-shell particles can be made with good uniformity and low porous shell thickness, decreasing both the *A* and *C* terms [54]. They also have small and uniform pores, reducing the *B* term. The mass transfer can increase if the shell thickness is reduced, which means lower elution times and higher efficiencies [60].

Based on their structure, there are several types of core-shell particles [61]. The most common is when the core is a single sphere covered by a porous shell (**Figure 7**). There are two possible methods for making these. One of them is when the core is indeed a single sphere. The other is when the core is made by aggregating several smaller spheres. They can either be used as such or covered to make a nearly perfect sphere for the core [62].

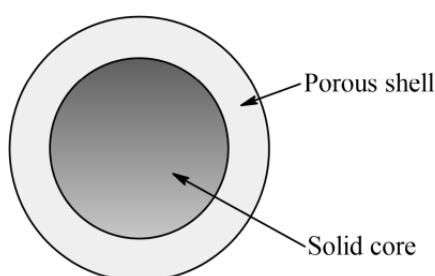


Figure 7. The structure of a core-shell particle

Most core-shell particles used in chromatography are made by the layer-by-layer (LbL) method [56]. This method uses electrostatic interaction to fabricate the shell. For this approach, either the surface of the core should have a charge, or a charged layer is needed to cover the core; for example, a polymer or charged nanospheres. In this case,

this surface-charged sphere is submerged in nanoparticles with opposite charges. These two submerges alternate until the desired shell thickness is achieved. There is also a rinsing step between each submerging to remove the excess, unbound particles. The last step is a thermal treatment, mostly to remove the organic polymers. This process has relatively low productivity, and the multilayer-by-multilayer (MLbML) approach was developed to accelerate the process. This method utilizes the aggregation of nanoparticles before they adsorb on the core particle [63,64]. This method also produces good-quality particles. However, it is important to note that the shell porosity will be higher compared to that achieved by the LbL method.

Depending on the pore size, these particles are adequate for separating different analytes. For the separation of smaller molecules, pore sizes of 8–10 nm are suitable [58], and 16-nm pores can be used for separating peptides and small proteins (up to 15 kDa) [65]. They can also be optimized for protein separation if the pore size is around 40 nm [66].

Core-shell particles can also be further coated to make specified selectors. *Paek et al.* coated 2.7 μm superficially porous particles with carbon after a thin layer of Al(III) to make catalytic sites for carbon deposition to use them for fast LC \times LC. These carbon-clad particles were found to have good peak shapes with high efficiency [67]. *Lomsadze et al.* were the first to publish a method making and testing core-shell particles coated with chiral selectors [68]. They used cellulose *tris*(4-chloro-3-methylphenylcarbamate) and coated fully porous particles to compare their performances. They found that the selectivities of the separations were higher on core-shell particles, especially at higher flow rates.

2.7. Amino acids

The most abundant biological macromolecules in all living cells are proteins. These can have different functions; for example, they can be enzymes, hormones, antibodies, transporters, etc. These proteins are built up from 20 amino acids through covalent bonding. All these amino acids are α -amino acids and they are chiral, except glycine. However, there are many more amino acids, both in larger structures or in a free form.

For a long time, it was thought that amino acids, with exception of α -L-amino acids, had only a minor function in a biological system. An example is D-serine, a co-agonist of the *N*-methyl-D-aspartate receptors responsible for memory and learning [69]. On the other hand, they can also be used as biomarkers or indicators of different diseases or

disorders. Several studies conducted in this field found several markers. D-Aspartic acid and D-alanine for Alzheimer's disease [70,71], D-alanine for Renal disease [72], D-serine for Parkinson's disease [73], and there are also several others also [74,75].

β -Amino acids have an additional C atom between the carboxyl and amino groups. This extra C atom can result in various secondary structures in peptides (β -peptides). This unnatural secondary structure explains the enhanced stability against hydrolysis or enzymatic degradation, which opens up new possibilities, for example, in pharmaceutical research [76–79]. Stability can also be enhanced with further functionalization [80]. There are two types of β -amino acids based on their structure – β^2 - and β^3 -amino acids. The number gives the position of the functional group connecting to the base amino acid chain. These structures can be seen in **Figure 8**.

Fluorinated amino acids have gained increased attention in the last 15 years. The exchange of a H atom to a F atom can cause different characteristics for the molecule due to the strength of the C–F bond [81]. The advantageous effects of fluorination were studied by several research groups and found a wide range of possibilities. For example, they can have therapeutic value [82], work as enzyme inhibitors [83], and exhibit antibacterial activity [84,85]. Furthermore, molecules containing fluorinated amino acids can also be used as antifungal agents [86].

Proline is also an attractive target amino acid due to its unique structure. It contains an α -imino group in a five-membered ring. When incorporated into peptides or peptidomimetics, the unique ring structure may develop special properties, such as conformational rigidity and enhanced chemical stability. Moreover, proline within a peptide chain may lead to the appearance of *cis/trans* isomerization [87,88] and it induces the formation strong type-II β -turns [89]. The biological importance of proline, especially the role of D-proline and its metabolism in living organisms, has recently been reviewed in several scientific papers and book chapters [90–92]. A few papers have focused on the enantiomeric separation of its α -substituted analogs, but chiral analysis of hydroxyproline [93] and different α -substituted proline analogs [94,95] were performed on its *N*-derivatized form.

3. Experimental

3.1. Chromatography system

The experiments were carried out on a Waters® ACQUITY UPLC® H-Class PLUS System (Waters Incorporation, Milford, MA, USA). The system contained the following modules: a quaternary solvent manager, a sample manager, a column manager, a PDA detector, and a QDa mass spectrometry detector. The system was managed by Empower 3 software (Waters).

3.2. Applied columns

Chiral columns were available in two different internal diameters (i.d.), 3.0 mm and 2.1 mm (abbreviated as -3.0 and -2.1, respectively), and all columns were 100 mm long. Chiral selectors are based on teicoplanin (TeicoShell; **T-3.0** and **T-2.1**), modified teicoplanin (NicoShell; **N-3.0**), teicoplanin aglycone (TagShell; **TAG-3.0** and **TAG-2.1**), vancomycin (VancoShell; **V-3.0** and **V-2.1**), isopropyl carbamate functionalized cyclofructan-6 (LarihcShell-P; **CF-P-3.0**), and *Cinchona* alkaloid-based *tert*-butyl carbamate quinine (Q-Shell; **Q-3.0**). All columns were provided by AZYP (LLC, Arlington, TX, USA). Their courtesy is highly appreciated.

3.3. Chemicals

Methanol (MeOH), acetonitrile (MeCN), and water (H₂O) were used as the base of the eluents, and all were LC-MS grade. Triethylamine (TEA), glacial acetic acid (AcOH), trifluoroacetic acid (TFA), formic acid (FA), ammonium formate (NH₄HCOO), and ammonium acetate (NH₄OAc) were used as polar modifiers in the eluent, and they were of analytical reagent grade. All chemicals were from VWR International (Radnor, PA, USA).

3.4. Investigated analytes

The studied analytes can be grouped into three categories: β^2 -amino acids (**B2-**), fluorinated β -phenylalanines (**BPA-**), and α -substituted proline analogs (**Pr-**). The base structures are shown for each group in **Figure 8**, and all exact structures can be found in the **Appendix (Figure A1–A3)**.

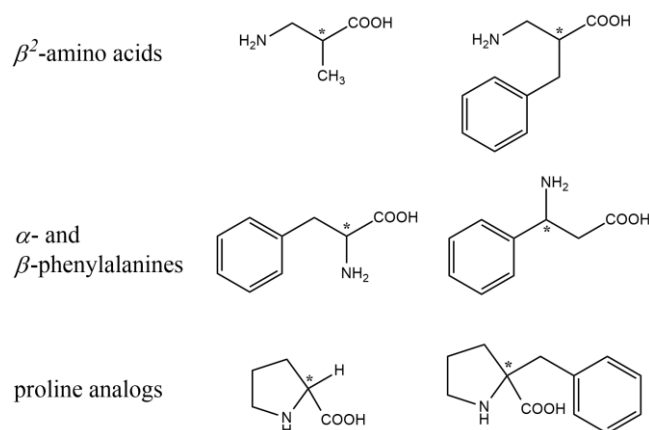


Figure 8. Base structures of the analytes

The synthesis of β^2 -amino acids can be found in a previous article [96].

α -Phenylalanine (**BPA-1**) was purchased from Sigma-Aldrich (St Louis, MO, USA). The racemic mixture of **BPA-2** was prepared through ring cleavage of racemic 4-phenylazetidin-2-one with 18% HCl [97]. **BPA-3** to **BPA-7** were synthesized through condensation of the corresponding aldehydes with malonic acid in the presence of NH_4OAc in EtOH [98]. Ring cleavage of 4-phenylazetidin-2-one catalyzed by CAL-B (*Candida antarctica* lipase B) resulted in phenyl-substituted β -amino acid (*S*)-**BPA-2** with excellent *ee* (enantiomeric excess) (99%) [97]. Enantiomeric fluorophenyl-substituted β -amino acids (*S*)-**BPA-3–7** (*ee* \geq 99%) were prepared through hydrolysis of the corresponding racemic β -amino carboxylic ester hydrochlorides catalyzed by lipase PSIM (*Burkholderia cepacia*) [98].

All α -substituted proline analogs were purchased from BioQuadrant Inc. (Quebec, Canada).

4. Results and discussion

4.1. Effect of mobile phase composition

Studying the effect of different bulk mobile phase compositions is nearly always the first step in improving or optimizing separations. The bulk solvent contained H₂O, MeOH, MeCN, or a mixture of two selected solvents. All three solvents have different effects on the interactions between the analytes and selectors. H₂O is the most polar of them. MeOH is a less polar protic solvent, while MeCN is an aprotic solvent. This means that water suppresses ionic interactions the most, while acetonitrile promotes them, but acetonitrile also interferes with the π – π interactions. The other main attribute is their effect on the H-bonding interactions. H₂O and MeOH are protic solvents and make H-bonding interactions less relevant between the analytes and selectors. On the other hand, MeCN as an aprotic solvent promotes these interactions. In all further experiments, one or the mixture of two of these solvents together with mobile phase additives were applied as mobile phases.

4.1.1. β^2 -Amino acids

To find the appropriate bulk solvent composition for the enantioseparation of β^2 -amino acids, the solvent composition was changed between H₂O/MeOH 90/10–10/90 (v/v). **B2-3** and **B2-9** amino acids containing an aliphatic propyl or an aromatic methylphenyl group, respectively, were used as analytes. For the experiments, TeicoShell and TagShell columns were used, and for some of these measurements, triethylammonium acetate (TEAA) was applied as a polar modifier. The corresponding results are presented in **Figure 9**.

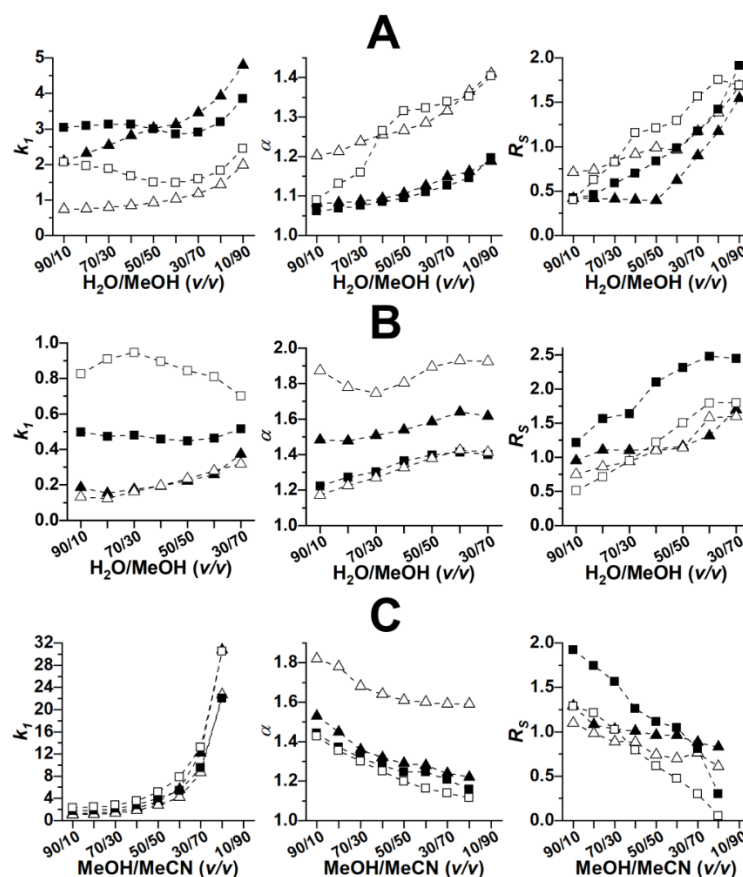


Figure 9. Effects of bulk solvent composition on the enantioseparation of two β^2 -amino acids

Chromatographic conditions: columns: **T-3.0** and **TAG-3.0**; eluent, **A:** H₂O/MeOH, **B:** H₂O/MeOH containing 20 mM TEAA, pH_a = 5.0, **C:** MeOH/MeCN containing 20 mM TEAA; flow rate: 0.3 ml/min; temperature: 20 °C; symbols for analytes: on **T-3.0** **B2-3** \blacktriangle , **B2-9** \blacksquare , on **TAG-3.0** **B2-3** \triangle , **B2-9** \square

Unbuffered H₂O/MeOH mixtures as mobile phases were studied first. With increasing MeOH content, increasing retention times were observed for **B2-3** on both columns. This can be partly explained by the changing solubility of the analyte and partly by the lower polar character of MeOH. The retention time of **B2-9** generally showed a slight increase too; however, it has a minimum between 50/50 and 30/70 (v/v) H₂O/MeOH compositions. The observed retention behavior is probably due to the increased effects of the hydrophobic interactions at increased MeOH content. The α and R_s values generally increased with increasing MeOH content. Comparing the TeicoShell and TagShell columns, the retentions were higher, while the α and R_s values were lower on the TeicoShell column, indicating that nonselective interactions contributed markedly to the retention properties in the case of the TeicoShell column.

Significant differences can be observed using TEAA as an additive in the eluent. TEAA as a polar modifier was “produced *in situ*” by adding 0.1% TEA into the eluent, then AcOH was added in an equimolar amount. The pH reported here is the apparent pH (pH_a). Apparent pH_a means that pH was adjusted to $\text{pH}_a = 5.0$ directly in the $\text{H}_2\text{O}/\text{MeOH}$ solvent mixture containing 0.1% TEAA by addition of AcOH. Notably, the apparent pH ($\text{pH}_a = 5.0$) was the same for each eluent applied in these experiments. In the presence of 20 mM TEAA, retentions were lower in all cases, while α and R_s were higher than those in the unbuffered systems. Based on these observations, it can be assumed that the buffer suppressed the non-selective interactions between the analytes and the selectors.

These experiments were also carried out with MeOH/MeCN containing 20 mM TEAA eluent. The retention times increased with increasing MeCN content with macrocyclic glycopeptide CSPs in all cases. At high MeCN content, the solvation of amino acids decreases, resulting in higher retention times. In contrast, both α and R_s decreased with the increase of MeCN in the eluent. This suggests that H-bonding does not play an essential role in enantioseparations under the applied conditions.

4.1.2. Fluorinated β -phenylalanines

For the separation of fluorinated β -phenylalanines, the efficiency of five columns – TeicoShell, TagShell, VancoShell, LarihcShell-P, and Q-Shell, all with 3.0 mm i.d – was tested. The measurements were conducted in reversed-phase (A: RP, $\text{H}_2\text{O}/\text{MeOH}$; B: RP, $\text{H}_2\text{O}/\text{MeCN}$) or polar ionic mode (C: PIM, MeOH/MeCN).

Despite the variation of the mobile phase composition, preliminary experiments showed that the TeicoShell column did not exhibit significant enantiorecognition ability in separating fluorinated β -phenylalanines. In RP, the TagShell column showed some separation abilities for some analytes, while the VancoShell column showed the best separation efficiency. The chromatographic data obtained are presented in **Figure 10**.

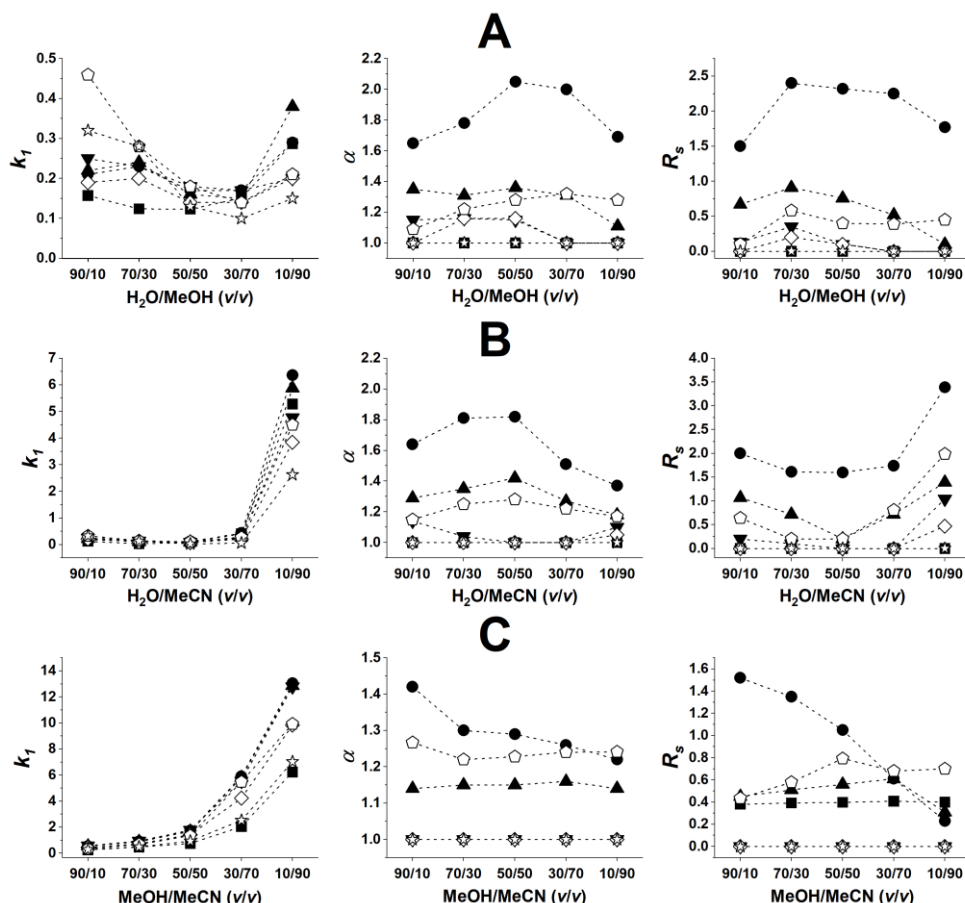


Figure 10. Effects of bulk solvent composition on the VancoShell column

Chromatographic conditions: column: V-3.0; eluent, **A**: H₂O/MeOH containing 0.1% TEAA, **B**: H₂O/MeCN containing 0.1% TEAA, **C**: MeOH/MeCN containing 0.1% TEAA; flow rate: 0.3 ml/min; temperature: 20 °C; symbols for analytes: **BPA-1** ■, **BPA-2** ●, **BPA-3** ▲, **BPA-4** ▼, **BPA-5** ◇, **BPA-6** □, **BPA-7** ☆

With the VancoShell column in RP conditions, the composition of H₂O/MeOH or H₂O/MeCN bulk solvent was changed between 90/10–10/90 (v/v), and both eluent systems contained 0.1% TEAA. The retention curve of the first analyte showed a minimum in all cases at around 30/70 (v/v), both with MeOH and MeCN. This is a typical hydrophobic chromatographic behavior. The increase in the retention time at higher water content is caused by the decrease of the solvation shell of the ionized analyte. The retention times are higher with MeCN in all cases, which is probably due to the lower solubility of the amino acids compared to that in MeOH. The selectivity showed a maximum curve for most cases, with a maximum at around 50/50–30/70 (v/v) composition.

In PIM, the eluent was composed of MeOH and MeCN (90/10–10/90 v/v) containing 0.1% TEAA. TEAA was prepared by adding 0.1% TEA and an equimolar amount of

AcOH into the mixture. The retention showed a steep increase with increasing MeCN content, suggesting rapidly decreasing solubility of the polar analytes in the eluent. The α and R_s values showed a relatively low dependence on the eluent composition in most cases, but higher MeOH content seems more favorable. These results suggest a minor role of H-bonding in enantiorecognition.

Similar experiments were also performed with the teicoplanin aglycone-based CSP, but this CSP could partially separate the enantiomers of only three analytes, **BPA-1**, **BPA-6**, and **BPA-7**. The trends were similar to the ones observed on vancomycin. The complementary enantiorecognition of the selectors can happen in two different ways: (i) if one glycopeptide cannot separate the enantiomers of a molecule, then there can be a structurally similar one that can separate the enantiomers; (ii) two different glycopeptides can separate the same enantiomers, but the enantiomeric order is reversed. In these experiments, the first case can be observed. The teicoplanin aglycone-based CSP was able to separate α -phenylalanine (**BPA-1**) but it could not separate β -phenylalanine (**BPA-2**), while the vancomycin-based CSP was able to separate β -phenylalanine but not α -phenylalanine.

A LarihcShell-P column was also studied with eluent systems composed of MeOH/MeCN 90/10–10/90 (v/v) containing TFA and TEA in various concentrations. First, the effects of TFA:TEA ratio were studied. The eluent contained MeOH/MeCN 10/90 (v/v) and 0.20% TEA with varying amounts of TFA (0.10–0.60%). The increase of the TFA concentration decreased the retentions for all four analytes (**BPA-1**, **BPA-2**, **BPA-3**, **BPA-7**), while the selectivities and resolutions increased only slightly (**Figure A4 A**). TFA:TEA 3:2 as the best performing ratio was used in all further experiments. Second, the effects of the concentration of the polar modifier were studied. The TFA:TEA concentration was changed between 0.15:0.10–0.60:0.40 (v/v), keeping the 3:2 ratio. Retention times decreased in all cases with increasing counter ion concentration; however, the selectivity did not change, while the resolution decreased slightly (**Figure A4 B**). To explore the effects of the bulk solvent composition, the MeOH/MeCN composition was changed between 90/10–10/90 (v/v), and all eluents contained 0.3% TFA and 0.2% TEA. The analytes did not have significant retention, when MeOH/MeCN varied between 90/10–50/50 (v/v), while retention times increased with MeCN content higher than 50% (**Figure A4 C**). This trend is similar to the results discussed previously on the TeicoShell, TagShell, and VancoShell columns. However, there is a difference in selectivity and resolution, since both α and R_s increased with

increasing MeCN content. This suggests that stereoselective H-bonding interactions are present between the analytes and the isopropyl carbamate moiety of CF6-P CSP.

We could observe the complementary attribute comparing the macrocyclic glycopeptide-based CSPs with the cyclofructane-6 (LarihcShell-P) and *Cinchona* alkaloid-based (Q-Shell) CPSs. The enantiomeric elution order on the glycopeptide-based CSPs was $S < R$, but the opposite, that is $R < S$, was observed on the other two.

4.1.3. α -Substituted proline analogs

First, the VancoShell and TagShell columns were compared for the separation of proline and α -substituted proline analogs. Analytes **Pr-1**, **Pr-2**, **Pr-4**, **Pr-5**, **Pr-6**, and **Pr-10** were selected, and MeOH/MeCN 100/0–20/80 (v/v) containing 20 mM AcOH as eluent were used. The retention times increased on both columns with the increase of MeCN content, suggesting that the protic MeOH promotes the solvation of the amino acids. The α and R_s values decreased, indicating that the nonselective interactions are becoming more dominant. Comparing the two columns, the retention times were always higher on the TagShell column.

MeOH/MeCN containing 20 mM TEAA was also used to repeat these experiments with analytes **Pr-4**, **Pr-5**, **Pr-6**, and **Pr-10** (**Pr-1** and **Pr-2** were not separable under this condition). Chromatographic data are presented in **Figure 11**. Similar trends have been observed on all studied columns; however, retention times were lower than in the eluent containing AcOH (data not shown). Interestingly, the NicoShell column showed some separation ability using MeOH/MeCN containing 20 mM TEAA eluent. The exact structure of the selector of the NicoShell column is unknown. The only available information is that it is a modified teicoplanin. This CSP was developed to separate the enantiomers of nicotine [99], but it can also separate several other molecules, too [100,101].

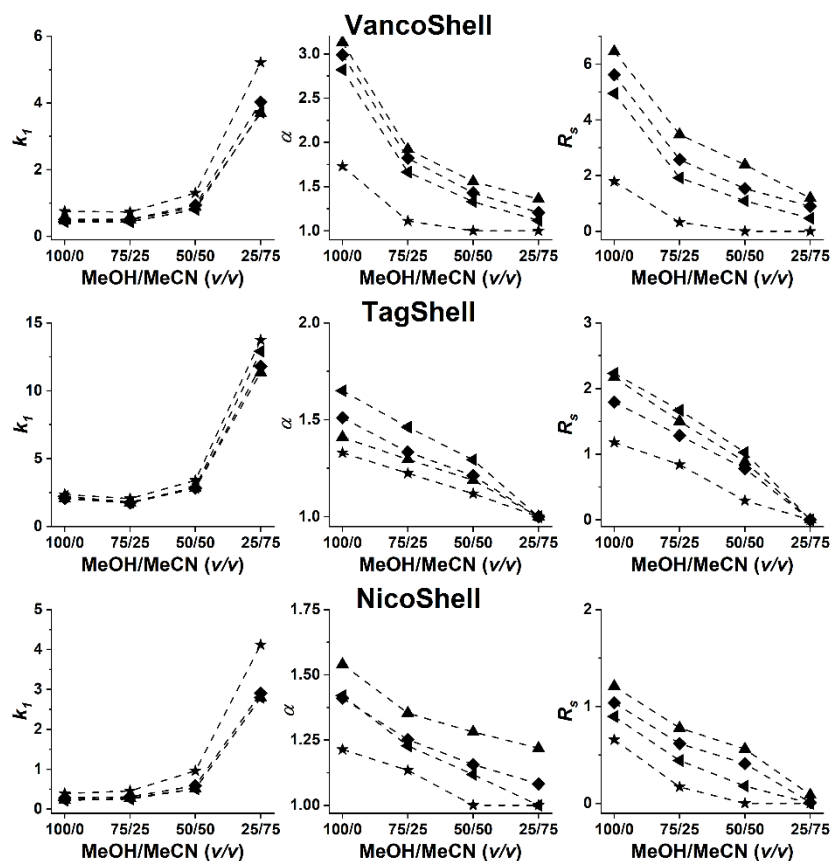


Figure 11. Effects of bulk solvent composition on the enantioseparation α -substituted proline analogs

Chromatographic conditions: columns: V-3.0, TAG-3.0, and N-3.0; eluent: MeOH/MeCN containing 20 mM TEAA; flow rate: 0.3 ml/min, temperature: 20 °C; symbols for analytes: *Pr-4* ▲, *Pr-5* ◆, *Pr-6* ◀, *Pr-10* ★

In summary, investigating the effect of the bulk solvent composition of the mobile phase, the retention times were lowest in the H₂O/MeOH eluent system containing polar modifiers, while for the H₂O/MeOH eluent without modifiers, somewhat higher retention times were registered. Application of MeCN in H₂O/MeCN containing TEAA or MeOH/MeCN containing TEAA eluent system, the retention times were significantly higher and immensely increased with increasing MeCN content. As concerns the enantioselectivities, they increased (or reached a maximum) with increasing MeOH content in H₂O/MeOH or H₂O/MeOH containing TEAA system; however, in the MeCN-containing mobile phases, α decreased with increasing MeCN content, especially in PIM.

4.2. Effects of nature of mobile phase additives

4.2.1. β^2 -Amino acids

The effects of five additives on the enantioseparation of β^2 -amino acids (**B2-3** and **B2-9**) were studied on TeicoShell and TagShell columns by applying NH_4HCOO , NH_4OAc , TEAA, FA, and AcOH. The bulk solvent was $\text{H}_2\text{O}/\text{MeOH}$ 90/10 (v/v) containing 20 mM additive. The pH_a was adjusted to 5.0 with the corresponding acid, when a salt was used as a modifier. The obtained results are presented in **Figure 12**.

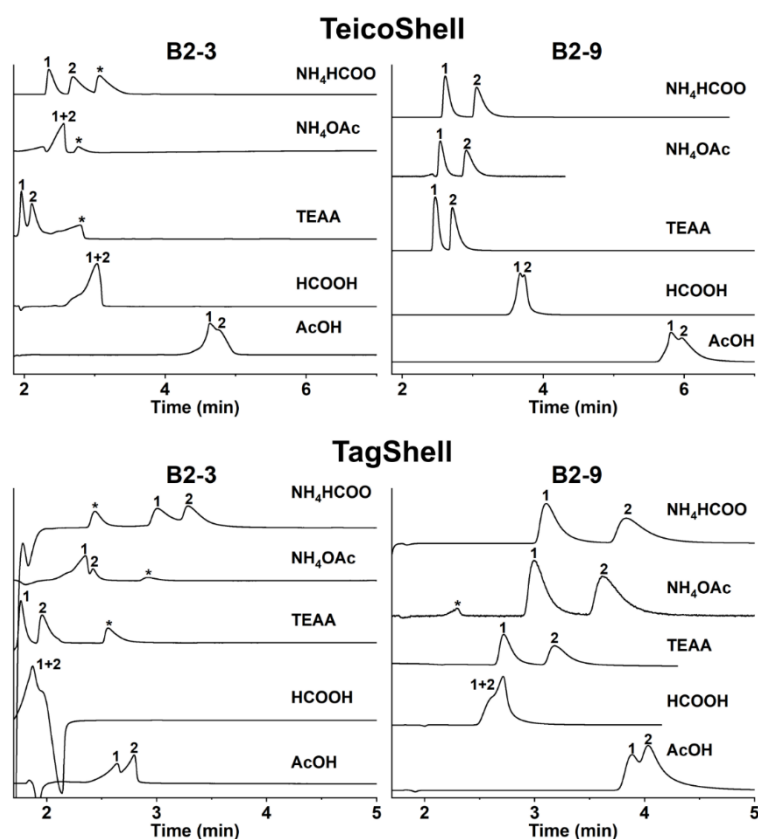


Figure 12. Effects of polar modifiers on the enantioseparation of two β^2 -amino acids with TeicoShell and TagShell columns

Chromatographic conditions: columns: **T-3.0** and **TAG-3.0**; eluent: $\text{H}_2\text{O}/\text{MeOH}$ 90/10 (v/v) containing 20 mM polar additive; flow rate: 0.3 ml/min, temperature: 20 °C; * unknown components

Application of FA and AcOH resulted in no or incomplete separations with poor peak shapes in some cases. TEAA produced the best peak shapes of the three salts applied and the lowest retention times with sufficient selectivities and resolutions. However, it is important to note that TEAA is not a suitable modifier when MS-based detection is necessary. NH_4OAc offered comparable separation performances with higher retention times, which can be suggested as a viable alternative in the case of MS detection.

4.2.2. α -Substituted proline analogs

The effects of polar modifiers on the enantioseparation of α -substituted proline analogs were studied on VancoShell and TagShell columns with FA, TFA, AcOH, TEAA, NH_4HCOO , and NH_4OAc , and the results obtained with *Pr-5* are shown in Figure 13.

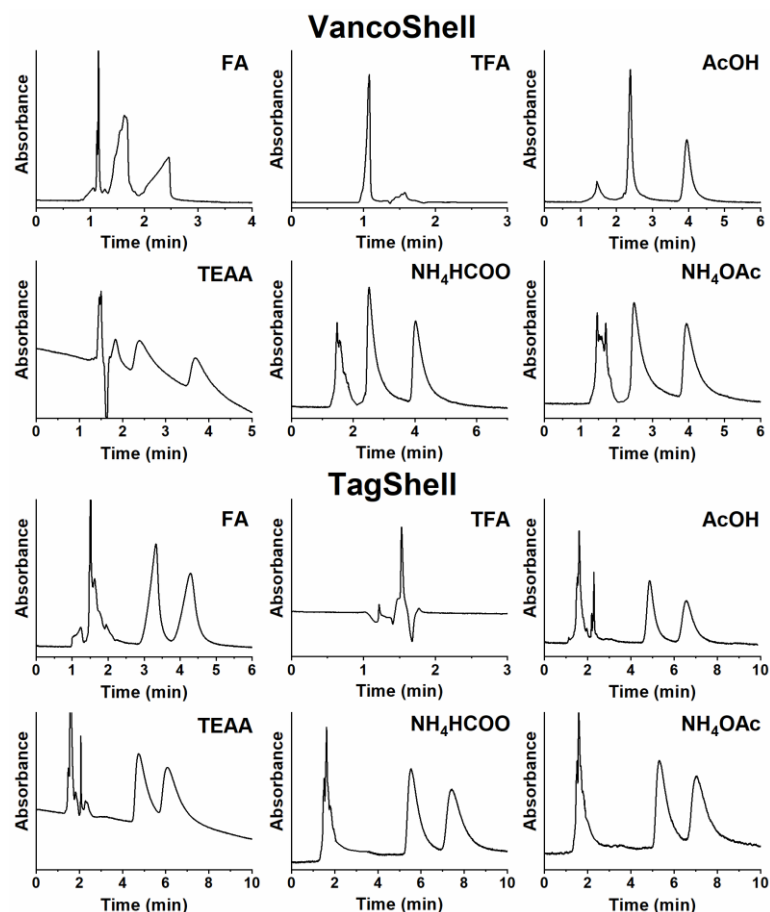


Figure 13. Effects of polar modifiers on the enantioseparation of *Pr-5* applying VancoShell and TagShell columns

Chromatographic conditions: columns: **V-3.0** and **TAG-3.0**; eluent: MeOH/MeCN 80/20 (v/v) containing 20 mM polar additives; flow rate: 0.3 ml/min; temperature: 20 °C

Using only an acid additive resulted in more symmetric peak shapes, however, the analytes had no significant retention with TFA, probably due to its high acidity. There are two possible explanations: either TFA can make a high ion concentration in the eluent, which crowds out the analytes (**Section 4.3.**), or the abundance of the ions causes the formation of ion-pairs that have low retention on the column. Utilizing a weaker acid increases the retention times, supporting the previous assumption. The application of AcOH led to higher resolutions than FA and it is also an MS-compatible additive. From

a chromatographic point of view, applying TEAA proved to be the most advantageous, resulting in better separations than AcOH in most cases.

The nature of the acidic or salt additives strongly affected retentions and separations. TEAA was an effective additive and often used in enantioselective chromatography, applying macrocyclic glycopeptide selectors and spectrophotometric detection. Regarding MS detection, application of NH_4OAc , NH_4HCOO , or AcOH, especially in the case of proline analogs, is more favorable.

4.3. Effect of counter ion concentration, application of the stoichiometric displacement model

All applied selectors possess carboxyl and amino groups, which can form ionic interactions. The stoichiometric displacement model has generally been applied to characterize the role of ionic interactions in chromatographic separations [102]. It predicts a linear relationship between the logarithm of the retention factor and the logarithm of the counter ion concentration:

$$\log k = \log K_Z - Z \log c_{\text{counter ion}} \quad (10)$$

where K_Z describes the ion-exchange equilibrium and Z is the effective charge.

Plotting $\log k$ as a function of $\log c_{\text{counter ion}}$ will result in a straight line if an ion-exchange mechanism is present. The slope of the line will be proportional to the effective charge, and the intercept will give information about the equilibrium constant.

4.3.1. β^2 -Amino acids

The applicability of the stoichiometric displacement model was tested with the TeicoShell and TagShell columns using **B2-3** and **B2-9** analytes. The experiments were performed in RP ($\text{H}_2\text{O}/\text{MeOH}$ 90/10 v/v) and in PIM (MeOH/MeCN 90/10 v/v), with both eluents containing 5.0-160 mM TEAA as a counter ion. Data illustrating the results of the linear regressions are presented in **Figure 14**.

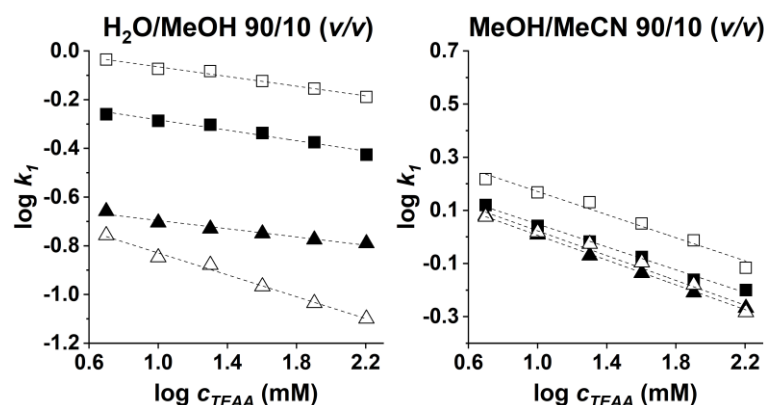


Figure 14. Effect of counter ion concentration on the retention factor of the first eluting enantiomer for β^2 -amino acids

Chromatographic conditions: columns: T-3.0 and TAG-3.0; symbols: on T-3.0 for B2-3 ▲ and B2-9 ■; on TAG-3.0 for B2-3 △ and B2-9 □; flow rate: 0.3 ml/min; temperature: 20 °C

According to literature data, the slopes for zwitterionic CSPs are mostly between -0.5 – -0.2, while they are around -1.0 in the case of monoionic ion exchangers [103,104]. In this study, the slopes calculated for the TeicoShell and TagShell columns are very similar in all cases, with values between -0.225 and -0.085 in RP and between -0.233 and -0.215 in PIM. This means that only weak ionic interactions are present between the analytes and selectors [105,106]. In such cases, increasing the counter ion concentration always decreases the retentions to a limited range. It can be stated that there is no significant difference between the two studied CSPs and the two modes in terms of retention times with varying counter ion concentrations.

4.3.2. Fluorinated β -phenylalanines

The applicability of the stoichiometric displacement model was tested for α -, and β -phenylalanines and their fluorinated analogs with optimized H₂O/MeOH, H₂O/MeCN, and MeOH/MeCN eluents, each containing 0.90–14.35 mM TEAA. Data presenting the linear fits are shown in **Figure 15**. In all cases, the increase of TEAA concentration decreased the retentions. The slopes were between -0.25 and -0.10 for the VancoShell, and between -0.011 and -0.01 for the TagShell column. These results prove that weak ionic interactions are present and they affect retentions; however, they do not play an essential role in the enantiomeric recognition.

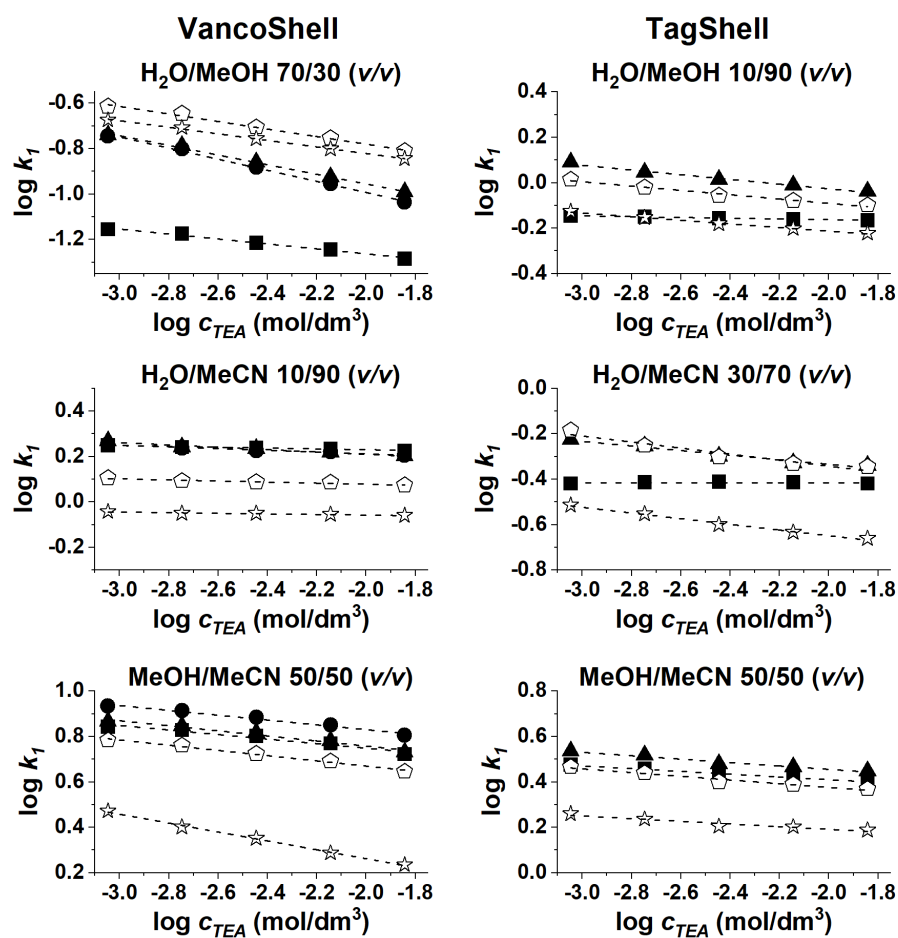


Figure 15. Effect of counter ion concentration on the retention factor of the first eluting enantiomer of β -phenylalanines

Chromatographic conditions: columns: **V-3.0** and **TAG-3.0**; flow rate: 0.3 ml/min; temperature: 20 °C; symbols for analytes: **BPA-1** ■, **BPA-2** ●, **BPA-3** ▲, **BPA-6** ◇, **BPA-7** ☆

4.3.3. α -Substituted proline analogs

In the case of proline and its α -substituted analogs, 100% MeOH containing 2.5, 5.0, 10.0, 20.0, or 40.0 mM AcOH eluents were used for the experiments to probe the validity of the stoichiometric displacement model. It is important to note that acetic acid is a weak acid, and its dissociation is further reduced by employing MeOH as a solvent. TEAA was not used in these experiments because of its incompatibility with MS detection. Employing stronger acids caused worse peak shapes or no retention for the analytes.

Correlation coefficients for all fitted lines exceed the $R^2 > 0.98$ value (**Figure 16**). The slopes were between -0.092 and -0.067 on VancoShell and -0.150 and -0.050 on TagShell column. These results indicate, even though the measurement conditions are not ideal, that only weak ion-exchange interactions are present between the analytes and

selectors, and they have just a slight effect on the retentions and the enantiomeric recognition.

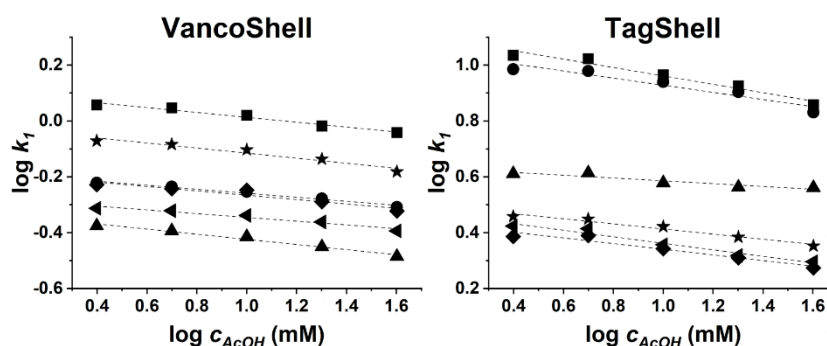


Figure 16. Effect of counter ion concentration on the retention factor of the first eluting enantiomer for proline analogs

Chromatographic conditions: columns: **V-3.0** and **TAG-3.0**; flow rate: 0.3 ml/min; temperature: 20 °C; symbols for analytes: *Pr-1* ■, *Pr-2* ●, *Pr-4* ▲, *Pr-5* ◆, *Pr-6* ◄, *Pr-10* ★

The increase in counter ion concentration decreased the retentions for all three groups of analytes independently of the applied column. The absolute value of slopes was relatively small in all cases, indicating that only weak ionic interactions are present. It should be noted that the k_2 values for the second eluting enantiomers give practically the same slopes with increasing counter ion content. This means that the selectivity does not change significantly with the increasing amount of counter ion, that is, counter ion concentration has only a limited effect on enantioselectivity.

4.4. Structure–retention relationships

4.4.1. β^2 -Amino acids

To study the structure–retention relationships, screening was made for all 19 β^2 -amino acids with three eluent systems: **A**: H₂O/MeOH 30/70 (v/v); **B**: H₂O/MeOH 30/70 (v/v) containing 2.5 mM TEA and 5.0 mM AcOH and **C**: MeOH/MeCN 70/30 (v/v) containing 2.5 mM TEA and 5.0 mM AcOH. The TeicoShell and TagShell columns were used with 3.0 mm and 2.1 mm i.d.

All amino acids were separated on at least one of the columns, and some were separated on both. The **C** eluent produced the highest retention times; however, the **B** eluent was the most favorable overall, producing comparable selectivities with lower retention times. The chromatographic data are shown in **Table A1** for the TeicoShell column, and **Table A2** for the TagShell column.

Regarding structure–retention relationships, a strong correlation could be observed for β^2 -amino acids possessing an aliphatic side chain. Steric effects may play an essential role in enantioselective liquid chromatography, in particular, when the selector is a (macro)cyclic molecule. In these cases, interactions between the selector and analyte mainly take place in the cavity of the selector molecule, and the size of the molecule is expected to affect molecular recognition. The so-called Meyer parameter (V^a) was used to describe this relationship, where V^a is the volume of the different substituents in the examined molecules; the volume of the same “base” structure is omitted [107]. The V^a values for Me (**B2-1**), Et (**B2-2**), Pr (**B2-3**), Bu (**B2-4**), 2-Pr (**B2-5**), and 2-Bu (**B2-6**) moieties are 2.84, 4.31, 4.78, 4.79, 5.74, and $6.21 \times 10^{-2} \text{ nm}^3$, respectively (no value is available for 6-methylheptanoic (**B2-7**) and 5-cyclohexylpentanoic (**B2-8**) moieties.). Both k_1 and α show a good correlation with V^a , confirming that the larger the volume of the functional group, the more significant impact it has (**Figure 17**). Retention times decrease with increasing V^a , while selectivity increases. It is worth mentioning that k_2 is also decreasing, but not as much as k_1 . As a result, an increase in selectivities can be observed. The results are similar with all three eluent systems and with both column sizes.

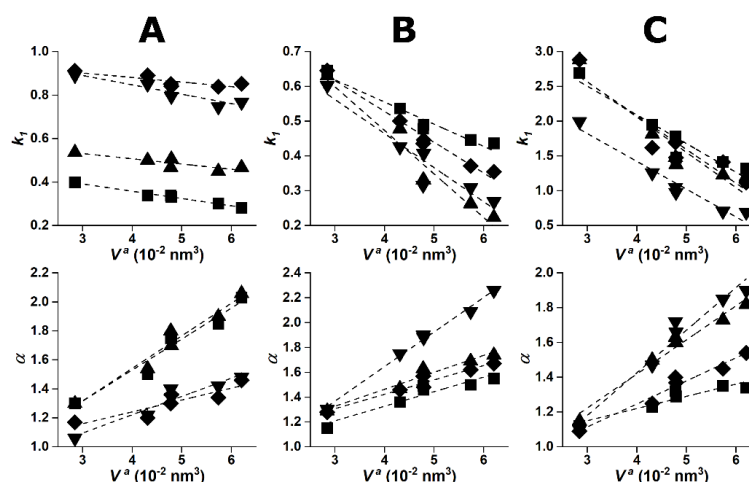


Figure 17. Dependence of retention and selectivity on the size of the functional group of β^2 -amino acids on TeicoShell and TagShell columns

Chromatographic conditions: columns: **T-3.0**, **T-2.1** and **TAG-3.0**, **TAG-2.1**; mobile phase; **A:** H₂O/MeOH 30/70 (v/v); **B:** H₂O/MeOH 30/70 (v/v) containing 2.5 mM TEA and 5.0 mM AcOH and **C:** MeOH/MeCN 70/30 (v/v) containing 2.5 mM TEA and 5.0 mM AcOH; flow rate: 0.3 ml/min; temperature: 20 °C; symbols for columns: **T-3.0** ■, **TAG-3.0** ▲, **T-2.1** ◆, **TAG-2.1** ▼

For β^2 -amino acids possessing an aromatic side chain, generally higher resolutions were observed for all three eluent systems (**Table A1** and **A2**). There was at least one

system, where $R_s > 1.5$ could be observed for most of them, and only **B2-12** and **B2-13** showed poorer resolutions. The better resolution of compounds possessing aromatic moiety is probably due to presence of π - π interactions with the selectors.

B2-9 contains no additional function on the phenyl group, **B2-11** has a methyl, **B2-12** a dimethylamine, **B2-13** a chlorine, and **B2-14** a hydroxy group in the *para* position on the ring. Substitution on the aromatic ring in the *para* position increased the retention times in all cases, especially for **B2-12** (Table A1 and Table A2). However, both selectivity and resolution decreased. The high retention of **B2-12** is probably due to the additional amino group that is protonated in the presence of an acid, resulting in additional ionic interactions. **B2-14** and **B2-15** contain a hydroxy group in the *para* or *meta* position. Retention times, selectivities, and resolutions were generally higher for **B2-15**, indicating that the substitution in the *meta* position is sterically more favorable for chiral recognition.

B2-16 contains an oxoethyl group and it has an additional chain compared to **B2-14**. Both can form H-bonding interactions, but **B2-16** is affected more by steric effects. The retentions and selectivities are similar, but the resolutions are higher for **B2-16** on the TeicoShell column, indicating faster adsorption–desorption kinetics. However, on the TagShell column, retention times are higher, while selectivities and resolutions are lower, indicating stronger nonselective interactions. These differences are observed for **B2-16** to **B2-19** analytes, each with an additional larger-size function on the phenyl ring. The teicoplanin and teicoplanin aglycone form a basket-like structure. Teicoplanin has three additional sugar moieties compared to teicoplanin aglycone. These are on the “outside” of the basket and mainly contribute to steric effects, primarily to steric repulsion. The addition of a bigger functional group onto the phenyl ring causes additional interactions with these sugar units.

B2-18 and **B2-19** have the highest retentions in addition to **B2-12**. **B2-18** has a 1,3-benzodioxole functional group, while **B2-19** has a naphthyl moiety. Both structures have a larger delocalized electron system contributing to the selector–analyte interactions, accounting for the higher retentions. The two O atoms in **B2-18** can also contribute to π - π interactions and H-bondings.

4.4.2. Fluorinated β -phenylalanines

The structure–retention relationship studies could effectively be conducted on the VancoShell and LarihcShell-P columns. On the TagShell and Q-Shell columns, only a

small number of analytes could be separated, and the available data are limited. However, it is important to note that the TagShell column separated the enantiomers of **BPA-1**, while the VancoShell column could separate **BPA-2**, as mentioned in **Section 4.1**.

Three eluent systems were used for the studies: **A**: H₂O/MeOH 70/30 (v/v) containing 0.1% TEAA, **B**: H₂O/MeCN 10/90 (v/v) containing 0.1% TEAA, and **C**: MeOH/MeCN 70/30 (v/v) containing 0.1% TEAA. All three eluents could separate most of the enantiomers of the analytes (**BPA-1** and **BPA-7** could not be separated on the VancoShell column), but eluent **C** was the least effective. The experiments were performed at 0.3 ml/min flow rate and 20 °C column temperature. Data are presented in **Table 2**.

Table 2. Chromatographic parameters of β -phenylalanines on the VancoShell column

Analyte	Eluent	k_I	α	R_S
BPA-1	A	0.12	1.00	0.00
	B	5.28	1.00	0.00
	C	0.12	1.00	0.00
BPA-2	A	0.19	1.96	2.20
	B	6.37	1.37	3.39
	C	0.81	1.33	1.32
BPA-3	A	0.20	1.37	0.91
	B	5.88	1.18	1.39
	C	0.81	1.15	0.54
BPA-4	A	0.23	1.18	0.32
	B	4.77	1.10	1.04
	C	0.86	1.00	0.00
BPA-5	A	0.18	1.17	0.20
	B	3.85	1.05	0.47
	C	0.69	1.00	0.00
BPA-6	A	0.28	1.22	0.45
	B	4.50	1.17	1.99
	C	0.31	1.19	0.45
BPA-7	A	0.24	1.00	0.00
	B	2.63	1.00	0.00
	C	0.28	1.00	0.00

Chromatographic conditions: column: **V-3.0**; mobile phases: **A**: H₂O/MeOH 70/30 (v/v) containing 0.1% TEAA, **B**: H₂O/MeCN 10/90 (v/v) containing 0.1% TEAA and **C**: MeOH/MeCN 70/30 (v/v) containing 0.1% TEAA; flow rate: 0.3 ml/min; temperature: 20 °C

The retention times are similar for all analytes on the VancoShell column with eluent **A**. The highest selectivity and resolution were observed for **BPA-2**, both steeply decreasing with the increasing number electron-withdrawing of F atoms on the phenyl ring. This indicates that π - π interactions have an important role in the enantiomeric recognition. Interestingly, higher retention but lower selectivity and resolution were observed for **BPA-6** than for **BPA-3**. Both have one F atom but in different positions (*ortho* for **BPA-3**, *para* for **BPA-6**), and **BPA-6** has an extra methyl group in the *para* position. This means that the methyl group somewhat offsets the electron-withdrawing effect of fluorine and, consequently, the *para* position is favorable for the retention. This is also supported by results obtained with **BPA-4** and **BPA-5**. Both of them have two F atoms but in different positions. **BPA-4** has one F atom in *meta* and one in *para* position and has higher retention, selectivity, and resolution. On **BPA-5**, both F atoms are in *meta* (3,5) positions. The lower chromatographic parameters confirm the disadvantageous *meta* position. Enantiomers of **BPA-7** could not be separated due to the high number of electron-withdrawing atoms.

Similar trends were obtained with eluent **B**. However, retention times are much longer in all cases, which is probably due to the lower solubility of the analytes in MeCN. MeCN also interferes with π - π interactions, and this explains the lower selectivities despite the higher retentions.

Eluent **C** was the least effective, and **BPA-4** and **BPA-5** could not be enantioseparated.

MeOH/MeCN 10/90 (v/v) containing 0.3 mM TFA and 0.2 mM TEA eluent was effective with the LarihcShell-P column, as data show in **Table 3**. This system was able to separate all analytes, at least partially. **BPA-4** had the highest retention but one of the lowest selectivity and resolution. The presence of an electronegative F atom results in increased retention time, but its ring position is more important. The retention time increases if a F atom is in the *para* position, whereas the enantioseparation decreases. **BPA-5** has lower retention but higher selectivity, confirming the previously described relationship. The *ortho* position is the most favorable when comparing the functional group positions on the phenyl ring. **BPA-6** and **BPA-7** have lower retention times than the others but have higher selectivity, except **BPA-1**. **BPA-1** has the highest selectivity and second highest resolution, indicating that both α -amino acid structure and the unmodified proline are favorable.

Table 3. Chromatographic parameters of β -phenylalanines on LarihcShell-P column

Analyte	k_I	α	R_s
BPA-1	2.05	1.19	1.37
BPA-2	1.93	1.08	0.60
BPA-3	2.23	1.06	0.50
BPA-4	2.56	1.06	0.60
BPA-5	2.04	1.11	1.30
BPA-6	1.64	1.09	1.48
BPA-7	1.92	1.10	1.14

Chromatographic conditions: column: **CF6-P-3.0**; eluent: MeOH/MeCN 10/90 (v/v) containing 0.3 mM TFA and 0.2 mM TEA; flow rate: 0.3 ml/min; temperature: 20 °C

4.4.3. α -Substituted proline analogs

In enantioselective separations, there is a high demand for the development of MS-compatible eluents due to the advantageous features of MS-based detection, such as high selectivity to the measured components and low limit of detection and quantitation. In enantioselective chromatography carried out on macrocyclic glycopeptide-based CSPs, TEA and its salts with AcOH (e.g., TEAA) are often applied as modifiers. Unfortunately, the base or its salt results in markedly reduced MS sensitivity. As proline and proline analogs with aliphatic side chains do not have significant UV absorption, MS-based detection and MS-compatible eluent must have been applied.

To gather data for the structure–retention (selectivity) relationships in the case of proline analogs, a study was performed with the VancoShell, TeicoShell, TagShell, and NicoShell columns with two eluent systems, **A**: 100% MeOH containing 20 mM AcOH, **B**: 100% MeOH containing 20 mM TEAA. Eluent **B** is not compatible with MS detection, because of the presence of TEA. Enantioselective chromatography generally requires an acid and a base as polar modifiers for sufficient separations. Ammonia can be used as a base, but it is not as effective in most cases as TEA.

Comparing all studied columns, lower retentions were obtained on the VancoShell and NicoShell columns with both eluents; however, the resolution and selectivity in many cases were significantly higher, in particular, in the case of proline analogs with aromatic side chains, indicating different retention mechanisms (**Table A3** and **A4**).

Regarding proline analogs with aliphatic side chains, the enantiomers of **Pr-1** could only be separated on the VancoShell column, whereas **Pr-3** was separated on the TagShell column with 100% MeOH containing 20 mM AcOH eluent. **Pr-1**, **Pr-2**, and

Pr-3 could not be studied with eluent **B** due to their poor UV absorbance, and eluent **B** is not compatible with MS. **Pr-2** was separated on both the TeicoShell and TagShell columns, but the resolution was higher on the TagShell column with similar selectivity.

By comparing the enantioselectivities obtained for proline analogs with aromatic side chains, namely **Pr-5**, **Pr-6**, **Pr-7**, and **Pr-10**, we can observe the effect of the group in the *para* position. The selectivity increased with the addition of a methyl group. This indicates that the more electron-rich the aromatic system, the better the enantiomeric recognition. The selectivity significantly decreases when introducing a F atom into the *para* position. A Br atom in that position also decreases the selectivity, but to a lesser extent, which is probably due to its lower electronegativity. **Pr-12** showed superior selectivity and resolution due to the naphthyl moiety, although with somewhat higher retention time, compared to **Pr-5**.

Based on the obtained results, it can be stated that a group in the *ortho* position is disadvantageous compared to the *meta* and *para* positions. Both **Pr-8** and **Pr-9** have a Cl atom in the *meta* and *ortho* positions, respectively. The selectivity changes from 2.34 to 1.52 on the VancoShell column with eluent **A** (see related data is in **Table A3**), and a similar change can be observed on all columns. The resolution also decreased significantly. The negative impact of the *ortho* position is also confirmed by **Pr-10** and **Pr-11**. In this case, the Br atom is in the *para* or *ortho* position. If it is in the *ortho* position, it decreases the enantioseparation, but this change is smaller than the change found with the *meta* to *para* position, described previously. It suggests that the *meta* position is the most advantageous in the case of enantioseparation on these columns. These differences can be seen with eluent **B**, too, especially in cases, when there was no enantioseparation with *ortho* position, for example, in the case of **Pr-11**.

Generally, the selectivity was higher on the TagShell column. In most cases, the selectivity on the TeicoShell column was lower than 1.15. Both selectors have the same glycopeptide structure, but teicoplanin has three sugar units. If the differences in the enantioselective free energies are calculated and plotted, the effect of the sugar units can be visualized (**Figure 18**). The negative value of free energy differences means that the separation is more advantageous on TagShell phases, while the positive value refers to more efficient separation on TeicoShell columns.

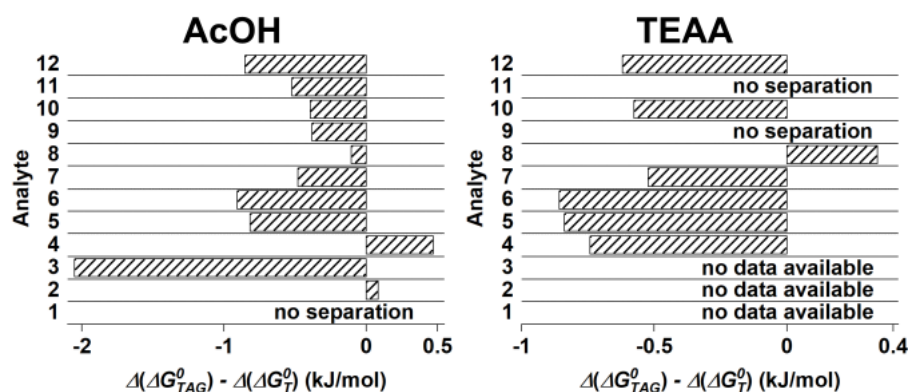


Figure 18. Effect of the sugar units on the enantioseparations of α -substituted proline analogs

Chromatographic conditions: columns: **T-3.0** and **TAG-3.0**; eluent: 100% MeOH containing 20 mM additive, AcOH or TEAA; flow rate: 0.3 ml/min; temperature: 20 °C

This graph also helps to understand the similar performance of vancomycin and teicoplanin aglycone selectors. Their base structure is similar, but vancomycin has only a single sugar moiety explaining the lower performance. *Berthod et al.* investigated the effects of the sugar moieties by comparing teicoplanin and teicoplanin aglycone [26]. The sugar units may intervene in the chiral recognition in different ways. Specifically, they may (i) sterically hinder the access of the molecules to binding sites on the aglycone basket; (ii) block the two phenol hydroxy groups on the aglycone, where two sugar units are attached; (iii) and block the alcohol moiety on the aglycone where the third sugar unit is linked.

In summary, a strong correlation can be observed between the separation performance and the structures of the analytes and selectors can be observed. For the β^2 -amino acids, the effect of the size of the aliphatic side chains was studied. The results showed a strong relationship between the size of the aliphatic side chain and retention or selectivity. In addition, the nature and position of a substituent on the aromatic side chain of β^2 -amino acids greatly affected chiral discrimination. It revealed that the substitution at the *para* position was favored regarding retention. However, regarding selectivity and resolution, it was not observed in all cases. Substituents capable of H-bonding or ionic-interaction, substituents with delocalized electron system capable of π - π interaction or steric-interactions (repulsion) may have a positive or negative effect on chiral discrimination.

Data for the separation of fluorinated β -phenylalanines showed that the number and position of F atoms with electron-withdrawing character possess a strong effect.

H₂O/MeOH containing acid and base additives was the best choice for mobile phases. The increasing number of F atoms generally has a negative effect on selectivity, while the influence of their *ortho* and *para* position depends on the CSP applied.

The best eluent for the α -substituted proline analogs with aliphatic side chain was the H₂O/MeOH mobile phase containing AcOH with MS detection. For the analogs with aromatic side chains, TEAA as additive was also successfully applied. It was also registered that a substituent on the aromatic ring with electron-donating properties was favorable, while the electron-withdrawing character was less favorable in enantiomer separation. Regarding the position of substituents, the *para* or *meta* position was the most advantageous, while the *ortho* position caused significant steric hindrance in enantiorecognition.

In the case of α -substituted proline analogs, the differences in the enantioselective free energies calculated for TagShell and TeicoShell CSPs shed light on the role of sugar units in enantiorecognition.

4.5. Influence of the temperature

Enantioselective separations are generally influenced more by temperature than achiral ones. Studying the effects of temperature change on chromatographic behavior by evaluating the van't Hoff equation (**equation 8**) is a technique used regularly [108,109]. It is important to note that with this method, the contribution of enantioselective and non-selective interactions cannot be differentiated [110].

4.5.1. β^2 -Amino acids

In the case of β^2 -amino acids, the thermodynamic studies were carried out both in RP (**A**: H₂O/MeOH 30/70 (v/v), 20 mM TEAA concentration, pH_a = 5.0) and PIM (**B**: MeCN/MeOH 30/70 (v/v), 20 mM TEAA concentration). The temperature was changed between 5–50 °C, and **B2-8** (possessing an aliphatic side chain) and **B2-9** (bearing an aromatic side chain) were used as analytes. Data are presented in **Table 4**.

Comparing the results obtained with two mobile phases and the TeicoShell column, quite different values can be seen for both $-\Delta(\Delta H^0)$ and $-\Delta(\Delta S^0)$. These differences are the results of different selectivities. These values are negative for both analytes, indicating that the adsorption/desorption kinetics are enthalpically favored. As observed most frequently, both k and α decreased with increasing temperature. These trends are

also valid for the TagShell column, and there is no significant difference in the thermodynamic values of **B2-8** and **B2-9**.

The Q value ($Q = \Delta(\Delta H^0)/[298 \text{ K} \times \Delta(\Delta S^0)]$) or enthalpy/entropy ratio tells us that a chiral separation is enthalpy- or entropy-driven. For these separations, the Q value was always greater than 1.0, indicating that all chiral separations were enthalpically driven.

Table 4. Thermodynamic parameters of β^2 -amino acids on TeicoShell and TagShell columns

Analyte	Eluent	$-\Delta(\Delta H^0)$ (kJ/mol)	$-\Delta(\Delta S^0)$ (J/(mol \times K))	$-\Delta(\Delta G^0)_{298K}$ (kJ/mol)	Q
TeicoShell					
B2-8	A	3.55	7.59	1.28	1.57
	B	1.43	2.72	0.62	1.77
B2-9	A	2.05	3.57	0.99	1.93
	B	1.30	2.31	0.61	1.89
TagShell					
B2-8	A	2.04	4.42	0.73	1.55
	B	2.56	5.14	1.02	1.67
B2-9	A	2.06	4.24	0.79	1.63
	B	2.11	4.78	0.68	1.48

Chromatographic conditions: columns: **T-3.0** and **TAG-3.0**; mobile phases: **A**: H₂O/MeOH 30/70 (v/v) containing 20 mM TEAA (pH_a = 5.0) and **B**: MeCN/MeOH 30/70 (v/v) containing 20 mM TEAA; temperature: 5-50 °C

4.5.2. Fluorinated β -phenylalanines

The thermodynamic characterization of fluorinated β -phenylalanines was carried out on VancoShell and LarihcShell-P columns. The study was performed both in RP and PIM on VancoShell. Since the retention and enantioselectivity strongly depended on the eluent composition, multiple eluent systems were used for the experiments.

On the VancoShell column in RP, H₂O/MeOH 70/30 and 10/90 (v/v), and H₂O/MeCN 70/30 and 10/90 (v/v), in PIM MeOH/MeCN 70/30 and 30/70 (v/v) mobile phases were used, all containing 0.1% TEAA (**Table A5**). Retention and selectivity decreased with increasing temperature in all cases. $\Delta(\Delta H^0)$ and $\Delta(\Delta S^0)$ all showed negative values with **BPA-2** to **BPA-5**. This is a similar behavior discussed for the β^2 -amino acids. (**BPA-1** and **BPA-7** were not examined because they could not be separated under the applied conditions.)

The van't Hoff equation describes the function of the selectivity on the temperature as a linear correlation. However, it can be different in some cases, and this behavior was observed on VancoShell with **BPA-6** (Figure 19).

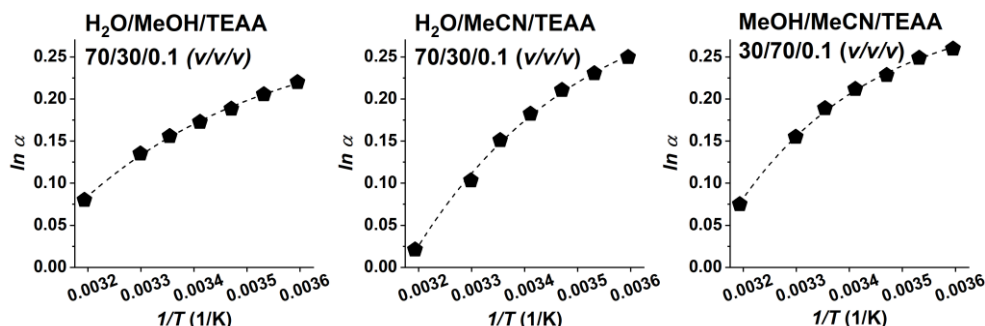


Figure 19. $\ln \alpha$ vs. $1/T$ curves for **BPA-6** on VancoShell column

Chromatographic conditions: column: VancoShell (**V-3.0**); mobile phase, H₂O/MeOH 70/30 (v/v); H₂O/MeCN 70/30 (v/v) and MeOH/MeCN 30/70 (v/v) all containing 0.1% TEAA; flow rate: 0.3 ml/min; temperature: 5–40 °C

All other analytes had a good linear correlation ($R^2 > 0.97$), while an exponential correlation was observed with **BPA-6**. During the thermodynamic studies, we assume that the mechanisms are the same at all temperatures, only the rate of the adsorptions/desorptions changes, and a linear correlation is valid. The non-linear behavior indicates that the overall binding situation changes in this temperature range. Unfortunately, we could not make further investigations to better understand this effect. In PIM, similar behaviors were observed, as previously mentioned, including **BPA-6**, but **BPA-4** and **BPA-5** could not be enantioseparated.

MeOH/MeCN 10/90 (v/v) containing 0.3% TFA and 0.2% TEA eluent was used with the LarihcShell-P column for thermodynamic evaluation. The trends were similar to those observed on the VancoShell column, showing similar values with the PIM experiments (Table 5). On the LarihcShell-P column, α - and β -phenylalanine (**BPA-1** and **BPA-2**) exhibited the most negative $\Delta(\Delta H^\circ)$ and $\Delta(\Delta S^\circ)$ values, suggesting that fluoro substitution reduced the differences experienced by the enantiomers in the process of chiral recognition.

All Q values were higher than 1.0, indicating that the contribution of enthalpy was more significant to the free energy than the contribution of entropy.

Table 5. Thermodynamic parameters measured on LarihcShell-P column with β -phenylalanines

Analyte	$-\Delta(\Delta H^0)$ (kJ/mol)	$-\Delta(\Delta S^0)$ (J/(mol \times K))	$-\Delta(\Delta G^0)_{298K}$ (kJ/mol)	Q
BPA-1	2.62	7.51	0.38	1.17
BPA-2	1.60	4.82	0.26	1.11
BPA-3	1.26	3.78	0.13	1.12
BPA-4	1.41	3.34	0.12	1.04
BPA-5	1.49	4.25	0.22	1.18
BPA-6	0.91	2.37	0.20	1.28
BPA-7	0.60	1.25	0.23	1.61

Chromatographic conditions: column: **CF6-P-3.0**; eluent: MeOH/MeCN 10/90 (v/v) containing 0.3% FA and 0.2% TEA; flow rate: 0.3 ml/min; temperature: 5–50 °C

4.5.3. α -Substituted proline analogs

The effect of temperature on chromatographic parameters for **Pr-1** to **Pr-12** were studied on VancoShell and TagShell columns in the temperature range 5–50 °C. 100% MeOH containing 20 mM AcOH was used as mobile phase.

Both k and α values decreased with increasing temperature for nearly all analytes on both columns. The $\Delta(\Delta H^0)$ values on the VancoShell column ranged from –10.80 to –2.43 kJ/mol and from –6.45 to +1.15 kJ/mol on the TagShell column (**Table A6**). In cases, when $\Delta(\Delta H^0)$ was negative, $\Delta(\Delta S^0)$ was negative too, indicating the enthalpically favored kinetics. The values of $\Delta(\Delta S^0)$ depended on two effects: (i) on the difference in the number of degrees of freedom of the two enantiomers on the surface of the selector, and (ii) on the solvation-desolvation process on both selector and selectand.

The only exception from the decreasing selectivity trend was **Pr-4** on the TagShell column. In this case, the selectivity increased with the temperature; both $\Delta(\Delta H^0)$ and $\Delta(\Delta S^0)$ were positive, meaning that the entropically driven enantioseparation was favored.

The calculated Q values exceeded 1.0 for all experiments except for **Pr-4** on the TagShell column, further confirming the entropically driven enantioseparation in this case. In such cases, the retention of the second eluting enantiomer increases to a lower extent than the first one.

In this study, in the case of proline analogs possessing an aromatic moiety in α - position, the effect of the nature and position of substituents on the aromatic ring has a noticeable effect on the thermodynamic parameters. Comparing **Pr-5** with **Pr-6**, a

benzyl or 4-methylbenzyl moiety, respectively, similar $\Delta(\Delta H^0)$ and $\Delta(\Delta S^0)$ values are observed, but they are somewhat more negative in the case of **Pr-6**. This is probably caused by the presence of the electron-donating methyl group. It means that the more “electron rich” the phenyl group, the stronger the interaction becomes with these CSPs. This theory is also supported by the thermodynamic parameters of **Pr-7** and **Pr-10**. They contain a F or Br atom, both possessing electron-withdrawing properties. The $\Delta(\Delta H^0)$ and $\Delta(\Delta S^0)$ values are more negative for **Pr-10** (–4.05 and –11.28 kJ/mol), followed by **Pr-7** (–3.80 and –10.50 kJ/mol), indicating more negative values with the increasing electronegativity.

As discussed in **Section 4.4.3.**, the *meta* position is the most favored because of steric interactions. This is also confirmed by the thermodynamic values when comparing **Pr-8** vs. **Pr-9** and **Pr-10** vs. **Pr-11**. In both comparisons, the thermodynamic values are less negative in the case of compounds with substituent in the *ortho* position. The other two positions have similar thermodynamic values but cannot be compared directly due to the different functional groups.

Further investigation and specific techniques, not available at present, would require to understand the positive $\Delta(\Delta H^0)$ and $\Delta(\Delta S^0)$ values for **Pr-4**.

The thermodynamic studies showed that most of the separations were enthalpically driven, implying that the retention and selectivity decreased with increasing temperature. Analyte **Pr-4** on the TagShell column possesses an entropy-driven separation mechanism. The $-\Delta(\Delta H^0)$ and $-\Delta(\Delta S^0)$ values for β^2 -amino acids on TeicoShell and TagShell CSPs and for fluorinated β -phenylalanines on VancoShell and LarihcShell-P CSPs, with a few exceptions, changed in a relatively narrow range, while this range for proline analogs was larger. Another interesting observation was the non-linear $\ln \alpha$ vs. $1/T$ curve for **BPA-6** on the VancoShell column, indicating a change in the retention mechanisms in the investigated temperature range.

4.6. Kinetic studies

The kinetics of the selector–selectand interactions are commonly studied by preparing van Deemter curves, as discussed in **Section 2.5**. All studied columns were available in two internal diameters (2.1 and 3.0 mm i.d.); thus, their performances could be evaluated and compared. The linear flow rate (u) is independent of the internal diameter, and the kinetic plots of the columns can be represented on the same graph, making the comparison and interpretation easier.

Water-containing eluents can have considerable viscosity, which can cause high backpressures at higher flow rates. According to Darcy's law, backpressure relates to the viscosity and linear velocity of the mobile phase [111]. On the basis of this information, the eluents were carefully selected to be able to perform the van Deemter analysis.

Due to the high flow rates and pressures, it is inevitable to have fractional heating in the column. Thermal imaging was made by *Makarov et al.* using a 50×2.1 mm C18 column filled with $1.7 \mu\text{m}$ FPPs, and higher than 10°C axial temperature difference could be observed above 300 bar operating pressure [112]. The fractional heating can cause decreased selectivity in chromatography, but it can be corrected by thermostating the column [113].

4.6.1. β^2 -Amino acids

Two mobile phases were used to perform the van Deemter analysis for β^2 -amino acids, $\text{H}_2\text{O}/\text{MeOH}$ (30/70 v/v) and MeCN/MeOH (30/70 v/v), both containing 2.5 mM TEA and 5.0 mM AcOH. **B2-6** and **B2-9**, an aliphatic and an aromatic analyte, were used.

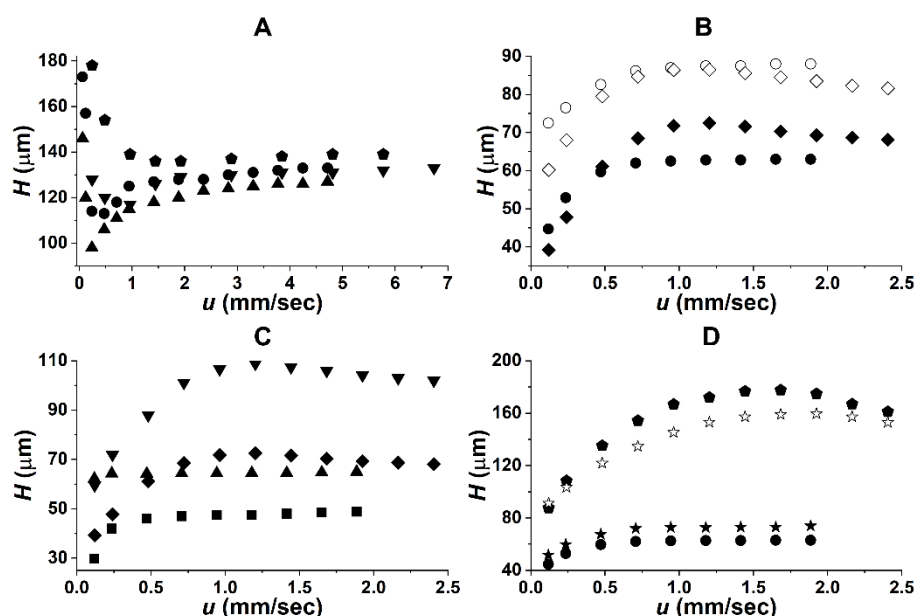


Figure 20. van Deemter plots measured on **T-3.0** and **T-2.1** and **TAG-3.0** and **TAG-2.1** columns with analytes **B2-6** and **B2-9**

Chromatographic conditions: columns: **T-3.0** and **T-2.1** and **TAG-3.0** and **TAG-2.1**; eluent: **A**, MeOH/MeCN 70/30 (v/v) containing 2.5 mM TEA and 5.0 mM AcOH, **B**, **C**, and **D**: $\text{H}_2\text{O}/\text{MeOH}$ 30/70 (v/v) containing 2.5 mM TEA and 5.0 mM AcOH; temperature: 20°C , symbols for analytes: **B2-6** on **T-3** H_1 \blacktriangle , H_2 \triangle , on **T-2.1** H_1 \blacktriangledown , H_2 \triangledown , on **TAG-3** H_1 \bullet , H_2 \circ , on **TAG-2.1** H_1 \blacklozenge , H_2 \lozenge ; **B2-9** on **T-3** H_1 \blacksquare , H_2 \square , **B2-9** on **T-2.1** H_1 \blacklozenge , H_2 \lozenge , on **TAG-3** \star and on **TAG-2.1** \star , H_1 and H_2 are the plate heights of the first and second eluting enantiomer, respectively

In PIM, curves with characteristic minima are observed with analyte **B2-6** on TeicoShell and TagShell columns (**Figure 20**). Comparing the 3.0 mm i.d. columns with the 2.1 mm i.d. ones, lower plate heights can be seen on the 3.0 mm columns in both cases, indicating better kinetic performance. The wall effect can explain the lower kinetic performance [114]. The molecules next or closer to the wall are left behind more resulting from the higher friction causing a more elongated parabolic flow profile, resulting in wider peaks. The difference can be particularly seen by comparing the minimums: 0.25 mm/sec on T-3.0 vs. 1.0 mm/sec on T-2.1 and 0.4 mm/sec on TAG-3.0 vs. 1.5 mm/sec on T-2.1. Comparing the two stationary phases, the curves obtained on the TeicoShell columns are always under the curves of the TagShell columns.

Figure 20 B depicts the differences between the plate heights of the first and second eluting enantiomers. The difference depends on the structure of the analyte and the selector and the properties of the eluent. The plate heights of the second enantiomers were around twice as high in nearly all cases. The curve shapes are nearly identical, indicating similar kinetics for both enantiomers.

The plate heights measured for **B2-6** and **B2-9** on the 3.0 mm and 2.1 mm columns are compared in the graphs of **Figure 20 C** and **D**. On both TeicoShell columns, the respective enantiomer of **B2-9** had lower plate heights than that of **B2-6**. In nearly all cases, the aliphatic analytes produced higher plate heights than the aromatic ones. However, on the TagShell column, **B2-6** had slightly lower plate heights for the first enantiomer.

It is important to note that most of the curves do not show the shape of a typical van Deemter curve. These curves show a particular shape, where the plate height constantly increases (efficiency decreases) with the flow rate. This effect was observed by other research groups, too, especially on macrocyclic antibiotic CSPs and for some achiral separations, too [115]. According to *Felletti et al.*, this effect is a combination of strong retention and the absence of diffusion in the solid phase [116]. The longitudinal diffusion of the analytes is also negligible at a lower flow rate, because they are absorbed in the stationary phase where there is no diffusion.

Based on the results discussed above, we can conclude that kinetics depends not only on the structure of the analyte and selector, but on the composition of the eluent as well. **B2-6** showed the typical van Deemter curve shapes on the TeicoShell columns (both on 3.0 and 2.1 mm i.d.) with MeOH/MeCN eluent, but they differed with H₂O/MeOH containing TEAA eluent (**Figure 20 A** and **C** graphs, respectively).

4.6.2. Fluorinated β -phenylalanines

VancoShell and LarihcShell-P columns were selected to determine the van Deemter plots with β -phenylalanines. On VancoShell, H₂O/MeCN 30/70 (v/v) containing 0.1% TEAA, on LarihcShell-P MeOH/MeCN 10/90 (v/v) containing 0.3 mM FA and 0.2 mM TEA eluent was used as mobile phase. The flow rate was changed between 0.025–2.0 ml/min, and the column temperature was set at 20 °C. Data are presented in **Figure 21**.

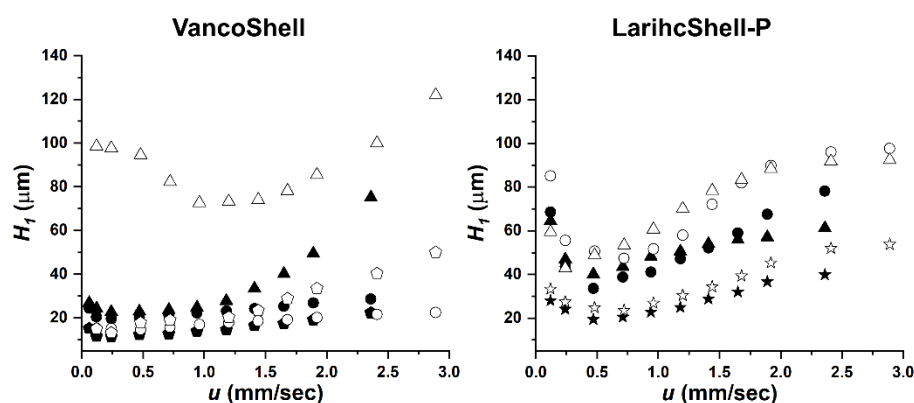


Figure 21. van Deemter plots on V-3.0, V-2.1 and CF6-P-3.0, CF6-P-2.1 columns

Chromatographic conditions: columns: V-3.0 and V-2.1 and CF6-P-3.0 and CF6-P-2.1; mobile phases: on V: H₂O/MeCN 30/70 (v/v) containing 0.1% TEAA, and on CF6-P: MeOH/MeCN 10/90 (v/v) containing 0.3 mM FA and 0.2 mM TEA; temperature: 20 °C; symbols for analytes: on 3 mm i.d. columns: BPA-2 ●, BPA-3 ▲, BPA-6 ◆ and BPA-7 ★; on 2.1 mm i.d. columns: BPA-2 ○, BPA-3 △, BPA-6 ◇ and BPA-7 ☆

The curves on the VancoShell column are similar to a typical van Deemter curve without the steep first part. All curves show a minimum at around 0.2–0.3 mm/sec flow rate. Only BPA-3 on the 2.1 mm i.d. column is an exception, with a minimum of 0.8 mm/sec. Interestingly, the plot of BPA-2 on the 2.1 mm i.d. column runs slightly under the curve on the 3.0 mm i.d. column.

The primary importance of these results is that the increase of the H_1 value with increasing flow rate is relatively low in some cases. Accordingly, markedly higher flow rates can be applied to achieve shorter retention times without significant loss in the performance.

All plot shapes were similar on the LarihcShell-P column, with minimums around 0.5 mm/sec. In all cases, the results on the 2.1 mm i.d. column were higher than on the 3.0 mm i.d. column, indicating the impact of the wall effect. Comparing the two columns, H_1 values were generally higher on the LarihcShell-P columns.

4.6.3. α -Substituted proline analogs

Pr-1, *Pr-2*, *Pr-4*, *Pr-5*, *Pr-6*, and *Pr-10* analytes were used to study the kinetic efficiency of the VancoShell and the TagShell columns applying 100% MeOH containing 20 mM AcOH as eluent. The column temperature was set at 20 °C, and the linear flow rate was changed between 0.1–1.0 ml/min on the 3.0 mm i.d. columns and between 0.05–0.5 ml/min on the 2.1 mm i.d. columns. The obtained results are presented in **Figure 22**.

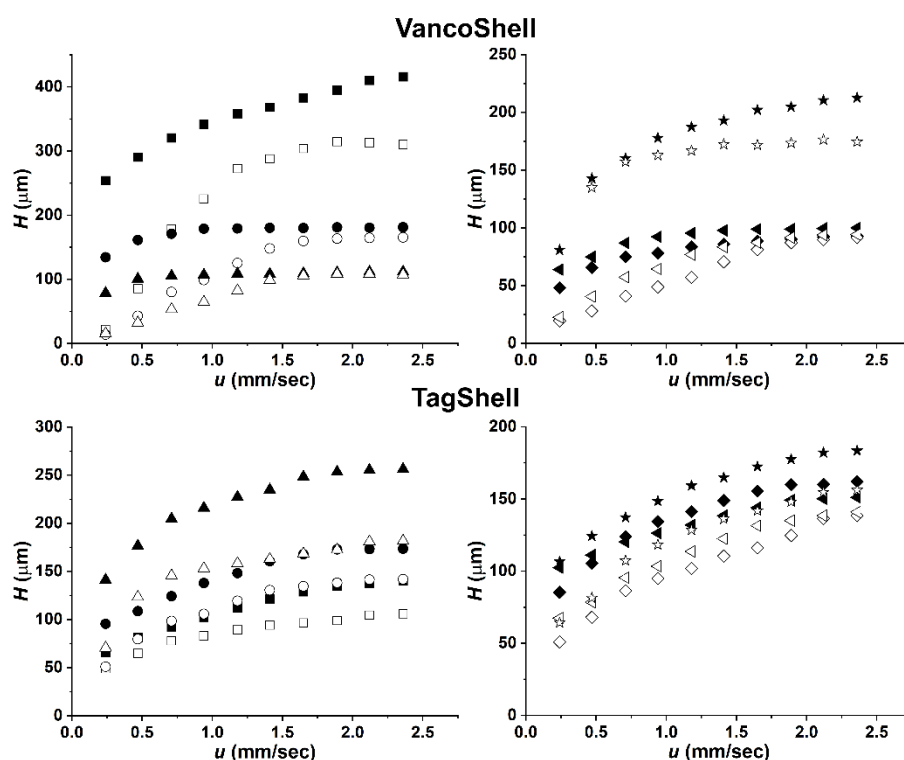


Figure 22. van Deemter plots of α -substituted proline analogs measured on VancoShell and TagShell columns

Chromatographic conditions: columns: **V-3.0**, **V-2.1** and **TAG-3.0**, **TAG-2.1**; mobile phase: 100% MeOH containing 20 mM AcOH; symbols for analytes: on 3.0 mm i.d. columns: **Pr-1** ■; **Pr-2** ●; **Pr-4** ▲; **Pr-5** ◆; **Pr-6** ◄; **Pr-10** ★; on 2.1 mm i.d. columns: **Pr-1** □; **Pr-2** ○; **Pr-4** △; **Pr-5** ◇; **Pr-6** ◁; **Pr-10** ☆

Unexpectedly, for the proline analogs, unusual van Deemter curves were observed; namely, no H minima vs. linear velocity can be identified for the studied analytes. The aromatic analytes, *Pr-5*, *Pr-6*, and *Pr-10*, show lower plate heights on the TagShell column. The curve shapes are similar, indicating a similar kinetic behavior on both columns.

The *Pr-1*, *Pr-2*, and *Pr-4* analytes show different behavior. The curve shapes are similar on both columns, but their order is different. On the VancoShell column, *Pr-1* has

the highest plate heights, *Pr-4* has the lowest, while *Pr-1* has the lowest on the TagShell column. This behavior can be related to the fact that the VancoShell column could separate the enantiomers of *Pr-1* but not *Pr-4*. In contrast, TagShell could separate *Pr-4* and could not separate *Pr-1*, utilizing the same eluent.

Interestingly, the *H-u* plots on the 2.1 mm i.d. columns run below the respective 3.0 mm plots in all cases. This is the opposite of the results in the previous studies using the same columns, where the 2.1 mm columns showed reduced efficiency due to the wall effect. The exact reasons are unknown at this moment; however, it is important to note that the analytes and the eluents are different, affecting both retentions and separations.

All these findings draw attention to an important fact. That is, the kinetic performance of a column depends not only on the geometric size and the mobile phase composition, as described often in the literature, but also on the nature of analytes.

It is important to note that the determined plate heights were higher than expected, although data were not corrected with the extra-column volume of the instrument. Reduction of the extra-column effects (e.g., by altering the tubing of the UHPLC) would probably result in lower plate heights. The shape of the curves and their minimum position depend not only on the geometrical size (i.d.) of the column, but on the structure of the analytes and even on the nature of the mobile phase as well. The unusual van Deemter curves in the case of proline analogs and, in a few cases of the β^2 -amino acids and fluorinated β -phenylalanine (*BPA-2*) indicate that the plate heights and the shapes of the curves are strongly influenced by numerous factors of chiral separation.

5. Summary

My research work utilized columns filled with superficially porous particles on a UHPLC system for the enantioseparation of natural and modified amino acids. Several selectors, primarily macrocyclic glycopeptides and quinine and cyclofructan-6 were also studied in the enantioseparation of three analyte groups, namely, β^2 -amino acids, β -phenylalanines, and proline analogs.

First, the effect of the mobile phase composition was studied. Most analytes were measured in RP with or without a polar modifier and in PIM. In most cases, RP with a polar modifier gave the lowest retention times, followed by the RP without a modifier. An eluent that contains MeCN increased retention times but could also result in considerable selectivity and resolutions. The RP eluent containing polar modifiers was the best overall choice in most cases. For the LarihcShell-P column, the MeOH/MeCN eluent containing TFA and TEA was effective for separating fluorinated β -phenylalanines. All analytes were separated with good selectivity with at least one column–eluent combination.

The nature of the mobile phase additives strongly affected both retentions and separations. In most cases, TEAA was observed to be the most effective, but it is not an MS-compatible additive. Other additives were also utilized, mainly to search for effective MS-compatible ones. With β^2 -amino acids, NH_4OAc gave good results, while for the proline analogs, AcOH proved to be effective with macrocyclic glycopeptide selectors.

The effects of the counter ion concentration were evaluated by applying the stoichiometric displacement model. In all cases, retentions decreased with the increase of the counter ion concentration. Still, all results showed that ionic interactions have a weak role in retentions and enantiomeric recognitions. However, their presence contributes to a more effective separation.

The structure of the analytes and selectors strongly affected both retentions and separations. In all cases, the presence of an aromatic moiety in the analyte increased the retention times, but selectivity and resolution also depended on the modifier groups on the aromatic ring. An important observation could be made on the effect of the position of the modifier group(s) on the aromatic ring for all three analyte groups. Generally, the *meta* or *para* position proved to be more advantageous for the separations, while the *ortho* position induced significant steric hindrance in most cases.

Thermodynamic studies were also made by changing the column temperature. The results showed that nearly all separations were enthalpically driven, implying that retentions and selectivities decreased with increasing temperature. This observation was further confirmed by the calculated Q values, which were higher than 1.0 in most cases. The only exception was **Pr-4** on the TagShell column, indicating that separations were entropically driven. According to the van't Hoff equation, the results show a linear correlation on an $\ln \alpha$ vs. $1/T$ plot. This correlation was valid in most cases; the only exception was **BPA-6** on the VancoShell column, suggesting a change in the binding mechanism in the studied temperature range.

Kinetic studies also gave either typical or unusual van Deemter curves, depending on the selector, the analyte, and the applied mobile phase. β -Phenylalanines showed typical curve shapes in nearly all cases. In contrast, the curves with the proline analogs were unusual in most cases. According to other research groups, this effect comes from strong retention and the absence of diffusion in the solid phase. The effect of the eluent on the kinetics could be observed with β^2 -amino acids. **B2-6** showed the typical van Deemter curve shapes on the TeicoShell columns with the MeOH/MeCN eluent, but differed with H₂O/MeOH containing TEAA eluent.

References

- [1] W. Walther, T. Netscher, *Chirality*. **8**, 397–401 (1996).
- [2] K. M. Rentsch, *J. Biochem. Biophys. Methods*. **54**, 1–9 (2002).
- [3] L. A. Nguyen, H. He, C. Pham-Huy, *Int. J. Biomed. Sci.* **2**, 85–100 (2006).
- [4] B. K. Matuszewski, M. L. Constanzer, *Chirality*. **4**, 515–519 (1992).
- [5] L. Yu, S. Wang, S. Zeng, in *Chiral Separations*, G. K. E. Scriba, Ed. (Humana Press, Totowa, NJ, 2013; http://link.springer.com/10.1007/978-1-62703-263-6_13), vol. 970 of *Methods in Molecular Biology*, pp. 221–231.
- [6] G. Gübitz, M. G. Schmid, *Chiral Separation: Method and protocol* (Human Press: Totowa, New Jersey, 2004).
- [7] M. Lämmerhofer, *J. Chromatogr. A*. **1217**, 814–856 (2010).
- [8] F. Jenő, K. Róbert, F. Szabolcs, *Modern folyadékkromatográfia* (Kromkorm Kft., Budapest, 2017).
- [9] L. H. Easson, E. Stedman, *Biochem. J.* **27**, 1257–1266 (1933).
- [10] G. M. Henderson, H. G. Rule, *Nature*. **141**, 917–918 (1938).
- [11] C. E. Dalglish, *J. Chem. Soc. Resumed*, 3940 (1952).
- [12] W. H. Pirkle, T. C. Pochapsky, *Chem. Rev.* **89**, 347–362 (1989).
- [13] V. A. Davankov, *Chirality*. **9**, 99–102 (1997).
- [14] G. K. E. Scriba, in *Chiral Separations*, G. K. E. Scriba, Ed. (Humana Press, Totowa, NJ, 2013; http://link.springer.com/10.1007/978-1-62703-263-6_1), vol. 970 of *Methods in Molecular Biology*, pp. 1–27.
- [15] A. D. Mesecar, D. E. Koshland, *Nature*. **403**, 614–615 (2000).
- [16] A. Berthod, *Anal. Chem.* **78**, 2093–2099 (2006).
- [17] R. B. Kasat, E. I. Franses, N.-H. L. Wang, *Chirality*. **22**, 565–579 (2010).
- [18] D. W. Armstrong, Y. Zhou, *J. Liq. Chromatogr.* **17**, 1695–1707 (1994).
- [19] D. W. Armstrong *et al.*, *Anal. Chem.* **66**, 1473–1484 (1994).
- [20] P. Franco, A. Senso, L. Oliveros, C. Minguillón, *J. Chromatogr. A*. **906**, 155–170 (2001).
- [21] K. H. Ekborg-Ott, Y. Liu, D. W. Armstrong, *Chirality*. **10**, 434–483 (1998).
- [22] K. H. Ekborg-Ott, G. A. Zientara, J. M. Schneiderheinze, K. Gahm, D. W. Armstrong, *ELECTROPHORESIS*. **20**, 2438–2457 (1999).
- [23] R. Berkecz, D. Tanács, A. Péter, I. Ilisz, *Molecules*. **26**, 3380 (2021).
- [24] D. P. Levine, *Clin. Infect. Dis.* **42**, S5–S12 (2006).
- [25] J. M. McGuire, R. N. Wolfe, D. W. Ziegler, *Antibiot. Annu.* **3**, 612–618 (1955).
- [26] A. Berthod *et al.*, *Anal. Chem.* **72**, 1767–1780 (2000).
- [27] A. Berthod, T. L. Xiao, Y. Liu, W. S. Jenks, D. W. Armstrong, *J. Chromatogr. A*. **955**, 53–69 (2002).
- [28] J. C. J. Barna, D. H. Williams, D. J. M. Stone, T. W. C. Leung, D. M. Doddrell, *J. Am. Chem. Soc.* **106**, 4895–4902 (1984).
- [29] A. H. Hunt, R. M. Molloy, J. L. Occolowitz, G. G. Marconi, M. Debono, *J. Am. Chem. Soc.* **106**, 4891–4895 (1984).
- [30] P. Pelletier, J. Caventou, *Ann. Chim. Phys.*, 337–365 (1820).
- [31] A. Strecker, *Ann. Chem. Pharm.* **91**, 349–351 (1854).
- [32] S. Izumoto, U. Sakaguchi, H. Yoneda, *Bull. Chem. Soc. Jpn.* **56**, 1646–1651 (1983).
- [33] K. Miyoshi, M. Natsubori, N. Dohmoto, S. Izumoto, H. Yoneda, *Bull. Chem. Soc. Jpn.* **58**, 1529–1534 (1985).
- [34] C. Pettersson, G. Schill, *J. Liq. Chromatogr.* **9**, 269–290 (1986).
- [35] C. Pettersson, C. Gioeli, *J. Chromatogr. A*. **435**, 225–228 (1988).

- [36] C. Rosini, C. Bertucci, D. Pini, P. Altemura, P. Salvadori, *Chromatographia*. **24**, 671–676 (1987).
- [37] M. Lämmerhofer, W. Lindner, *J. Chromatogr. A*. **741**, 33–48 (1996).
- [38] M. Kawamura, T. Uchiyama, T. Kuramoto, Y. Tamura, K. Mizutani, *Carbohydr. Res.* **192**, 83–90 (1989).
- [39] S. Kushibe, R. Sashida, Y. Morimoto, *Biosci. Biotechnol. Biochem.* **58**, 1136–1138 (1994).
- [40] P. Sun, C. Wang, Z. S. Breitbach, Y. Zhang, D. W. Armstrong, *Anal. Chem.* **81**, 10215–10226 (2009).
- [41] M. Sawada *et al.*, *Carbohydr. Res.* **217**, 7–17 (1991).
- [42] D. W. Armstrong, W. DeMond, *J. Chromatogr. Sci.* **22**, 411–415 (1984).
- [43] C. Wang, P. Sun, D. W. Armstrong, in *Chiral Recognition in Separation Methods*, A. Berthod, Ed. (Springer Berlin Heidelberg, Berlin, Heidelberg, 2010; http://link.springer.com/10.1007/978-3-642-12445-7_4), pp. 77–96.
- [44] R. Berkecz, G. Némethi, A. Péter, I. Ilisz, *Molecules*. **26**, 4648 (2021).
- [45] D. Roy, D. W. Armstrong, *J. Chromatogr. A*. **1605**, 360339 (2019).
- [46] H. Chen, Cs. Horváth, *J. Chromatogr. A*. **705**, 3–20 (1995).
- [47] K. S. Yun, C. Zhu, J. F. Parcher, *Anal. Chem.* **67**, 613–619 (1995).
- [48] F. Gritti, G. Guiochon, *J. Chromatogr. A*. **1115**, 142–163 (2006).
- [49] M. Wang, J. Mallette, J. F. Parcher, *J. Chromatogr. A*. **1218**, 2995–3001 (2011).
- [50] E. Caiali, V. David, H. Y. Aboul-Enein, S. C. Moldoveanu, *J. Chromatogr. A*. **1435**, 85–91 (2016).
- [51] L. Lapidus, N. R. Amundson, *J. Phys. Chem.* **56**, 984–988 (1952).
- [52] J. J. van Deemter, F. J. Zuiderweg, A. Klinkenberg, *Chem. Eng. Sci.* **5**, 271–289 (1956).
- [53] F. Svec, *J. Chromatogr. A*. **1217**, 902–924 (2010).
- [54] N. Wu, A. M. Clausen, *J. Sep. Sci.* **30**, 1167–1182 (2007).
- [55] K. K. Unger, R. Skudas, M. M. Schulte, *J. Chromatogr. A*. **1184**, 393–415 (2008).
- [56] G. Guiochon, F. Gritti, *J. Chromatogr. A*. **1218**, 1915–1938 (2011).
- [57] R. W. Brice, X. Zhang, L. A. Colón, *J. Sep. Sci.* **32**, 2723–2731 (2009).
- [58] J. J. DeStefano, S. A. Schuster, J. M. Lawhorn, J. J. Kirkland, *J. Chromatogr. A*. **1258**, 76–83 (2012).
- [59] J. O. Omamogho, J. P. Hanrahan, J. Tobin, J. D. Glennon, *J. Chromatogr. A*. **1218**, 1942–1953 (2011).
- [60] L. E. Blue, J. W. Jorgenson, *J. Chromatogr. A*. **1218**, 7989–7995 (2011).
- [61] R. Hayes, A. Ahmed, T. Edge, H. Zhang, *J. Chromatogr. A*. **1357**, 36–52 (2014).
- [62] X. Zhang, H. Niu, W. Li, Y. Shi, Y. Cai, *Chem. Commun.* **47**, 4454 (2011).
- [63] M. Spasova *et al.*, *J. Mater. Chem.* **15**, 2095 (2005).
- [64] H. Dong, J. D. Brennan, *Chem Commun.* **47**, 1207–1209 (2011).
- [65] S. A. Schuster, B. E. Boyes, B. M. Wagner, J. J. Kirkland, *J. Chromatogr. A*. **1228**, 232–241 (2012).
- [66] S. A. Schuster, B. M. Wagner, B. E. Boyes, J. J. Kirkland, *J. Chromatogr. A*. **1315**, 118–126 (2013).
- [67] C. Paek, Y. Huang, M. R. Filgueira, A. V. McCormick, P. W. Carr, *J. Chromatogr. A*. **1229**, 129–139 (2012).
- [68] K. Lomsadze, G. Jibuti, T. Farkas, B. Chankvetadze, *J. Chromatogr. A*. **1234**, 50–55 (2012).
- [69] H. Wolosker *et al.*, *Proc. Natl. Acad. Sci.* **96**, 721–725 (1999).
- [70] G. H. Fisher *et al.*, *Brain Res. Bull.* **26**, 983–985 (1991).

- [71] A. D’Aniello, J. M. Lee, L. Petrucelli, M. M. Di Fiore, *Neurosci. Lett.* **250**, 131–134 (1998).
- [72] Y. Nagata, R. Masui, T. Akino, *Experientia*. **48**, 986–988 (1992).
- [73] M. L. Chouinard, D. Gaitan, P. L. Wood, *J. Neurochem.* **61**, 1561–1564 (1993).
- [74] C. R. McCudden, V. B. Kraus, *Clin. Biochem.* **39**, 1112–1130 (2006).
- [75] K. Kalíková, T. Šlechtová, E. Tesařová, *Separations*. **3**, 30 (2016).
- [76] G. Cardillo, L. Gentilucci, P. Melchiorre, S. Spampinato, *Bioorg. Med. Chem. Lett.* **10**, 2755–2758 (2000).
- [77] M. Jin, M. A. Fischbach, J. Clardy, *J. Am. Chem. Soc.* **128**, 10660–10661 (2006).
- [78] M.-I. Aguilar *et al.*, *Org. Biomol. Chem.* **5**, 2884 (2007).
- [79] K. Gach-Janczak *et al.*, *Peptides*. **95**, 116–123 (2017).
- [80] D. F. Hook, F. Gessier, C. Noti, P. Kast, D. Seebach, *ChemBioChem*. **5**, 691–706 (2004).
- [81] J. Han *et al.*, *J. Fluor. Chem.* **239**, 109639 (2020).
- [82] X.-G. Li, M. Lähtie, L. T. Kanerva, *Tetrahedron Asymmetry*. **19**, 1857–1861 (2008).
- [83] V. Peddie *et al.*, *Synthesis*. **2010**, 1845–1859 (2010).
- [84] Y. Gong, K. Kato, *J. Fluor. Chem.* **111**, 77–80 (2001).
- [85] Y. Gong, K. Kato, *J. Fluor. Chem.* **125**, 767–773 (2004).
- [86] K. Nakayama *et al.*, *Org. Lett.* **2**, 977–980 (2000).
- [87] A. Yaron, F. Naider, S. Scharpe, *Crit. Rev. Biochem. Mol. Biol.* **28**, 31–81 (1993).
- [88] J. Jacob, H. Duclohier, D. S. Cafiso, *Biophys. J.* **76**, 1367–1376 (1999).
- [89] J. A. Robinson, *Synlett*. **2000**, 429–441 (2000).
- [90] J. M. Phang, *Antioxid. Redox Signal.* **30**, 635–649 (2019).
- [91] M. Endicott, M. Jones, J. Hull, *Amino Acids*. **53**, 1169–1179 (2021).
- [92] T. Miyamoto, H. Homma, *J. Biochem. (Tokyo)*. **170**, 5–13 (2021).
- [93] H. Zahradníčková, S. Opekar, L. Řimnáčová, P. Šimek, M. Moos, *Amino Acids*. **54**, 687–719 (2022).
- [94] A. Péter, E. Vékes, A. Árki, D. Tourwé, W. Lindner, *J. Sep. Sci.* **26**, 1125–1132 (2003).
- [95] A. Péter, G. Török, E. Vékes, J. Van Betsbrugge, D. Tourwé, *J. Liq. Chromatogr. Relat. Technol.* **27**, 17–29 (2004).
- [96] I. Ilisz *et al.*, *J. Chromatogr. A*. **1334**, 44–54 (2014).
- [97] E. Forró, T. Paál, G. Tasnádi, F. Fülöp, *Adv. Synth. Catal.* **348**, 917–923 (2006).
- [98] S. Shahmohammadi, F. Fülöp, E. Forró, *Molecules*. **25**, 5990 (2020).
- [99] G. Hellinghausen, J. T. Lee, C. A. Weatherly, D. A. Lopez, D. W. Armstrong, *Drug Test. Anal.* **9**, 944–948 (2017).
- [100] G. Hellinghausen *et al.*, *J. Pharm. Biomed. Anal.* **155**, 70–81 (2018).
- [101] G. Hellinghausen *et al.*, *Chromatographia*. **82**, 221–233 (2019).
- [102] W. Kopaciewicz, M. A. Rounds, J. Fausnaugh, F. E. Regnier, *J. Chromatogr. A*. **266**, 3–21 (1983).
- [103] C. V. Hoffmann, M. Laemmerhofer, W. Lindner, *J. Chromatogr. A*. **1161**, 242–251 (2007).
- [104] G. Lajkó *et al.*, *J. Chromatogr. A*. **1467**, 188–198 (2016).
- [105] C. V. Hoffmann, R. Reischl, N. M. Maier, M. Lämmerhofer, W. Lindner, *J. Chromatogr. A*. **1216**, 1157–1166 (2009).
- [106] T. Orosz *et al.*, *J. Pharm. Biomed. Anal.* **145**, 119–126 (2017).
- [107] A. Y. Meyer, *J. Chem. Soc. Perkin Trans. 2*, 1567 (1986).
- [108] S. Allenmark, V. Schurig, *J. Mater. Chem.* **7**, 1955–1963 (1997).
- [109] T. Fornstedt, P. Sajonz, G. Guiochon, *J. Am. Chem. Soc.* **119**, 1254–1264 (1997).

- [110] L. D. Asnin, M. V. Stepanova, *J. Sep. Sci.* **41**, 1319–1337 (2018).
- [111] C. L. Barhate, M. F. Wahab, Z. S. Breitbach, D. S. Bell, D. W. Armstrong, *Anal. Chim. Acta.* **898**, 128–137 (2015).
- [112] A. A. Makarov *et al.*, *Anal. Chim. Acta.* **1018**, 1–6 (2018).
- [113] M. M. Fallas, M. R. Hadley, D. V. McCalley, *J. Chromatogr. A.* **1216**, 3961–3969 (2009).
- [114] R. A. Shalliker, B. Scott Broyles, G. Guiochon, *J. Chromatogr. A.* **994**, 1–12 (2003).
- [115] F. Gritti, G. Guiochon, *J. Chromatogr. A.* **1392**, 10–19 (2015).
- [116] S. Felletti *et al.*, *J. Chromatogr. A.* **1630**, 461532 (2020).

Acknowledgments

I would like to thank my supervisor Professor István Ilisz, Head of the Institute of Pharmaceutical Analysis, for allowing me to make my Ph.D. work there and giving me great advice and help with my studies.

I would like to express my thanks to Professor Antal Péter, who also guided my work and helped me in many ways during my studies. Without their help and support, I would not have started my research work in this field.

I also wish my thanks to my colleagues, Dr. Gyula Lajkó, Dr. Attila Bajtai, Dr. Tímea Orosz, Gábor Németi, Dr. Róbert Berkecz, Dr. Tímea Körmöczi and Gabriella Vasas, who also helped me and gave various advice during my work and made an excellent working atmosphere. I also would like to thank all other members of the Institute of Pharmaceutical Analysis.

I want to thank Professor Árpád Molnár for proofreading my thesis.

I would like to give my greatest thanks to my parents and brother, who always helped and supported me, and to my extended family, who also believed in me.

This work was supported by UNKP-21-3-SZTE-274 and UNKP-22-3-SZTE-162 New National Excellence Program of the Ministry for Culture and Innovation from the source of the National Research, Development and Innovation Fund, and by the National Research, Development and Innovation Office-NKFIA through project K137607. Project no. TKP2021-EGA-32 has been implemented with the support provided by the Ministry of Innovation and Technology of Hungary from the National Research, Development and Innovation Fund, financed under the TKP2021-EGA funding scheme.

Appendix

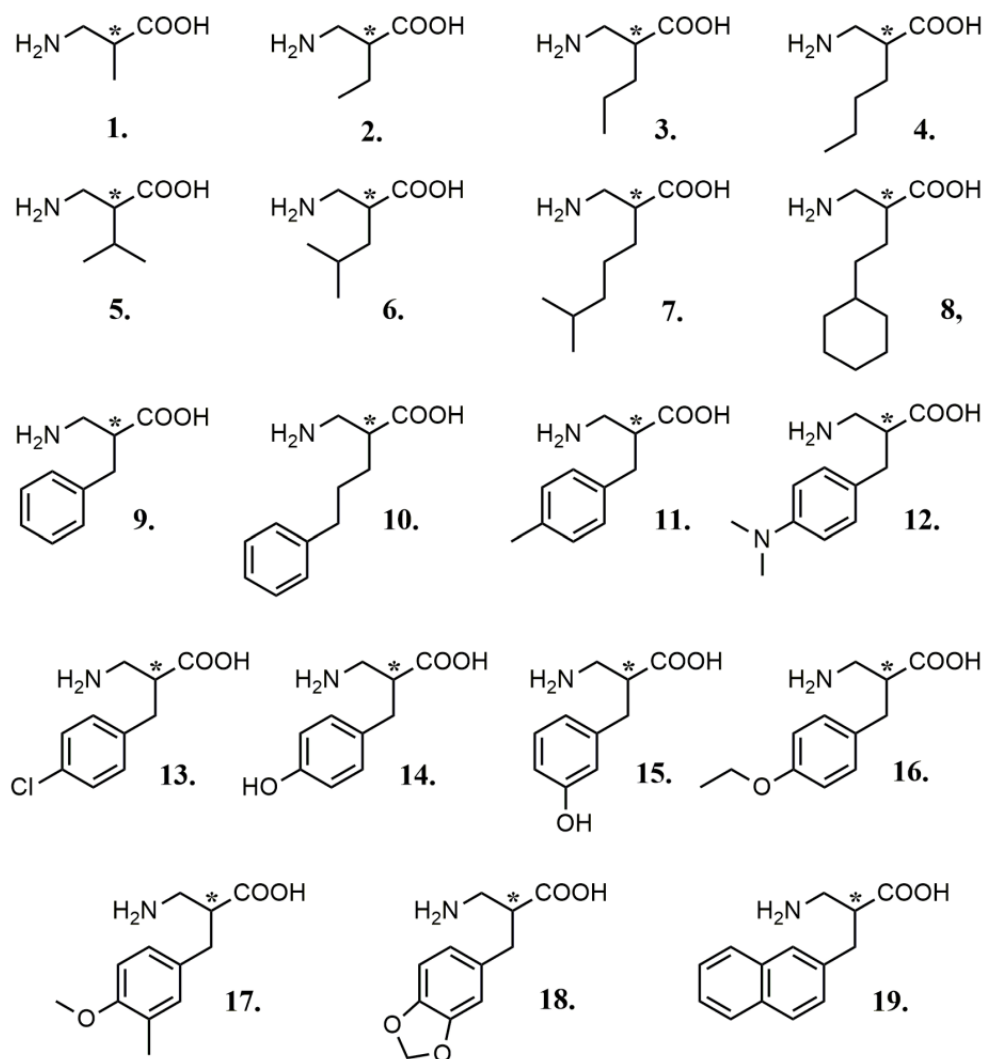


Figure A1. Structure of β^2 -amino acid analytes

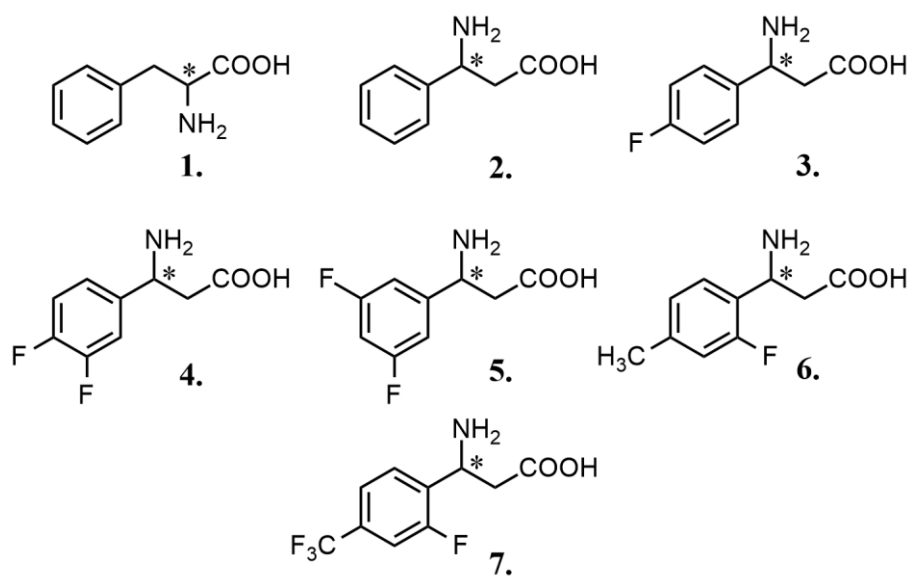


Figure A2. Structure of α - and fluorinated β -phenylalanines

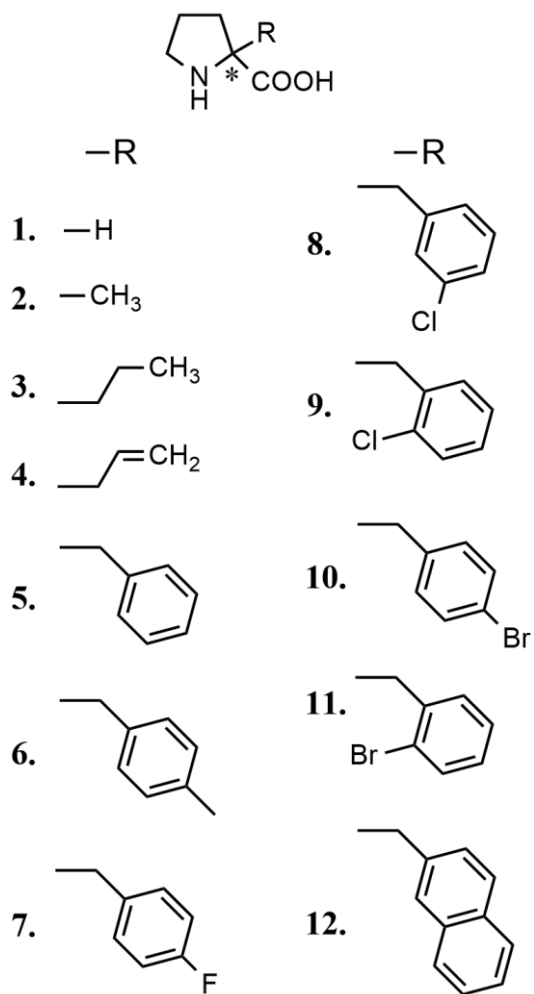


Figure A3. Structure of α -substituted proline analogs

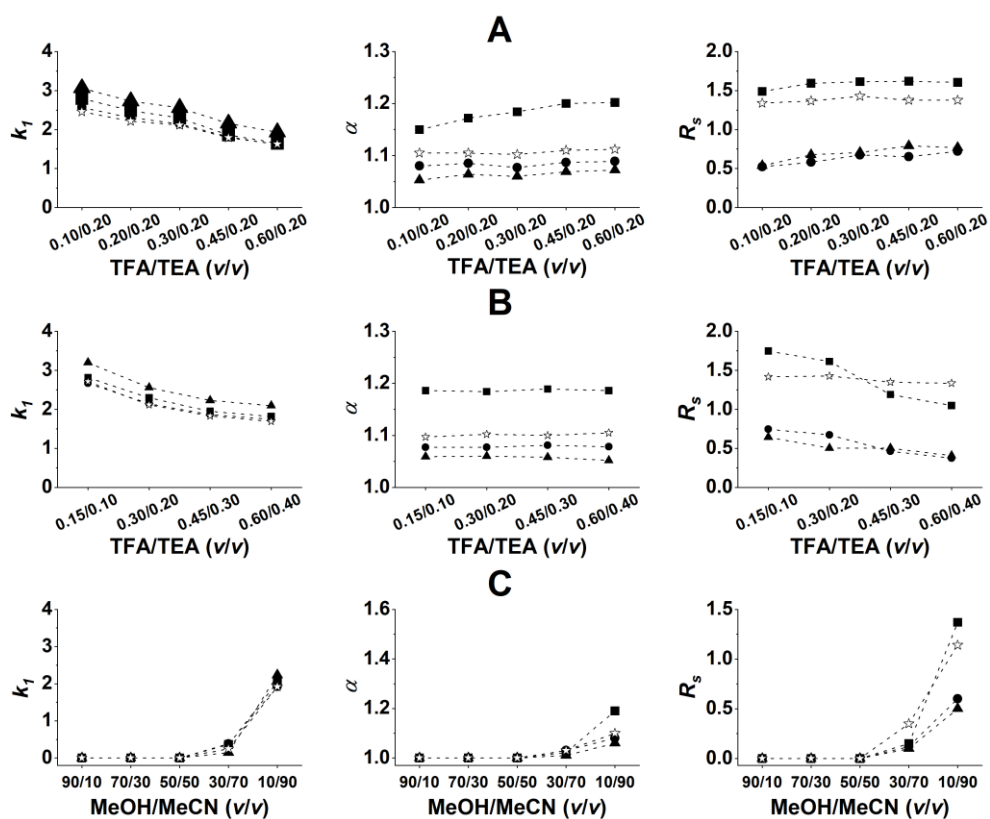


Figure A4. Effect of the eluent composition on LarihcShell-P column

Chromatographic conditions: column: **CF6-P-3.0**; mobile phase: **A, B**: MeOH/MeCN 10/90 (v/v) containing TFA/TEA; **C**: MeOH/MeCN containing TFA/TEA 0.3/0.2 (v/v); flow rate: 0.3 ml/min, temperature: 20 °C; symbols for analytes, *BPA-1* ■, *BPA-2* ●, *BPA-3* ▲, and *BPA-7* ☆

Table A1. Chromatographic data of β^2 -amino acids on TeicoShell column in different eluent systems

Analyte	Eluent system	k_I	α	R_S
<i>B2-1</i>	A	0.40	1.30	1.01
	B	0.65	1.16	0.65
	C	2.69	1.12	0.45
<i>B2-2</i>	A	0.34	1.50	1.42
	B	0.53	1.36	1.32
	C	1.95	1.23	0.70
<i>B2-3</i>	A	0.34	1.75	2.48
	B	0.47	1.49	1.15
	C	1.78	1.32	1.30
<i>B2-4</i>	A	0.33	1.76	2.07
	B	0.49	1.46	1.16
	C	1.48	1.29	1.17
<i>B2-5</i>	A	0.30	1.86	1.71
	B	0.44	1.50	0.78
	C	1.40	1.35	0.95
<i>B2-6</i>	A	0.28	2.03	2.50
	B	0.43	1.55	1.21
	C	1.32	1.34	1.39
<i>B2-7</i>	A	0.27	1.81	1.97
	B	0.47	1.43	1.03
	C	1.09	1.28	1.04
<i>B2-8</i>	A	1.10	1.59	2.05
	B	0.57	1.38	0.91
	C	1.37	1.26	0.95
<i>B2-9</i>	A	0.82	1.36	1.75
	B	0.62	1.48	1.99
	C	2.13	1.31	1.42
<i>B2-10</i>	A	0.97	1.50	1.74
	B	0.62	1.69	2.77
	C	1.88	1.43	1.76
<i>B2-11</i>	A	0.90	1.32	1.24
	B	0.64	1.39	1.70
	C	2.04	1.24	1.12
<i>B2-12</i>	A	2.37	1.12	0.40
	B	1.57	1.17	1.27
	C	2.63	1.24	1.07
<i>B2-13</i>	A	0.89	1.23	1.03
	B	0.73	1.18	1.32
	C	2.36	1.12	0.58
<i>B2-14</i>	A	0.84	1.30	1.08
	B	0.67	1.46	1.84
	C	2.14	1.28	1.23

Table A1. (continued) Chromatographic data of β^2 -amino acids on TeicoShell column in different eluent systems

Analyte	Eluent system	k_I	α	R_S
B2-15	A	0.86	1.40	1.57
	B	0.59	1.50	3.10
	C	2.31	1.36	1.38
B2-16	A	1.08	1.25	1.06
	B	0.68	1.34	1.51
	C	2.12	1.19	0.92
B2-17	A	1.00	1.32	1.33
	B	0.67	1.45	1.82
	C	2.64	1.24	0.90
B2-18	A	1.19	1.35	1.58
	B	0.74	1.47	2.09
	C	2.37	1.32	1.48
B2-19	A	1.17	1.45	1.98
	B	0.75	1.64	2.71
	C	2.27	1.36	1.55

Chromatographic conditions: column: **T-3.0**; mobile phase: **A**: H₂O/MeOH 30/70 (v/v), **B**: H₂O/MeOH 30/70 (v/v) containing 20 mM TEAA, pH_a = 5.0, **C**: MeCN/MeOH 30/70 (v/v) containing 2.5 mM TEA and 5.0 mM AcOH; flow rate: 0.3 ml/min, temperature: 20 °C

Table A2. Chromatographic data of β^2 -amino acids on TagShell column in different eluent systems

Analyte	Eluent system	k_I	α	R_S
B2-1	A	0.53	1.30	1.05
	B	0.63	1.29	0.87
	C	2.87	1.15	0.40
B2-2	A	0.50	1.54	1.35
	B	0.48	1.47	0.75
	C	1.82	1.50	0.36
B2-3	A	0.47	1.80	2.66
	B	0.33	1.63	1.22
	C	1.49	1.63	1.71
B2-4	A	0.51	1.70	1.25
	B	0.33	1.60	1.20
	C	1.37	1.60	1.70
B2-5	A	0.45	1.90	1.35
	B	0.26	1.69	0.85
	C	1.02	1.73	1.37
B2-6	A	0.46	2.06	2.39
	B	0.22	1.74	1.30
	C	1.15	1.82	2.02

Table A2. (continued) Chromatographic data of β^2 -amino acids on TagShell column in different eluent systems

Analyte	Eluent system	k_I	α	R_S
B2-7	A	0.66	1.64	1.80
	B	0.28	1.62	1.14
	C	1.08	1.60	1.77
B2-8	A	0.46	1.62	1.17
	B	0.38	1.54	0.81
	C	1.55	1.56	1.75
B2-9	A	1.00	1.49	1.82
	B	0.91	1.49	1.94
	C	2.38	1.38	1.25
B2-10	A	1.19	1.73	2.83
	B	1.10	1.74	3.02
	C	2.05	1.71	2.06
B2-11	A	1.12	1.43	1.68
	B	1.02	1.41	1.78
	C	2.27	1.35	1.11
B2-12	A	1.84	1.17	0.42
	B	2.01	1.18	0.76
	C	2.62	1.33	1.06
B2-13	A	1.39	1.25	1.08
	B	1.33	1.26	1.22
	C	3.04	1.15	0.52
B2-14	A	0.83	1.48	1.89
	B	0.95	1.96	3.32
	C	2.63	1.43	1.38
B2-15	A	0.82	2.10	2.58
	B	n.d.	n.d.	n.d.
	C	n.d.	n.d.	n.d.
B2-16	A	1.12	1.37	1.48
	B	1.07	1.36	1.63
	C	2.32	1.30	1.00
B2-17	A	0.92	2.00	2.91
	B	0.93	1.93	3.16
	C	2.91	1.70	2.14
B2-18	A	1.05	1.73	2.72
	B	1.07	1.66	2.75
	C	2.50	1.55	1.68
B2-19	A	1.53	1.75	2.77
	B	1.62	1.73	2.97
	C	2.95	1.53	1.50

Chromatographic conditions: column: **TAG-3.0**; mobile phases: **A**: H₂O/MeOH 30/70 (v/v), **B**: H₂O/MeOH 30/70 (v/v) containing 20 mM TEAA, pH_a = 5.0, **C**: MeCN/MeOH 30/70 (v/v) containing 2.5 mM TEA and 5.0 mM AcOH; flow rate: 0.3 ml/min; temperature: 20 °C, n.d.: no data available

Table A3. Chromatographic data of α -substituted proline analogs on different columns

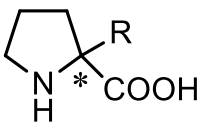
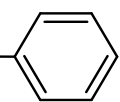
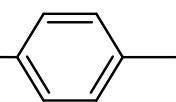
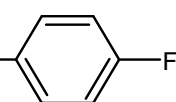
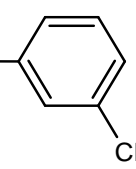
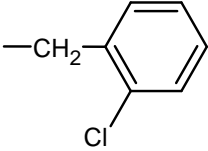
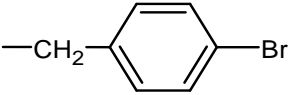
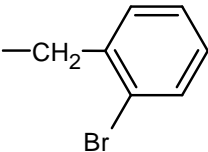
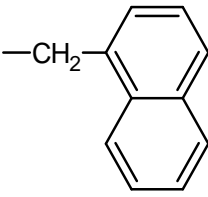
Analyte (R)	Column	<i>k</i> _I	α	<i>R</i> _S
				
Pr-1 —H	V-3.0	1.04	1.27	1.26
	T-3.0	7.56	1.00	0.00
	TAG-3.0	9.74	1.00	0.00
	N-3.0	0.64	1.00	0.00
Pr-2 —CH ₃	V-3.0	0.57	1.00	0.00
	T-3.0	8.15	1.46	1.65
	TAG-3.0	9.19	1.41	2.52
	N-3.0	0.38	1.00	0.00
Pr-3 —CH ₂ —CH ₂ —CH ₃	V-3.0	0.31	1.00	0.00
	T-3.0	7.64	1.00	0.00
	TAG-3.0	2.54	2.32	1.90
	N-3.0	0.25	1.00	0.00
Pr-4 —CH ₂ —CH=CH ₂	V-3.0	0.37	1.00	0.00
	T-3.0	4.59	1.31	1.62
	TAG-3.0	4.56	1.07	0.21
	N-3.0	0.16	1.62	0.92
Pr-5 —CH ₂ — 	V-3.0	0.51	3.03	3.62
	T-3.0	1.93	1.08	<0.10
	TAG-3.0	2.24	1.53	1.90
	N-3.0	0.26	1.71	1.67
Pr-6 —CH ₂ — 	V-3.0	0.40	2.96	3.68
	T-3.0	1.88	1.13	0.71
	TAG-3.0	2.31	1.67	2.16
	N-3.0	0.15	1.98	1.96
Pr-7 —CH ₂ — 	V-3.0	0.52	1.52	1.49
	T-3.0	1.74	1.10	0.15
	TAG-3.0	2.04	1.34	1.22
	N-3.0	0.29	1.50	1.32
Pr-8 —CH ₂ — 	V-3.0	0.55	2.34	3.36
	T-3.0	1.49	1.13	0.18
	TAG-3.0	2.10	1.18	0.60
	N-3.0	0.30	1.59	1.80

Table A3. (continued) Chromatographic data of α -substituted proline analogs on different columns

Analyte (R)	Column	<i>k</i> _I	α	<i>R</i> _S
Pr-9 	V-3.0	0.48	1.52	0.96
	T-3.0	1.70	1.00	0.00
	TAG-3.0	3.49	1.17	0.55
	N-3.0	0.28	1.43	0.89
Pr-10 	V-3.0	0.74	1.54	1.66
	T-3.0	1.69	1.14	0.40
	TAG-3.0	2.66	1.36	1.28
	N-3.0	0.37	1.44	1.37
Pr-11 	V-3.0	0.59	1.33	0.80
	T-3.0	2.68	1.00	0.00
	TAG-3.0	4.22	1.24	0.85
	N-3.0	0.29	1.60	1.22
Pr-12 	V-3.0	0.77	2.31	2.87
	T-3.0	2.89	1.00	0.00
	TAG-3.0	5.18	1.42	1.39
	N-3.0	0.38	1.56	1.62

Chromatographic conditions: columns: **V-3.0**, **T-3.0**, **TAG-3.0** and **N-3.0**; mobile phase: 100% MeOH containing 20 mM AcOH; flow rate: 0.3 ml/min; detection: MS

Table A4. Chromatographic data of α -substituted proline analogs on different columns

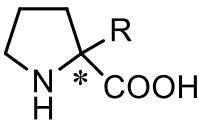
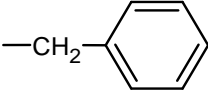
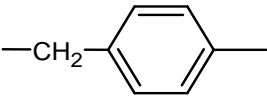
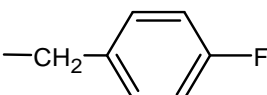
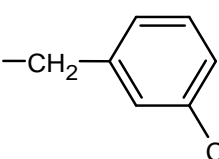
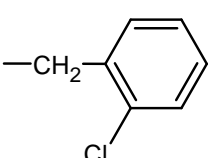
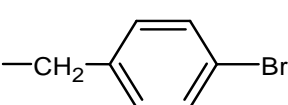
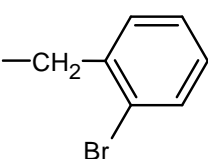
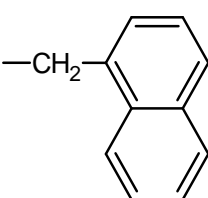
Analyte (R)	Column	<i>k</i> _I	α	<i>R</i> _S
				
Pr-4 $-\text{CH}_2-\text{CH}=\text{CH}_2$	V-3.0	0.48	3.13	6.45
	T-3.0	1.81	1.04	0.10
	TAG-3.0	2.05	1.41	2.17
	N-3.0	0.23	1.54	1.21

Table A4. (continued) Chromatographic data of α -substituted proline analogs on different columns

Analyte (R)	Column	<i>k</i> _I	α	<i>R</i> _S
Pr-5 	V-3.0	0.51	2.99	5.62
	T-3.0	1.92	1.07	0.25
	TAG-3.0	2.06	1.51	1.79
	N-3.0	0.28	1.41	1.04
Pr-6 	V-3.0	0.44	2.82	4.95
	T-3.0	1.92	1.07	0.25
	TAG-3.0	2.06	1.71	2.22
	N-3.0	0.28	1.41	0.92
Pr-7 	V-3.0	0.51	1.41	1.30
	T-3.0	1.23	1.00	0.00
	TAG-3.0	1.58	1.24	0.48
	N-3.0	0.28	1.00	0.00
Pr-8 	V-3.0	0.54	2.12	2.54
	T-3.0	0.98	1.15	0.40
	TAG-3.0	1.81	1.00	0.00
	N-3.0	0.32	1.00	0.00
Pr-9 	V-3.0	0.50	1.41	0.71
	T-3.0	1.73	1.00	0.00
	TAG-3.0	3.16	1.00	0.00
	N-3.0	0.28	1.00	0.00
Pr-10 	V-3.0	0.75	1.43	1.79
	T-3.0	1.96	1.05	< 0.10
	TAG-3.0	2.35	1.33	1.18
	N-3.0	0.39	1.21	0.66
Pr-11 	V-3.0	0.79	1.00	0.00
	T-3.0	2.03	1.00	0.00
	TAG-3.0	4.01	1.00	0.00
	N-3.0	0.35	1.00	0.00
Pr-12 	V-3.0	0.88	1.91	1.18
	T-3.0	2.52	1.00	0.00
	TAG-3.0	4.45	1.29	0.55
	N-3.0	0.47	1.00	0.00

Chromatographic conditions: columns: **V-3.0**, **T-3.0**, **TAG-3.0** and **N-3.0**; mobile phase: 100% MeOH containing 20 mM TEAA; flow rate: 0.3 ml/min; detection: PDA, 258-282 nm

Table A5. Effects of eluent composition on the thermodynamic parameters of analytes **BPA-2–5** on VancoShell column

Analyte	Temp. range (°C)	$-\Delta(\Delta H^0)$ (kJ/mol)	$-\Delta(\Delta S^0)$ (J/(mol × K))	$-\Delta(\Delta G^0)_{298K}$ (kJ/mol)	Q
A mobile phase (H₂O/MeOH)					
		70/30	10/90	70/30	10/90
BPA-2	5–50	5.69	4.26	14.64	10.04
BPA-3	5–50	3.23	3.04	8.80	8.28
BPA-4	5–40	1.72	–	4.67	–
BPA-5	5–30	2.28	–	6.55	–
B mobile phase (H₂O/MeCN)					
		70/30	10/90	70/30	10/90
BPA-2	5–50	7.16	4.62	19.62	13.12
BPA-3	5–50	3.79	2.33	10.50	6.58
BPA-4	5–50	3.94*	1.19	12.85*	3.28
BPA-5	5–50	–	0.80	–	2.27
C mobile phase (MeOH/MeCN)					
		70/30	30/70	70/30	30/70
BPA-2	10–50	2.54	2.56	6.41	6.81
BPA-3	5–50	1.39	1.53	3.66	4.02

Chromatographic conditions: column: **V-3.0**; mobile phase: **A**: H₂O/MeOH 70/30 (v/v) and H₂O/MeOH 10/90 (v/v), **B**: H₂O/MeCN 70/30 (v/v) and H₂O/MeCN 10/90 (v/v), **C**: MeOH/MeCN 70/30 (v/v) and MeOH/MeCN 30/70 (v/v), all containing 0.1% TEAA; T_{iso} : temperature where the enantioselectivity cancels; $Q = \Delta(\Delta H^0)/[298 \times \Delta(\Delta S^0)]$; * temperature range: 5–25 °C

Table A6. Thermodynamic parameters, $-\Delta(\Delta H^0)$, $-\Delta(\Delta S^0)$, $-\Delta(\Delta G^0)$, correlation coefficient (R^2), T_{iso} and Q values of analytes **Pr-1–12** on VancoShell and TagShell columns

Analyte	$-\Delta(\Delta H^0)$ (kJ/mol)	$-\Delta(\Delta S^0)$ (J/(mol \times K))	$-\Delta(\Delta G^0)_{298K}$ (kJ/mol)	<i>Corr. coeff.</i> R^2	Q
V-3.0					
Pr-1	2.43	6.29	0.56	0.992	1.29
Pr-5	9.89	24.71	2.52	0.995	1.34
Pr-6	10.80	27.91	2.48	0.992	1.30
Pr-7	4.21	10.97	0.94	0.989	1.29
Pr-8	8.60	22.31	1.95	0.993	1.29
Pr-9	6.14	17.65	0.88	0.970	1.17
Pr-10	5.19	14.22	0.95	0.992	1.23
Pr-11	5.36	15.86	0.63	0.985	1.13
Pr-12	8.92	23.64	1.87	0.991	1.27
TAG-3.0					
Pr-2	2.15	4.69	0.75	0.993	1.53
Pr-3	4.00	6.70	2.00	0.996	2.00
Pr-4	−1.15	−4.46	0.16	0.994	0.86
Pr-5	5.65	15.74	0.96	0.998	1.21
Pr-6	6.45	17.68	1.18	0.999	1.22
Pr-7	3.80	10.50	0.67	0.998	1.22
Pr-8	4.32	13.35	0.34	0.999	1.09
Pr-9	2.93	8.81	0.31	0.999	1.12
Pr-10	4.05	11.28	0.68	0.999	1.20
Pr-11	3.06	8.76	0.45	0.993	1.17
Pr-12	4.35	12.03	0.77	0.991	1.21

Chromatographic conditions: columns: **V-3.0** and **TAG-3.0**; mobile phase: MeOH containing 20 mM AcOH; R^2 , correlation coefficient of van't Hoff plots, $\ln \alpha$ vs. $1/T$ curves; T_{iso} , temperature, where the enantioselectivity cancels; $Q = \Delta(\Delta H^0)/[298 \times \Delta(\Delta S^0)]$; temperature range: 5–50 °C; enantiomers of analytes **2**, **3** and **4** while of analyte **1** were not separable on **V-3.0** and **TAG-3** CSPs, respectively

Publications related to the thesis



Enantioseparation of β^2 -amino acids by liquid chromatography using core-shell chiral stationary phases based on teicoplanin and teicoplanin aglycone

Dániel Tanács^a, Róbert Berkecz^a, Aleksandra Misicka^b, Dagmara Tymecka^b, Ferenc Fülöp^c, Daniel W. Armstrong^d, István Ilisz^{a,*}, Antal Péter^a

^a Institute of Pharmaceutical Analysis, Interdisciplinary Excellence Centre, University of Szeged, Somogyi B. u. 4, H-6720 Szeged, Hungary

^b Department of Chemistry, University of Warsaw, Pasteura str. 1, 02-093 Warsaw, Poland

^c Institute of Pharmaceutical Chemistry, University of Szeged, Eötvös utca 6, H-6720 Szeged, Hungary

^d Department of Chemistry and Biochemistry, University of Texas at Arlington, Arlington, TX 76019-0065, USA

ARTICLE INFO

Article history:

Received 30 April 2021

Revised 18 June 2021

Accepted 28 June 2021

Available online 5 July 2021

Keywords:

β^2 -amino acids
liquid chromatography
macrocytic glycopeptide-based chiral
stationary phases
kinetic and thermodynamic
characterization, core-shell particles

ABSTRACT

Enantioseparation of nineteen β^2 -amino acids has been performed by liquid chromatography on chiral stationary phases based on native teicoplanin and teicoplanin aglycone covalently bonded to 2.7 μ m superficially porous silica particles. Separations were carried out in unbuffered (water/methanol), buffered [aqueous triethylammonium acetate (TEAA)/methanol] reversed-phase (RP) mode, and in polar ionic (TEAA containing acetonitrile/methanol) mobile phases. Effects of pH in the RP mode, acid and salt additives, as well as counter-ion concentrations on chromatographic parameters have been studied. The structure of selectands (β^2 -amino acids possessing aliphatic or aromatic side chains) and selectors (native teicoplanin or teicoplanin aglycone) was found to have a considerable influence on separation performance. Analysis of van Deemter plots and determination of thermodynamic parameters were performed to further explore details of the separation performance.

© 2021 The Author(s). Published by Elsevier B.V.

This is an open access article under the CC BY license (<http://creativecommons.org/licenses/by/4.0/>)

1. Introduction

In the past decade, considerable interest has been paid to peptides containing β -amino acids (β -peptides). With an additional carbon atom between the amino and carboxylic groups, these β -amino acids can adopt various stable secondary structures with further functionalization possibilities enhancing the number of potential applications [1]. Unlike their analogs, these β -amino acids are not readily susceptible to hydrolysis or enzymatic degradation. Consequently, peptides with incorporated β -amino acids exhibit enhanced stability [2]. Additionally, chimeric peptides (mixed α - and β -peptides) consisting of α - and β -amino acids are of considerable interest as peptidomimetics in an increasing range of therapeutic applications [3,4]. Depending on the position of the side chain on the 3-aminoalkanoic acid skeleton β^2 - and β^3 -amino acids can be differentiated. The syntheses of β^2 -amino acids in enantiomerically pure form are much more challenging than their β^3 -

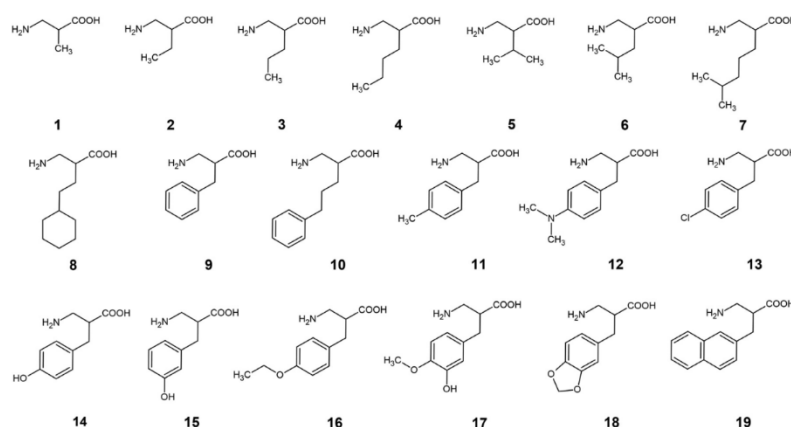
analogues [5]. The synthesis of β^2 -amino acids in racemic form and their subsequent enantioseparation currently is the most practical and effective approach to obtain enantiopure β^2 -amino acids. Chromatographic data related to the separation and identification of β^2 -amino acid enantiomers have been reported in the literature [6–8]. However, relatively little information is available on the separation of β^2 -amino acid enantiomers. The enantioseparation of a few β^2 -amino acids have recently been carried out by direct high-performance liquid chromatography (HPLC) methods on chiral stationary phases (CSPs) based on (+)-(18-crown-6)-2,3,11,12-tetracarboxylic acid [9,10], macrocyclic glycopeptides [11,12], and Cinchona alkaloids [13,14].

Core-shell particles (superficially porous particles, SPPs) and sub-2 μ m fully porous particles (FPPs) are expected to provide high-throughput and effective separations of a variety of chiral molecules in ultra-high-performance liquid chromatography (UHPLC). Teicoplanin, teicoplanin aglycone, vancomycin, or isopropylcyclofructan covalently bonded to sub-2 μ m or 2.7 μ m SPPs were successfully applied for the enantioseparation of native and *N*-protected α -amino acids and small peptides under LC [15–18], and supercritical fluid chromatography (SFC) conditions [19,20]. Te-

* Corresponding author: István Ilisz, Institute of Pharmaceutical Analysis, University of Szeged, Somogyi B. u. 4, H-6720 Szeged, Hungary
E-mail address: ilisztan@szte.hu (I. Ilisz).

<https://doi.org/10.1016/j.chroma.2021.462383>

0021-9673/© 2021 The Author(s). Published by Elsevier B.V. This is an open access article under the CC BY license (<http://creativecommons.org/licenses/by/4.0/>)

Figure 1. Structure of β^2 -amino acids

icoplanin and teicoplanin aglycone covalently attached to 1.9 μm FPP silica gel with narrow size distribution exhibited excellent separation performances for native proteinogenic amino acids in both LC and SFC modalities [21]. The new synthetic route developed for bonding teicoplanin to sub-2 μm or 2.7 μm SPPs and to sub-2 μm FPPs endowed the selector with a zwitterionic character [22,23]. Ion-exchange-type CSPs are also being developed for UHPLC purposes. For example, *tert*-butylcarbamoyl(8 *S*,9 *R*)-quinine was covalently bonded to 1.9 μm [22] or to 2.7 μm [24–30] SPPs, and to 3.0 μm and 1.7 μm FPPs [28]. Lämmerhofer *et al.* [30] in chiral \times chiral two-dimensional UHPLC applied *tert*-butylcarbamoyl(8 *S*,9 *R*)-quinine and *tert*-butylcarbamoyl(8 *R*,9 *S*)-quinidine selectors bonded to 2.7 μm SPPs for the separation of enantiomers of native proteinogenic α -amino acids after peptide hydrolysis. A survey of literature data revealed that enantioseparations under UHPLC conditions were performed for proteinogenic α -amino acids with the only exceptions being the enantioseparation of γ -aminobutyric acid [27] and β -Ala [28,34].

The present study provides results for the utilization of CSPs based on macrocyclic glycopeptides covalently bonded to 2.7 μm SPPs for the enantioseparation of 19 unusual β^2 -amino acids. Experiments were performed utilizing columns with 3.0 and 2.1 mm internal diameter (i.d.) based on teicoplanin- and teicoplanin aglycone. RP and polar-ionic mobile phases were applied in separations. Effects of the nature and concentration of the mobile phase components, acid and salt additives under various conditions, and pH in reversed-phase (RP) mode were studied. To gain detailed information about the chiral recognition process, structure-retention (selectivity) relationships were evaluated by taking into account the structural features of both the analytes and selectors. Analysis of van Deemter plots served as a basis for the kinetic investigations, while the temperature dependence study allowed thermodynamic characterization. In a few cases, elution sequences also were determined.

2. Experimental

2.1. Chemicals and materials

Nineteen racemic amino acids (1–19) were synthesized as described earlier [13]. (For structures see Fig. 1). Enantiomers (*R*)-2,

(*S*)-5 and (*S*)-6 were generous gifts from Prof. D. Tourwé (Vrije Universiteit Brussels, Brussels, Belgium).

Methanol (MeOH), acetonitrile (MeCN), and water of LC-MS grade, NH_3 dissolved in MeOH, triethylamine (TEA), formic acid (FA), glacial acetic acid (AcOH), ammonium formate (HCO_2NH_4), and ammonium acetate (NH_4OAc) of analytical reagent grade were from VWR International (Radnor, PA, USA). The pH reported for the reversed-phase mobile phase is the apparent pH (pH_a), which was adjusted directly in the aqueous triethylammonium acetate (TEAA)/MeOH solutions with the addition of AcOH.

2.2. Apparatus and chromatography

LC measurements were carried out on a Waters® ACQUITY UPLC® H-Class PLUS System with Empower 3 software (Waters) and components as follows: quaternary solvent manager, sample manager FTN-H, column manager, PDA detector, and QDa mass spectrometer detector. The parameters for the QDa detector were set as follows: positive ion mode, probe temperature, 600 $^\circ\text{C}$, capillary voltage, 1.5 V, cone voltage, 20 V.

Chiral columns, based on teicoplanin (TeicoShell, **T**) and teicoplanin aglycone (TagShell, **TAG**) attached covalently to the surface of 2.7 μm SPPs, were applied in this study. The core diameter and shell thickness of the SPPs were 1.7 μm and 0.5 μm , respectively. All columns (AZYP, LLC, Arlington, TX, USA) have 100 \times 3.0 mm i.d. or 100 \times 2.1 mm i.d. dimensions (abbreviations for columns: **T-3.0** and **T-2.1**; **Tag-3.0** and **Tag-2.1**).

Stock solutions of analytes (1–10 mg ml^{-1}) were prepared in MeOH and diluted with the mobile phase. The dead-time (t_0) of the columns was determined by 0.1% AcOH dissolved in MeOH and detected at 210 or 256 nm. In all experiments a flow rate of 0.3 ml min^{-1} provided efficiency and fast analysis for both column dimensions, while the column temperature was set at 20 $^\circ\text{C}$ (if not otherwise stated).

3. Results and discussion

Based on their side chain, the investigated β^2 -amino acids can be divided into two sub-groups: those that contain an aliphatic moiety or an aromatic moiety. The branch or the length of the aliphatic moiety or the nature and position of substituents on the

aromatic ring influences the size and polarity of the molecule and is expected to have a considerable effect on selector–analyte interactions.

3.1. Effect of pH on retention and separation performance

The pK value of carboxylic groups of teicoplanin and teicoplanin aglycone (playing important role in the retention mechanism) is approximately 2.5. The pK values of the amino groups of β^2 -amino acids **1–19** are in the range 10.16–10.32. The corresponding values for the carboxylic moieties of **1–12**, **19** are between 4.10–4.50, whereas for **13–18** they are between 3.20–3.60 (calculated with Marvin Sketch v. 17.28 software, ChemAxon Ltd., Budapest). Therefore, the charge of macrocyclic glycopeptide-based stationary phases and analytes is sensitive to pH and alters the interactions between the CSP and the analyte. To reveal the possible effects of pH_a on retention, selectivity, and resolution of β^2 -amino acids bearing aliphatic (**3**) and aromatic side chain (**9**) were selected and their retention behavior was investigated on **T-3.0** and **TAG-3.0** columns in the RP mode applying eluents consisting of *aq*.TEAA/MeOH (90/10 v/v and 30/70 v/v) with a constant TEAA concentration of 20.0 mM and varying pH_a of the mobile phase between pH_a 3.5–6.5. Under the studied conditions, the retention factors of the first eluting enantiomer (k_1) usually changed slightly with increasing pH_a for both analytes, and only analyte **9** exhibited moderate increases in the *aq*.TEAA/MeOH 30/70 (v/v) eluent (Fig. S1). Interestingly, α and R_s increased more significantly in both mobile phase systems, especially for analyte **3**, with the highest values obtained above pH_a 5.0 (Fig. S1). Based on their pK values, teicoplanin, teicoplanin aglycone, and β^2 -amino acids are present in ionized form under these mobile phase conditions. That is, the observed behavior is probably due to increased ionic interactions between the protonated amino group of the analyte and the deprotonated carboxylic group of the selector. The ionic structures affect either directly the Coulombic or dipolar interactions between the analyte and selector, or influence indirectly the retention by changing the conformation of the macrocyclic glycopeptides. To obtain the highest resolution and selectivity an eluent pH_a of 5.0 or above can be recommended for the enantioseparation of β^2 -amino acids.

3.2. Effects of mobile phase composition on the chromatographic performance

Employing analytes **3** and **9**, first, the effects of five different mobile phase additives (salts or acids, namely HCO₂NH₄, NH₄OAc, TEAA, FA, and AcOH) were studied on the chromatographic performance of **T-3.0** and **TAG-3.0** CSPs. Experiments were performed with a constant aqueous to organic solvent ratio (H₂O/MeOH 90/10 v/v) and a constant additive concentration (20.0 mM, calculated for the whole eluent system). In the case of organic salts, the pH_a was adjusted to 5.0 by the addition of the corresponding acid. Mobile phases containing solely 20.0 mM FA or AcOH (without pH adjustment) resulted in unresolved peaks with rather poor peak shapes (Fig. S2). In contrast, when HCO₂NH₄, NH₄OAc or TEAA were used as mobile phase additive, resolution could be obtained. Employing TEAA has led to symmetrical peak shapes, very good efficiencies, and selectivities. Therefore, in further experiments, TEAA was the favored mobile phase additive. It is worth mentioning that regarding MS-based detection, NH₄OAc offers higher sensitivity with acceptable peak shapes and resolution.

MeOH and MeCN organic modifiers are used commonly in amino acid separations [9]. The nature and concentration of the mobile phase components can exert considerable effects on retention and separation. Therefore, we next investigated the effects of organic modifiers on the enantioseparation of analytes **3**

and **9** utilizing **T-3.0** and **TAG-3.0** CSPs. Figure 2 shows the chromatographic figures of merit for the separations of analytes **3** and **9** in three different eluent systems. In unbuffered RP mode (**a**), mobile phase compositions of H₂O/MeOH 90/10–10/90 (v/v), in buffered RP mode (**b**), *aq*.TEAA/MeOH 90/10–30/70 (v/v) containing 20 mM TEAA and pH_a 5.0, and in polar-ionic mode (**c**), MeCN/MeOH 90/10–10/90 (v/v) containing 20 mM TEAA were applied.

In the unbuffered eluent system (Fig. 2 A), k_1 increases with increasing MeOH content, however, not in the whole range studied. The observed phenomenon is at least partly for the lower solubility of amino acids with polar character in the less polar MeOH. The observed minimum in the curve for analyte **9** indicates an increased hydrophobic interaction at higher water content. Regarding α and R_s values, they increase with increasing MeOH content. Interestingly, comparing the two CSPs, k_1 values were higher on the **T-3.0** column, while higher α and R_s values were registered on **TAG-3.0**, which may indicate reduced nonselective interactions in the latter case.

Under buffered RP conditions (Fig. 2B), similar to the unbuffered eluents, a slight increase in k_1 , α , and R_s values was registered with increasing MeOH content. As an exception, analyte **9** on the **TAG-3.0** column first showed a moderate increase, then a slight decrease for k_1 . Comparing these two eluent systems, a remarkable difference between chromatographic performances can be noted. In the presence of TEAA, higher α and R_s values are obtained with significantly lower retentions, suggesting a pronounced suppression of nonselective interactions between the analytes and the stationary phase by the salt addition.

The results obtained with the application of mixtures of MeCN and MeOH along with acid and base additives in the polar-ionic mode are depicted in Fig. 2 C. With variation in the composition of the eluent the acid–base equilibrium and proton activity will be changed. At high MeCN content, the solvation of polar amino acids in the aprotic solvent decreases resulting in high retentions, while the increasing ratio of protic MeOH favors the solvation of polar amino acids, i.e., retention decreases. The change of α and R_s values exhibited trends similar to those discussed above. The improved selectivity with increasing MeOH content suggests that hydrogen bonding may not play a major role in these enantioseparations.

3.3. Effects of the counter-ion concentration

The stoichiometric displacement model [31] is applied frequently to describe the retention behavior based on ion-pairing and ion-exchange mechanisms, predicting a linear relationship between the logarithm of the retention factor and the logarithm of the counter-ion concentration,

$$\log k = \log K_2 - Z \log c_{\text{counter-ion}} \quad (1)$$

where Z is the ratio of the number of charges of the cation and the counter-ion, while K_2 describes the ion-exchange equilibrium. If an ion-exchange mechanism exists, plotting $\log k$ against $\log c_{\text{counter-ion}}$ will result in a straight line with a slope proportional to the effective charge during the ion-exchange process, while the intercept provides information about the equilibrium constant.

To probe the potency of the simple displacement model in our case, experiments were carried out on **T-3.0** and **TAG-3.0** CSPs applying mobile phases **b**, *aq*.TEAA/MeOH (90/10 v/v, pH_a ≈ 5.5) and **c**, MeCN/MeOH (10/90 v/v) both containing 5.0–160 mM TEAA. In a cation exchange process in the presence of TEAA, the protonated triethylammonium ion acts as a competitor. The results presented in Fig. 3, definitely indicate the applicability of the stoichiometric displacement model, i.e., they support the involvement of ion-interaction processes in the retention mechanism. In

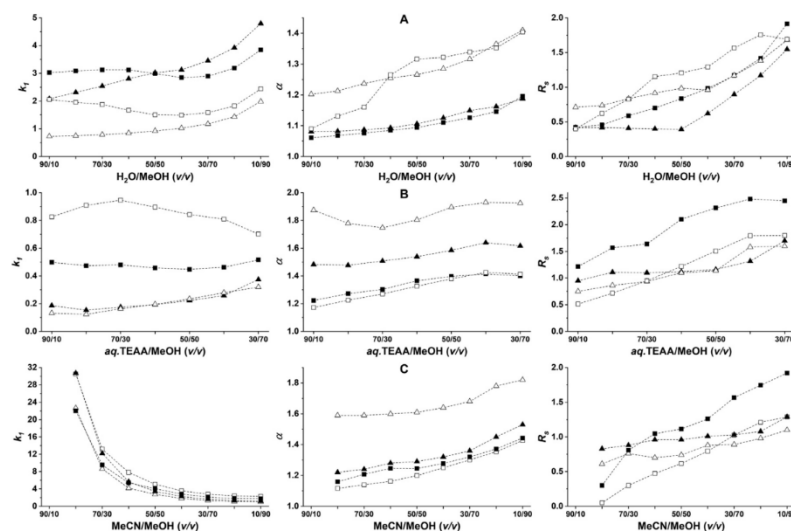


Figure 2. Effect of bulk solvent composition on chromatographic parameters for analyte **3** and **9** applying different mobile phase systems. Chromatographic conditions: column, T-3.0 and TAG-3.0; mobile phase, **a**, $\text{H}_2\text{O}/\text{MeOH}$ (90/10–10/90 v/v), **b**, $\text{aq.TEAA}/\text{MeOH}$ (90/10–30/70 v/v), concentration of TEAA in mobile phase 20.0 mM and the actual pH of the mobile phase, pH_i 5.0, **c**, MeCN/MeCN (90/10–10/90 v/v), concentration of TEAA in mobile phase, 20.0 mM; flow rate, 0.3 ml min⁻¹; detection, 210–258 nm; temperature, 20 °C; symbols, on T-3.0 for analyte **3**, \blacksquare , for analyte **9**, \square , on TAG-3.0 for analyte **3**, \blacktriangle , for analyte **9**, \triangle .

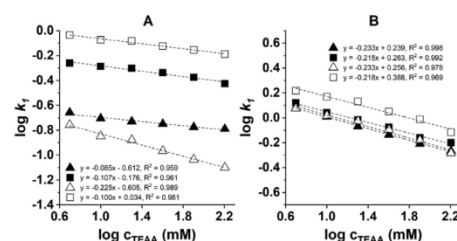


Figure 3. Effect of ion content on retention factor of the first eluting enantiomer, k_1 , for analytes **3** and **9**. Chromatographic conditions: column, T-3.0 and TAG-3.0; mobile phase, **A**, $\text{aq.TEAA}/\text{MeOH}$ (90/10 v/v), concentration of TEAA in mobile phase, 5.0–160 mM, **B**, MeCN/MeOH (10/90 v/v), concentration of TEAA in mobile phase, 5.0–160 mM; flow rate, 0.3 ml min⁻¹; detection, 210–258 nm; temperature, 20 °C; symbols, on T-3.0 for analyte **3**, \blacksquare , for analyte **9**, \square , on TAG-3.0 for analyte **3**, \blacktriangle , for analyte **9**, \triangle .

this study, linear relationships were found between $\log k_1$ vs. $\log c_{\text{counter-ion}}$, with slopes varying between about (–0.10) and (–0.23). In an earlier study, slopes around –1.0 were found for strong ion-exchangers, where the selector and selectand act in almost fully ionized form [32]. In absolute terms, the smaller slopes observed reveal a marked difference between the strong and weak ion-exchanger-based CSPs [33]. In the case of weak ion-exchanger CSPs, the retention (affected by the pH and the ionic state of the selector and analyte) can be reduced with the enhancement of the counter-ion concentration, but only to a limited range. It is worth mentioning that on both CSPs, practically equal slopes were calculated for each enantiomer, i.e., no significant difference could be observed

in the enantioselectivities with varying counter-ion concentration (data not shown).

3.4. Effects of structures of selector and analyte on retention and selectivity

The structure of both the chiral selector and the analyte affects considerably their interactions resulting in different retention and separation characteristics. To gain a set of chromatographic data, screening of the enantioseparation of 19 β^2 -amino acids was performed on four teicoplanin and teicoplanin aglycone-based columns in three different mobile phase systems: unbuffered RP (**a**, $\text{H}_2\text{O}/\text{MeOH}$ 30/70 v/v), buffered RP (**b**, $\text{aq.TEAA}/\text{MeOH}$ 30/70 v/v, containing 2.5 mM TEA and 5.0 mM AcOH, pH_i 5.5), and a polar-ionic mobile phase (**c**, MeCN/MeOH 30/70 v/v, containing 2.5 mM TEA and 5.0 mM AcOH). The related chromatographic data are summarized in Tables S1–S4. All studied β^2 -amino acids were baseline-separated on at least one CSP, and often with both CSPs within three to five minutes depending on the nature of analytes, mobile phase, and inner diameter of columns. The overall success rate of the enantioseparations is depicted in Fig. S3. Taking into account the time needed for the analyses, application of mobile phase **a** and **b** seemed to be more favorable (Tables S1–S4). It should be noted, that the analysis time obtained here is three to ten times lower than that observed earlier on 5 μm particles and 4.6 mm i.d. columns [10–13]. It was also observed that, in most cases, β^2 -amino acids possessing aliphatic side chains (analytes **1–8**) exhibited slightly smaller R_S values than analytes with aromatic side chains (**9–19**). This is in spite of their similar enantioselectivity ($1.30 < \alpha < 2.20$). For analytes **9–19**, in almost all cases, $R_S > 1.5$ was obtained on all four columns applied with any of the three mobile phase systems (exceptions were compounds **12** and **13**).

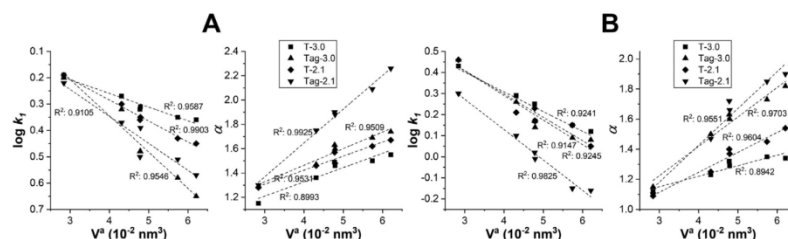


Figure 4. Dependence of retention factors of the first eluting enantiomer (k_1) and separation factors (α) of analytes 1–6 on the Meyer substituent parameter (V^0) Chromatographic conditions, column, T-3.0, T-2.1, TAG-3.0 and TAG-2.1; mobile phase, **A**, aq.TEAA/MeOH (30/70 v/v), concentration of TEA and AcOH in mobile phase 2.5 and 5.0 mM, respectively and the actual pH of the mobile phase, pH₅ 5.5, **B**, MeCN/MeOH (30/70 v/v), concentration of TEA and AcOH in mobile phase 2.5 and 5.0 mM, respectively; flow rate, 0.3 ml min⁻¹; detection, 210–258 nm; temperature, 20 °C; symbols, for T-3.0 ■, for TAG-3.0 ▲, for T-2.1 ● and for TAG-2.1 ▼.

In order to determine the specific structural effects of analytes possessing alkyl side chains on chromatographic data such as k_1 and α , the effect of the volume of the alkyl substituents (V^0) was investigated. The steric effect of a substituent on the reaction rate can be characterized by the size descriptor of the molecule, V^0 [34]. The V^0 values for Me, Et, Pr, Bu, 2-Pr, and 2-Bu moieties are 2.84, 4.31, 4.78, 4.79, 5.74, and $6.21 \times 10^{-2} \text{ nm}^3$, respectively. Note, that there are no V^0 values available for 6-methylheptanoic (7) and 5-cyclohexylpentanoic (8) moieties. Values of k_1 and α showed a good correlation with V^0 on all studied columns in all three eluent systems. As the data presented in Fig. 4 confirm the volume of the alkyl substituents markedly influenced k_1 : a bulkier substituent hindered the interactions between the selector and analyte leading to reduced retention. Since the difference in the interactions of the two enantiomeric analytes with the CSP differed considerably, an enhanced chiral recognition with higher V^0 values could be observed. It should be noted here, that not only the position and bulkiness of the substituent but also the steric effect may heavily influence retention behavior and chiral recognition of β^2 -amino acids.

Comparing the separation of analytes 9–19 possessing aromatic or substituted aromatic side chains to analytes 1–8, shows higher R_S values for analytes 9–19. In most cases, the R_S was above 1.5 and only analytes 12 and 13 exhibited poorer resolution (Table S1–S4). The most relevant and optimized data of separations are depicted in Table 1. The presence of an aromatic moiety instead of an aliphatic side chain in 9–19 probably improves π – π -interactions between the enantiomers and the chiral selector and contributes to better chiral recognition. Enantiomers of analyte 12 possessing an additional 4-dimethylamino moiety (pK_a 5.0, calculated with Marvin Sketch v. 17.28 software, ChemAxon Ltd., Budapest) were baseline-separated only in mobile phases **b** and **c**, where the ionic strength could be kept at a constant level.

Analytes 11, 13, and 14 possess a methyl, chlorine, or hydroxyl substituent at position 4 of the aromatic ring, giving π -basic or π -acidic character to the molecules. Figures 5 and S4 are chromatograms that illustrate the separation performance obtained on TAG-3.0 and T-3.0 CSPs in two different eluent systems. The methyl and chlorine moieties show slight effects on retention, selectivity, and resolution, while the hydroxyl moieties and their positions in analytes 14 vs. 15 affect considerably the separation performance. The 3-position of the hydroxyl moiety probably favors steric interactions between selector and analyte resulting in higher selectivity and resolution, in particular, on the TAG-3 CSP in H₂O/MeOH (30/70 v/v) mobile phase (Fig. 5 A). These differences, especially in resolution, can be observed in Fig. S4 A and S4B.

Analytes 16–18 possess an additional ether O-atom, which is capable of H-bond interactions, while 19 bears a naphthyl moiety,

which may facilitate stronger π – π -interactions. All these structural features led to higher α and R_S values as depicted in Fig. 5B and Fig. S4B.

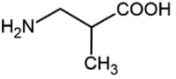
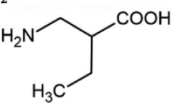
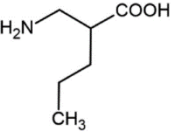
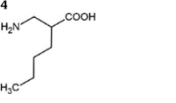
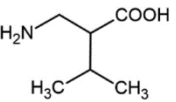
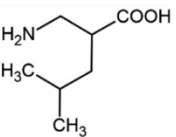
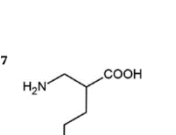
In addition to the chromatograms for analytes 11–19, Figure 6 depicts selected chromatograms for analytes 1–10 and 12 as well representing the separations obtained within three minutes. Using enantiopure analytes, elution sequences for analytes 2, 5, and 6 were determined and found to be the same for all columns and mobile phases, they were, $R < S$.

According to the data in Tables S1–S4, the separation factors, despite similar retention times and retention factors of the first eluting enantiomers, sometimes differ considerably on the teicoplanin- and teicoplanin aglycone-based CSPs, indicating a possible difference in the separation mechanism. In most cases, higher selectivities and resolutions were obtained with the aglycone-based CSP under all the studied conditions, while no clear trend could be observed for the variation in the retention times. As described earlier [35] the sugar units of the native teicoplanin may affect the chiral recognition process in different ways; they block the possible interaction sites on the aglycone, occupy the space inside the “basket”, and offer additional interaction sites since the three sugar units are themselves chiral. To quantitatively determine the effects of the sugar units, the equation $\Delta(\Delta G^\circ) = -RT \ln \alpha$ was applied for the calculation of the differences in enantioselective free energies between the two CSPs [$\Delta(\Delta G^\circ)_{\text{TAG}} - \Delta(\Delta G^\circ)_T$]. As illustrated in Fig. 7, the energy differences [$\Delta(\Delta G^\circ)_{\text{TAG}} - \Delta(\Delta G^\circ)_T$] with very few exceptions, are negative, i.e., the interaction between the free aglycone basket (without the sugar moieties) and analyte improves chiral recognition. By comparing the [$\Delta(\Delta G^\circ)_{\text{TAG}} - \Delta(\Delta G^\circ)_T$] values for analytes 1–6, it is interesting to note that in the case of molecules with a larger size, interactions between selector and analyte are favored. It should be noted that [$\Delta(\Delta G^\circ)_{\text{TAG}} - \Delta(\Delta G^\circ)_T$] values can vary with the amount of mobile phase additives.

3.5. van Deemter analysis

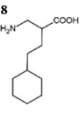
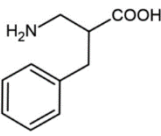
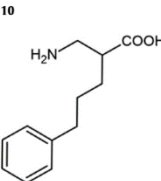
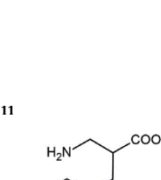
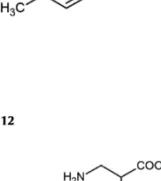
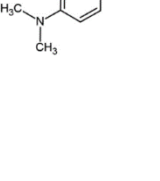



Organic components of eluents (MeOH and MeCN) used in this study in combination with water yield mobile phases with considerable viscosity, while combination of MeOH and MeCN result in low-viscosity eluent allowing higher flow rates without high backpressures. According to Darcy's law, backpressure relates to mobile phase viscosity and linear velocity [21,36]. For the investigation of van Deemter plots, mobile phases possessing low and moderate viscosity [mobile phase **b**, aq.TEAA/MeOH (30/70 v/v) and **c**, MeCN/MeOH (30/70 v/v, respectively) both containing 2.5 mM TEA and 5.0 mM AcOH] were selected, and plots were constructed on all four studied columns for analytes containing an aliphatic (6) or

Table 1
Selected chromatographic data for the separation of β^2 -amino acids.

Analyte	Column	Mobile phase	k_1	α	R_s
aliphatic β^2-amino acids					
1 	T-3.0	H ₂ O/MeOH (30/70 v/v)	0.40	1.30	1.01
	T-3.0	H ₂ O/MeOH (10/90 v/v)	0.20	1.46	0.90
	TAG-3	H ₂ O/MeOH (30/70 v/v)	0.70	1.30	1.05
	TAG-3	H ₂ O/MeOH (10/90 v/v)	1.82	1.22	0.72
	TAG-3.0	aq.TEAA/MeOH (10/90 v/v)	1.75	1.24	0.74
2 	T-3.0	aq.TEAA/MeOH (30/70 v/v)	0.53	1.35	1.32
	TAG-3.0	H ₂ O/MeOH (30/70 v/v)	0.50	1.54	1.35
	T-3.0	H ₂ O/MeOH (30/70 v/v)	0.34	1.75	2.48
	T-2.1	H ₂ O/MeOH (30/70 v/v)	0.86	1.30	1.58
	T-3.0	H ₂ O/MeOH (30/70 v/v)	0.47	1.80	2.66
3 	TAG-3.0	MeCN/MeOH (30/70 v/v)	1.49	1.63	1.71
	TAG-2.1	MeCN/MeOH (30/70 v/v)	1.04	1.72	1.53
	T-3.0	H ₂ O/MeOH (30/70 v/v)	0.33	1.76	2.07
	TAG-3.0	MeCN/MeOH (30/70 v/v)	1.37	1.60	1.70
	TAG-2.1	MeCN/MeOH (30/70 v/v)	0.97	1.66	1.40
4 	T-3.0	H ₂ O/MeOH (30/70 v/v)	0.30	1.85	1.71
	TAG-3.0	H ₂ O/MeOH (30/70 v/v)	0.45	1.90	1.35
	TAG-3.0	MeCN/MeOH (30/70 v/v)	1.02	1.73	1.37
	TAG-3.0	MeCN/MeOH (10/90 v/v)	1.09	1.51	1.58
	T-3.0	H ₂ O/MeOH (30/70 v/v)	0.28	2.03	2.50
5 	T-3.0	MeCN/MeOH (10/90 v/v)	1.45	1.45	0.83
	T-2.1	H ₂ O/MeOH (30/70 v/v)	0.85	1.46	1.64
	TAG-3.0	H ₂ O/MeOH (30/70 v/v)	0.95	2.06	2.39
	TAG-3.0	aq.TEAA/MeOH (30/70 v/v)	0.22	1.74	1.30
	TAG-3.0	aq.TEAA/MeOH (10/90 v/v)	0.73	2.24	2.88
6 	TAG-3.0	MeCN/MeOH (30/70 v/v)	1.15	1.82	2.02
	TAG-2.1	H ₂ O/MeOH (30/70 v/v)	0.77	1.48	1.72
	TAG-2.1	MeCN/MeOH (30/70 v/v)	0.69	1.90	1.89
	T-3.0	H ₂ O/MeOH (30/70 v/v)	0.27	1.81	1.97
	TAG-3.0	H ₂ O/MeOH (30/70 v/v)	0.66	1.64	1.80
7 	TAG-3.0	aq.TEAA/MeOH (20/80 v/v)	0.28	1.62	1.14
	TAG-3.0	aq.TEAA/MeOH (10/90 v/v)	0.79	1.80	2.08
	TAG-3.0	MeCN/MeOH (30/70 v/v)	1.08	1.60	1.77
	TAG-3.0	H ₂ O/MeOH (30/70 v/v)	0.66	1.64	1.80
	TAG-3.0	aq.TEAA/MeOH (20/80 v/v)	0.28	1.62	1.14

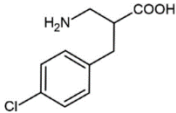
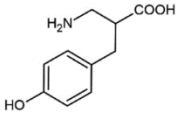
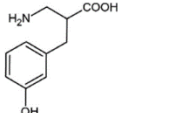
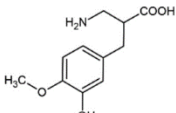
(continued on next page)

Table 1 (continued)

Analyte	Column	Mobile phase	k_1	α	R_s
8 	T-3.0	H ₂ O/MeOH (30/70 v/v)	1.10	1.59	2.05
	T-3.0	aq.TEAA/MeOH (10/90 v/v)	0.79	1.61	1.67
aromatic β^2-amino acids 9 	TAG-3.0	MeCN/MeOH (30/70 v/v)	1.55	1.56	1.75
	T-3.0	H ₂ O/MeOH (30/70 v/v)	0.82	1.36	1.75
10 	T-3.0	aq.TEAA/MeOH (30/70 v/v)	0.62	1.48	1.99
	T-2.1	H ₂ O/MeOH (30/70 v/v)	1.73	1.23	1.94
11 	T-2.1	aq.TEAA/MeOH (30/70 v/v)	0.69	1.53	1.73
	T-2.1	MeCN/MeOH (30/70 v/v)	2.43	1.39	1.68
12 	TAG-3.0	H ₂ O/MeOH (30/70 v/v)	1.00	1.49	1.82
	TAG-3.0	aq.TEAA/MeOH (30/70 v/v)	0.91	1.49	1.94
13 	TAG-2.1	H ₂ O/MeOH (30/70 v/v)	1.09	1.34	1.59
	TAG-2.1	aq.TEAA/MeOH (30/70 v/v)	0.72	1.60	1.72
14 	TAG-2.1	MeCN/MeOH (30/70 v/v)	1.67	1.48	1.68
	T-3.0	H ₂ O/MeOH (30/70 v/v)	0.97	1.50	1.74
15 	T-3.0	aq.TEAA/MeOH (30/70 v/v)	0.62	1.70	2.77
	T-3.0	MeCN/MeOH (30/70 v/v)	1.88	1.43	1.76
16 	T-2.1	H ₂ O/MeOH (30/70 v/v)	1.74	1.21	1.87
	T-2.1	aq.TEAA/MeOH (30/70 v/v)	0.72	1.72	2.40
17 	T-2.1	MeCN/MeOH (30/70 v/v)	2.07	1.52	2.08
	TAG-3.0	H ₂ O/MeOH (30/70 v/v)	1.19	1.73	2.83
18 	TAG-3.0	aq.TEAA/MeOH (30/70 v/v)	1.10	1.74	3.02
	TAG-3.0	MeCN/MeOH (30/70 v/v)	2.05	1.71	2.06
19 	TAG-2.1	H ₂ O/MeOH (30/70 v/v)	1.24	1.46	2.31
	TAG-2.1	aq.TEAA/MeOH (30/70 v/v)	0.89	1.75	2.50
20 	TAG-2.1	MeCN/MeOH (30/70 v/v)	1.45	1.80	2.54
	T-3.0	aq.TEAA/MeOH (30/70 v/v)	0.64	1.39	1.70
21 	T-2.1	H ₂ O/MeOH (30/70 v/v)	1.87	1.17	1.58
	T-2.1	aq.TEAA/MeOH (30/70 v/v)	0.72	1.46	1.59
22 	T-2.1	MeCN/MeOH (30/70 v/v)	2.30	1.33	1.46
	TAG-3.0	aq.TEAA/MeOH (30/70 v/v)	1.12	1.43	1.68
23 	TAG-3.0	MeCN/MeOH (30/70 v/v)	1.02	1.41	1.78
	TAG-2.1	H ₂ O/MeOH (30/70 v/v)	1.39	1.39	2.02
24 	TAG-2.1	aq.TEAA/MeOH (30/70 v/v)	0.81	1.51	1.64
	TAG-2.1	MeCN/MeOH (30/70 v/v)	1.58	1.45	1.64
25 	T-3.0	aq.TEAA/MeOH (30/70 v/v)	1.57	1.17	1.27
	T-3.0	aq.TEAA/MeOH (10/90 v/v)	1.88	1.44	1.97
26 	T-2.1	MeCN/MeOH (30/70 v/v)	2.95	1.32	1.37
	T-2.1	aq.TEAA/MeOH (10/90 v/v)	2.35	1.27	1.19
27 	TAG-3.0	MeCN/MeOH (30/70 v/v)	2.62	1.33	1.06
	TAG-3.0	MeCN/MeOH (10/90 v/v)	3.08	1.39	1.15
28 	TAG-2.1	MeCN/MeOH (20/80 v/v)	1.81	1.43	1.53

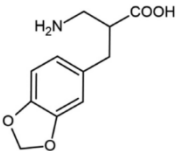
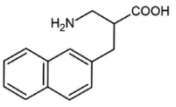
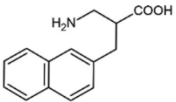
(continued on next page)

Table 1 (continued)

Analyte	Column	Mobile phase	k_1	α	R_s
13 	T-3.0	aq.TEAA/MeOH (30/70 v/v)	0.73	1.18	1.32
	T-3.0	aq.TEAA/MeOH (10/90 v/v)	1.30	1.32	1.56
	T-2.1	aq.TEAA/MeOH (30/70 v/v)	0.78	1.30	1.32
	T-2.1	aq.TEAA/MeOH (10/90 v/v)	1.62	1.40	1.91
	TAG-3.0	aq.TEAA/MeOH (30/70 v/v)	1.33	1.26	1.22
	TAG-3.0	aq.TEAA/MeOH (10/90 v/v)	2.08	1.28	1.07
	TAG-2.1	H ₂ O/MeOH (30/70 v/v)	1.60	1.28	1.47
	TAG-2.1	aq.TEAA/MeOH (30/70 v/v)	1.04	1.35	1.21
	TAG-2.1	aq.TEAA/MeOH (10/90 v/v)	1.49	1.38	1.46
	T-3.0	aq.TEAA/MeOH (30/70 v/v)	0.67	1.46	1.84
14 	T-2.1	H ₂ O/MeOH (30/70 v/v)	1.71	1.16	1.49
	T-2.1	aq.TEAA/MeOH (30/70 v/v)	0.73	1.51	1.74
	T-2.1	MeCN/MeOH (30/70 v/v)	2.47	1.37	1.59
	TAG-3.0	H ₂ O/MeOH (30/70 v/v)	0.83	1.48	1.89
	TAG-3.0	aq.TEAA/MeOH (30/70 v/v)	0.95	1.96	3.32
	TAG-3.0	MeCN/MeOH (30/70 v/v)	2.63	1.43	1.38
	TAG-2.1	H ₂ O/MeOH (30/70 v/v)	1.11	1.39	2.09
	TAG-2.1	aq.TEAA/MeOH (30/70 v/v)	0.74	2.13	2.78
	TAG-2.1	MeCN/MeOH (30/70 v/v)	1.88	1.53	1.91
	T-3.0	H ₂ O/MeOH (30/70 v/v)	0.86	1.40	1.57
15 	T-3.0	aq.TEAA/MeOH (30/70 v/v)	0.59	1.50	3.10
	T-3.0	MeCN/MeOH (30/70 v/v)	2.31	1.36	1.38
	TAG-3.0	H ₂ O/MeOH (30/70 v/v)	0.82	2.10	2.58
	T-3.0	aq.TEAA/MeOH (30/70 v/v)	0.68	1.34	1.51
	T-2.1	H ₂ O/MeOH (30/70 v/v)	1.92	1.16	1.50
	T-2.1	aq.TEAA/MeOH (30/70 v/v)	0.76	1.41	1.48
	TAG-3.0	H ₂ O/MeOH (30/70 v/v)	1.12	1.37	1.48
	TAG-3.0	aq.TEAA/MeOH (30/70 v/v)	1.07	1.36	1.63
	TAG-2.1	H ₂ O/MeOH (30/70 v/v)	1.47	1.34	1.90
	TAG-2.1	aq.TEAA/MeOH (30/70 v/v)	0.85	1.44	1.53
17 	TAG-2.1	MeCN/MeOH (30/70 v/v)	1.63	1.41	1.51
	T-3.0	aq.TEAA/MeOH (30/70 v/v)	0.67	1.45	1.82
	T-2.1	H ₂ O/MeOH (30/70 v/v)	1.86	1.18	1.57
	T-2.1	aq.TEAA/MeOH (30/70 v/v)	0.73	1.50	1.74
	TAG-3.0	H ₂ O/MeOH (30/70 v/v)	0.92	2.00	2.91
	TAG-3.0	aq.TEAA/MeOH (30/70 v/v)	0.93	1.93	3.16
	TAG-3.0	MeCN/MeOH (30/70 v/v)	2.91	1.70	2.14
	TAG-2.1	H ₂ O/MeOH (30/70 v/v)	1.26	1.74	3.00
	TAG-2.1	aq.TEAA/MeOH (30/70 v/v)	0.74	2.12	2.78
	TAG-2.1	MeCN/MeOH (30/70 v/v)	2.13	1.83	2.64

(continued on next page)

Table 1 (continued)

Analyte	Column	Mobile phase	k_1	α	R_s
18 	T-3.0	H ₂ O/MeOH (30/70 v/v)	1.19	1.35	1.58
	T-3.0	aq.TEAA/MeOH (30/70 v/v)	0.74	1.47	2.09
	T-3.0	MeCN/MeOH (30/70 v/v)	2.37	1.32	1.48
	T-2.1	H ₂ O/MeOH (30/70 v/v)	2.02	1.22	1.91
	T-2.1	aq.TEAA/MeOH (30/70 v/v)	0.84	1.52	1.94
	T-2.1	MeCN/MeOH (30/70 v/v)	2.71	1.40	1.74
	TAG-3.0	H ₂ O/MeOH (30/70 v/v)	1.05	1.73	2.72
	TAG-3.0	aq.TEAA/MeOH (30/70 v/v)	1.07	1.66	2.75
	TAG-3.0	MeCN/MeOH (30/70 v/v)	2.50	1.55	1.68
	TAG-2.1	H ₂ O/MeOH (30/70 v/v)	1.44	1.56	2.88
	TAG-2.1	aq.TEAA/MeOH (30/70 v/v)	0.84	1.77	2.46
	TAG-2.1	MeCN/MeOH (30/70 v/v)	1.76	1.66	2.27
	T-3.0	H ₂ O/MeOH (30/70 v/v)	1.17	1.45	1.98
	T-3.0	aq.TEAA/MeOH (30/70 v/v)	0.75	1.64	2.71
19 	T-3.0	MeCN/MeOH (30/70 v/v)	2.27	1.36	1.55
	T-2.1	H ₂ O/MeOH (30/70 v/v)	1.97	1.31	2.37
	T-2.1	aq.TEAA/MeOH (30/70 v/v)	0.88	1.70	2.57
	T-2.1	MeCN/MeOH (30/70 v/v)	2.96	1.45	1.94
	TAG-3.0	H ₂ O/MeOH (30/70 v/v)	1.53	1.75	2.77
19 	TAG-3.0	aq.TEAA/MeOH (30/70 v/v)	1.62	1.73	2.97
	TAG-3.0	MeCN/MeOH (30/70 v/v)	2.95	1.53	1.50
	TAG-2.1	H ₂ O/MeOH (30/70 v/v)	1.60	1.67	3.22
	TAG-2.1	aq.TEAA/MeOH (30/70 v/v)	1.04	1.86	2.83
	TAG-2.1	MeCN/MeOH (30/70 v/v)	2.12	1.69	2.30

Chromatographic conditions: column, **T-3.0**, **T-2.1**, **TAG-3.0** and **TAG-2.1**; mobile phase, H₂O/MeOH (30/70 v/v), aq.TEAA/MeOH (30/70 v/v) and MeCN/MeOH (30/70 v/v), the latter two contain 2.5 mM TEA and 5.0 mM AcOH; flow rate, 0.3 ml min⁻¹; detection, 210–258 nm; temperature, 20 °C

aromatic (**9**) side chain. van Deemter plots are shown in Figure 8 A (for analyte **6**) and Fig. S5 A (for analyte **9**) in polar-ionic mode. In the polar-ionic mode, the curves for the first eluting enantiomer show characteristic minima for analyte **6** on **T-3.0**, **T-2.1**, and **TAG-3.0** columns, and a slight minima on **TAG-2.1** at ~1.5 mm sec⁻¹ (Fig. 8 A). It should be noted that 2.1 mm i.d. columns are usually less efficient than 3.0 mm ones due to wall effects (Fig. 8 A). The H minima on **T-3.0** and **TAG-3.0** were registered at 0.24 mm sec⁻¹, while on **T-2.1** at 0.48 mm sec⁻¹ linear velocity, which corresponds to a flow rate of 0.1 ml min⁻¹. The van Deemter curves for teicoplanin-based columns run below the plots of the teicoplanin aglycone. Fig. S5 A depicts van Deemter plots for analyte **9** under the same conditions. The shape of the curve for columns with 3.0 mm i.d. are similar to plots obtained for analyte **6** (minima are in the range 0.24–0.48 mm sec⁻¹, i.e., 0.1–0.2 ml min⁻¹), while plots obtained on columns with 2.1 mm i.d. exhibited slight minima at lower flow rates (0.05–0.1 ml min⁻¹). Interestingly, the H-u plot for the teicoplanin aglycone column with 2.1 mm i.d. (**TAG-2.1**) runs below the same type of column with a larger i.d. (**TAG-3.0**). Figures 8B and S5B depict van Deemter plots for analytes **6** and **9** applying mobile phase **b**, aq.TEAA/MeOH (30/70 v/v) containing 2.5 mM TEA and 5.0 mM AcOH on teicoplanin- and te-

icoplanin aglycone-based columns possessing different internal diameters. The van Deemter curves at high flow rates (where the C-term dominates) on **T-3.0** columns exhibited a slight increase in plate height, while on **T-2.1** columns a decrease in plate height (slightly negative slope) was registered for both analytes at high flow rates. It is described several times that at high backpressures, two types of temperature gradients – axial and radial – exist together as the result of significant frictional heating [16,37–39]. Axial temperature differences ranging from 11 to 16 °C can readily be generated when pressure above 300 bar is applied [16,37]. In some cases, longitudinal frictional heating was found to increase the chiral resolution when small particles and high flow rates are used [16,21]. In Fig. 8 C, van Deemter plots for the first and second eluting enantiomer of analyte **6** on **TAG-3** and analyte **9** on the **T-2.1** column are depicted. It is interesting to note that identical kinetic plot shapes were recorded for both enantiomers with the curve for the second enantiomer shifted upwards. The similar shapes indicate that both enantiomers have similar adsorption/desorption kinetics (the same results were obtained under other conditions too; data not shown). In summary, comparing results obtained for van Deemter analyses and screening experiments of 19 β²-amino acids (registered at a flow rate of 0.3 ml min⁻¹), the following conclu-

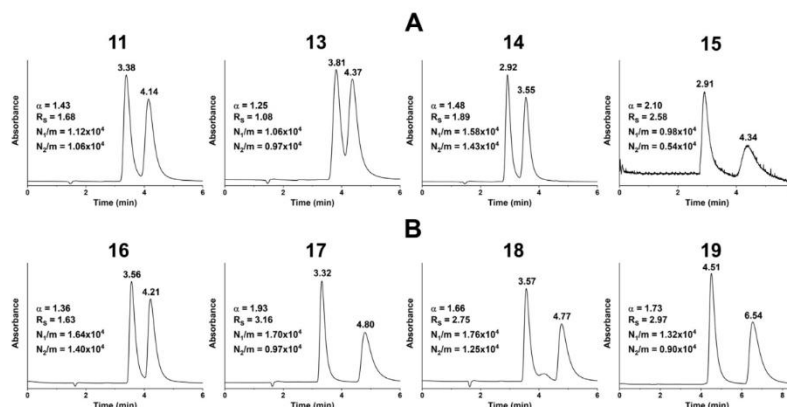


Figure 5. Effect of nature of substituents and chemical structure of analytes on chromatographic performance for analytes **11** and **13–19**. Chromatographic condition, column, TAG-3.0; mobile phase, **A**, H₂O/MeOH (30/70 v/v), **B**, aq.TEAA/MeOH (30/70 v/v), concentration of TEA and AcOH in mobile phase 2.5 and 5.0 mM, respectively and the actual pH of the mobile phase, pH₄ 5.5; flow rate, 0.3 ml min⁻¹; detection, 258 nm; temperature, 20 °C.

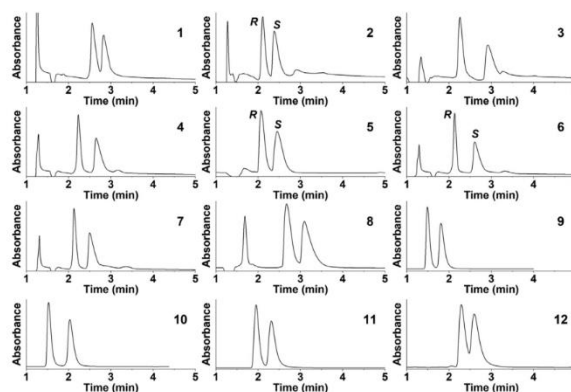


Figure 6. Selected chromatograms for analytes **1–10** and **12**. Chromatographic conditions, columns, for analytes **1**, **4**, **6**, **7**, and **8** T-3.0, for **2**, **3** and **5** TAG-3.0, for **9** and **10** T-2.1 and for **11** and **12** TAG-2.1; mobile phase, for analytes **1–7** and **11**, H₂O/MeOH (30/70 v/v), for **8–10** and **12** aq.TEAA/MeOH (30/70 v/v), concentration of TEA and AcOH in mobile phase 2.5 and 5.0 mM, respectively and the actual pH of the mobile phase, pH₄ 5.5; flow rate, 0.3 ml min⁻¹; detection, 258 nm; temperature, 20 °C.

sions can be drawn: (i) higher plate numbers were obtained on teicoplanin-based than on teicoplanin aglycone-based CSP (T-3.0 vs. TAG-3.0 and T-2.1 vs. TAG-2.1), (ii) in general, for SPPs of 2.7 μ m, the narrow bore columns (2.1 mm i.d.) show decreased efficiency compared to their counterparts with 3.0 mm i.d. Note, that the latter columns were expected to outperform the columns of 2.1 mm i.d. and this expectation was met under all the studied conditions. It must be emphasized, however, that column performance, in the practice, depends on both the nature of analytes and the mobile phase composition. H values for analytes possessing an alkyl side chain (**1–8**) were always smaller on columns of 3.0 mm i.d., while for analytes possessing an aromatic side chain (**9–19**), columns of 2.1 mm i.d. showed better performance (Table S1–S4 and Fig. S5 A). However, in the RP mode for analytes **9–19**, columns of 3.0 mm i.d. always outperformed the columns of 2.1 mm i.d. columns (Table S1–S4).

3.6. Temperature dependence and thermodynamic parameters

Studying the effects of temperature on retention and enantioselectivity in chiral separations is an often applied methodology to gather information on enantiomer recognition [40–43]. Theoretically, retention observed on chiral CSPs consists of chiral and nonchiral components [44–48], however, in this study, these two components are not differentiated. Keeping in mind the limitations of the approach, used herein the difference in the change in standard enthalpy $\Delta(\Delta H^\circ)$ and entropy $\Delta(\Delta S^\circ)$ for the enantiomer pairs were calculated using the relationship between $\ln \alpha$ (natural logarithm of the apparent selectivity factor) and T^{-1} (reciprocal of absolute temperature) as described by the van't Hoff equation:

$$\ln \alpha = -\frac{\Delta(\Delta H^\circ)}{RT} + \frac{\Delta(\Delta S^\circ)}{R} \quad (2)$$

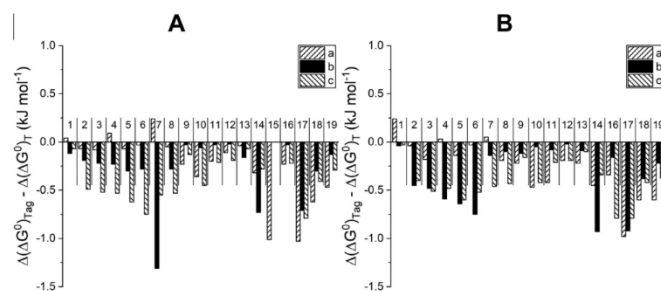


Figure 7. Enantioselectivity free energy differences $\Delta(\Delta G^0)_{\text{rag}} - \Delta(\Delta G^0)_{\text{r}}$ between aglycone and native teicoplanin selector Chromatographic condition, column, **A**, TAG-3.0 vs. T-3.0 and **B**, TAG-2.1 vs. T-2.1; mobile phase, **a**, H₂O/MeOH (30/70 v/v), **b**, aq.TEAA/MeOH (30/70 v/v), concentration of TEA and AcOH in the mobile phase 2.5 and 5.0 mM, respectively, and the actual pH of the mobile phase, pH_s 5.5; **c**, MeCN/MeOH (30/70 v/v), concentration of TEA and AcOH in the mobile phase 2.5 and 5.0 mM, respectively; flow rate, 0.3 ml min⁻¹; detection, 210–258 nm; temperature, 20 °C; symbols, mobile phase, **a**, mobile phase, **b**, and mobile phase, **c**.

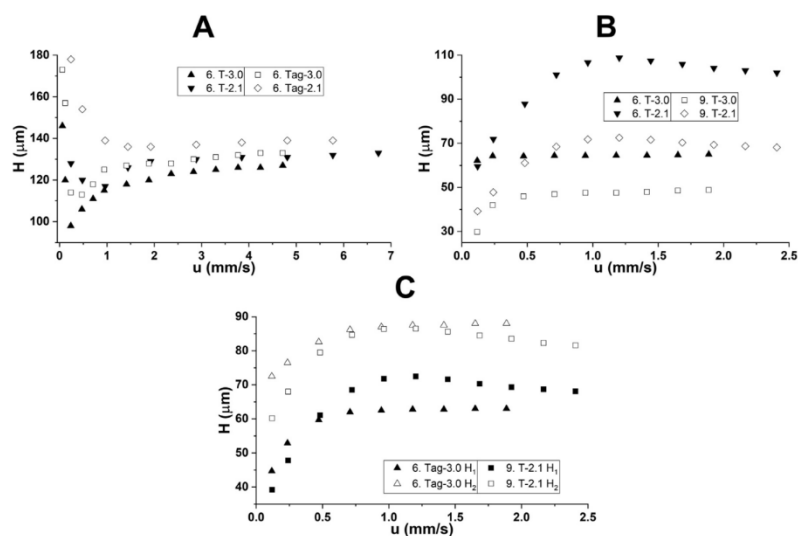


Figure 8. Plots of plate heights versus superficial velocities for analytes **6** and **9** on macrocyclic glycopeptide-based columns Chromatographic conditions: columns, **A**, T-3.0, T-2.1, TAG-3.0 and TAG-2.1, **B**, T-3.0, T-2.1 and **C**, TAG-3.0 and TAG-2.1; mobile phase, **A**, MeCN/MeOH (30/70 v/v), concentration of TEA and AcOH in the mobile phase 2.5 and 5.0 mM, respectively, **B** and **C**, aq.TEAA/MeOH (30/70 v/v), concentration of TEA and AcOH in the mobile phase 2.5 and 5.0 mM, respectively, and the actual pH_s of the mobile phase, pH_s 5.5; detection, 210–258 nm; temperature, 20 °C; symbols, **A**, analyte **6**, ▲ T-3.0, ▼ T-2.1, □ TAG-3.0, ◇ TAG-2.1; **B**, analyte **6**, ▲ T-3.0, ▼ T-2.1, □ TAG-3.0, ◇ TAG-2.1; **C**, analyte **6**, ▲ TAG-3.0 (first enantiomer), △ TAG-3.0 (second enantiomer), analyte **9**, ■ T-2.1 (first enantiomer), □ T-2.1 (second enantiomer).

where R is the universal gas constant. As discussed earlier, under UHPLC conditions operating with inlet pressures above 300 bars, the generated axial temperature differences can lead to a marked difference between real operational and set conditions [16,21,37]. To avoid the temperature differences caused by high backpressure, the nature of applied mobile phases and flow rates were carefully selected for this study. For example, CSPs with 2.1 mm i.d. were applied only in polar-ionic mode.

Dependence of the chromatographic parameters on temperature was studied on the four columns for analyte **8** possessing an aliphatic side chain, and for analyte **9** bearing an aromatic

side chain in the temperature range 5–50 °C. Experimental data with mobile phases of aq.TEAA/MeOH (30/70 v/v) and MeCN/MeOH (30/70 v/v) both containing 20 mM TEAA are presented in Table S5. As most frequently observed, both k and α decreased with increasing temperature in all cases. Resolution usually decreases with increasing temperature, while in a few cases, R_S , exhibited a maximum curve with the change of temperature (Table S5). Lower R_S values at low and high temperatures can be attributed to the lower kinetic and higher thermodynamic effect (decreased α values), respectively.

Table 2

Thermodynamic parameters, $\Delta(\Delta H^\circ)$, $\Delta(\Delta S^\circ)$, $\text{Tx}\Delta(\Delta S^\circ)$, $\Delta(\Delta G^\circ)$, correlation coefficients (R^2), T_{iso} and Q values of β^2 -amino acids in different separation modalities on **TeicoShell** and **TagShell** columns with 3.0 and 2.1 i.d., respectively.

Compound	Mobile phase	$-\Delta(\Delta H^\circ)$ (kJ/mol)	$-\Delta(\Delta S^\circ)$ (J/(mol·K))	Correlation coefficients (R^2)	$-\text{Tx}\Delta(\Delta S^\circ)_{298\text{K}}$ (kJ/mol)	$-\Delta(\Delta G^\circ)_{298\text{K}}$ (kJ/mol)	T_{iso} (°C)	Q
TeicoShell (3.0 mm I.D.)								
8	b	3.55	7.59	0.9960	2.26	1.28	194	1.57
	c	1.43	2.72	0.9790	0.81	0.62	255	1.77
	c	1.30	2.31	0.9976	0.69	0.61	289	1.89
TeicoShell (2.1 mm I.D.)								
8	c	1.96	4.32	0.9936	1.29	0.68	181	1.52
	c	1.99	3.99	0.9994	1.19	0.80	226	1.67
TagShell (3.0 mm I.D.)								
8	b	2.04	4.42	0.9912	1.32	0.73	189	1.55
	c	2.56	5.14	0.9949	1.53	1.02	225	1.67
	c	2.06	4.24	0.9810	1.26	0.79	212	1.63
9	b	2.11	4.78	0.9980	1.42	0.68	168	1.48
	c	2.02	3.34	0.9950	0.99	1.02	332	2.03
TagShell (2.1 mm I.D.)								
8	c	2.28	4.91	0.9989	1.46	0.81	191	1.56
	c							

Chromatographic conditions: columns, **TeicoShell** and **TagShell** with 3.0 and 2.1 i.d., respectively; mobile phase, **b**, aq.TEAA/MeOH/ (30/70 v/v), total concentration of TEAA in the mobile phase 20 mM, actual pH of mobile phase, $\text{pH}_\text{a} = 5.0$, **c**, MeCN/MeOH/ (30/70 v/v) containing 20 mM TEAA; detection, 215–256 nm; flow rates, 0.3 ml min⁻¹; T_{iso} , temperature where the enantioselectivity cancels; $Q = \Delta(\Delta H^\circ) / T \times \Delta(\Delta S^\circ)_{298\text{K}}$

The calculated $-\Delta(\Delta H^\circ)$ and $-\Delta(\Delta S^\circ)$ values are presented in Table 2. The $\Delta(\Delta H^\circ)$ values ranged from -1.30 to -3.55 kJ mol⁻¹. These negative values indicate that the adsorption/desorption kinetics are enthalpically favored. $\Delta(\Delta S^\circ)$ values ranged from -2.31 to -7.59 J mol⁻¹ K⁻¹. It is important to note that $\Delta(\Delta S^\circ)$ values are depended on (i) the difference in the number of degrees of freedom between the solutes bound on the CSP, and (ii) the number of solvent molecules leaving the solvated CSP and the analyte, when the analyte is associated with the CSP. The trends in the change in $\Delta(\Delta S^\circ)$ and $\Delta(\Delta H^\circ)$ were similar, that is, a more negative $\Delta(\Delta H^\circ)$ was accompanied by a more negative $\Delta(\Delta S^\circ)$.

Under the applied conditions more negative $\Delta(\Delta G^\circ)$ values (calculated at 298 K) were obtained on TagShell CSPs, in most cases, indicating that the differential binding to the aglycone-based selector was more favorable. For the representation of the relative contribution to the free energy of adsorption we calculated the enthalpy/entropy ratio, as $Q = \Delta(\Delta H^\circ) / [298 \times \Delta(\Delta S^\circ)]$. As indicated in Table 2, the enantioselective discrimination was enthalpically driven in all cases.

4. Conclusions

It was generally observed that an increase in the methanol content in the RP mode resulted in a slight increase in retention and moderate enhancement in selectivity and resolution. In the polar-ionic mode, retention considerably decreased, while selectivity and resolution moderately increased with increasing methanol content. The change of actual pH_a under RP conditions showed, that pH_a values higher than 5.0 were advantageous regarding retention, selectivity, and resolution. In the application of different organic acids and salts, the best chromatographic performances were observed with the TEAA additive.

Macrocyclic glycopeptide CSPs are expected to act as weak ion-exchangers and this concept was supported by the validated displacement model. Investigation of the effect of analyte and selector structures revealed that (i) there is a strong relationship between separation performance (retention and selectivity) and the size of the aliphatic side chain (Meyer's size descriptor), (ii) the nature of substituents on analytes with an aromatic ring (endowing π -acidic- or π -basic character for the molecule) affects separation performance slightly, while the position of a hydroxyl moiety has a considerable effect, and (iii) separation is thermodynamically favored in the case of selectors without sugar units (aglycone-based CSPs).

Analyses of van Deemter plots in the polar-ionic mode confirmed a typical shape with a plate height of minima, while no characteristic minima were registered when RP eluents were applied. Columns with 3.0 mm i.d. exhibited a slight increase in plate height, while a decrease in plate height was registered for the columns with 2.1 mm i.d. at high flow rates (axial temperature effect). In addition, in all three mobile phase systems, lower plate heights were obtained: (i) concerning native teicoplanin (**T**) vs. teicoplanin aglycone (**TAG**) for all analytes and (ii) concerning columns with 3.0 mm i.d. vs. columns with 2.1 mm i.d. for β^2 -amino acids possessing aliphatic side chains. For analytes with aromatic side chains, an opposite correlation was observed. Evaluation of the kinetic curves, in most cases, supports that the separation of two enantiomers takes place with the same adsorption/desorption kinetics, i.e., the shape and slope of van Deemter plots were similar. Let us note here, that the determined plate heights were higher than expected, although data were not corrected with the extra-column volume of the instrument. Reduction of the extra-column effects (e.g., by altering the tubing of the UHPLC) would probably result in lower plate heights. The flat C-term curves observed in many cases demonstrate the possibility for high-speed enantioseparations without significant loss in efficiency, thus the speed gain and the significant reduction in solvent consumption offered by the columns based on 2.7 μm SP particles compared to a traditional (5 μm FP particle-based) column are worth to utilize.

Thermodynamic parameters obtained by a temperature-dependence study revealed that enantioseparations were enthalpically driven and selectivity decreased with enhanced temperature under all studied conditions.

Elution sequences for analytes **2**, **5**, and **6** were determined to show an $R < S$ relationship.

Declaration of Competing Interest

The authors declare no conflict of interest.

Acknowledgments

This work was supported by the National Research Development and Innovation Office, project grant GINOP-2.3.2-15-2016-00034, the EU-funded Hungarian grant EFOP-3.6.1-16-2016-00008, and the Ministry of Human Capacities, Hungary grant TKP-2020.

Credit Author Statement

Dániel Tanács: Investigation, Writing – Original Draft, Visualization; **Róbert Berkecz:** Conceptualization, Writing – Original Draft, Review & Editing; **Aleksandra Misicka, Dagmara Tymecka:** Resources, Writing – Original Draft; **Ferenc Fülöp:** Writing-Review & Editing, **Daniel Armstrong:** Conceptualization, Writing-Original Draft, Review & Editing; **Antal Péter:** Conceptualization, Writing-Review & Editing; **István Ilisz:** Conceptualization, Writing-Original Draft, Review & Editing; Supervision, Project Administration, Funding Acquisition

Supplementary materials

Supplementary material associated with this article can be found, in the online version, at doi:10.1016/j.chroma.2021.462383.

References

- [1] D.F. Hook, F. Gessier, C. Noti, P. Kast, D. Seebach, Probing the proteolytic stability of β -peptides containing α -fluoro- and α -hydroxy- β -amino acids, *ChemBioChem* 5 (2004) 691–706, doi:10.1002/cbic.200300827.
- [2] M.J. Aguilar, A.W. Purcell, R. Devi, R. Lew, J. Rossjohn, A.I. Smith, P. Perlmutter, β -Amino acid-containing hybrid peptides – New opportunities in peptidomimetics, *Org. Biomol. Chem.* 5 (2007) 2884–2890 doi:10.1039/b708507 a.
- [3] K. Gach-Janczak, J. Piekielna-Ciesielska, A. Adamska-Bartłomiejczyk, R. Perlikowska, R. Kruszyński, A. Kluczyk, J. Krzywik, J. Sukienik, M.C. Cerlesie, G. Caloe, A. Wasilewski, M. Zielińska, A. Janicka, Synthesis and activity of opioid peptidomimetics with β^2 - and β^3 -amino acids, *Peptides* 95 (2017) 116–123, doi:10.1016/j.peptides.2017.07.015.
- [4] K.H.Y. Duong, V.G. Göz, I. Pintér, A. Percel, Synthesis of chimera oligopeptide including furanoid β -sugar amino acid derivatives with free OHs: mild but successful removal of the 1,2-O-isopropylidene from the building block, *Amino Acids* 53 (2021) 281–294, doi:10.1007/s00726-020-02923-3.
- [5] G. Lelais, D. Seebach, β^2 -amino acids-syntheses, occurrence in natural products, and components of β -peptides, *Biopolymers* 76 (2004) 206–243, doi:10.1002/bip.20088.
- [6] I. Ilisz, A. Bajtai, W. Lindner, A. Péter, Liquid chromatographic enantiomer separations applying chiral ion-exchangers based on Cinchona alkaloids, *J. Pharm. Biomed. Anal.* 159 (2018) 127–152, doi:10.1016/j.jpba.2018.06.045.
- [7] G. Lajkó, T. Orosz, N. Grecsó, B. Fekete, M. Palkó, F. Fülöp, W. Lindner, A. Péter, I. Ilisz, High-performance liquid chromatographic enantioseparation of cyclic β -aminohydroxamic acids on zwitterionic chiral stationary phases based on Cinchona alkaloids, *Anal. Chim. Acta*, 921 (2016) 84–94, doi:10.1016/j.aca.2016.03.044.
- [8] R. Sardella, F. Ianni, A. Lisanti, S. Scorroni, F. Marini, S. Sternativo, B. Natalini, Direct chromatographic enantioresolution of fully constrained β -amino acids: exploring the use of high-molecular-weight chiral selectors, *Amino Acids* 46 (2014) 1235–1242, doi:10.1007/s00726-014-1683-5.
- [9] R. Berkecz, I. Ilisz, A. Misicka, D. Tymecka, F. Fülöp, H.J. Choi, M.H. Hyun, A. Péter, HPLC enantioseparation of β^2 -homooamino acids using crown ether-based chiral stationary phase, *J. Sep. Sci.* 32 (2009) 981–987, doi:10.1002/jssc.200800561.
- [10] I. Ilisz, Z. Pataj, R. Berkecz, A. Misicka, D. Tymecka, F. Fülöp, H.J. Choi, M.H. Hyun, A. Péter, High-performance liquid chromatographic enantioseparation of β^2 -amino acids using a long-tethered (+)-(18-crown-6)-2,3,11,12-tetracarboxylic acid-based chiral stationary phase, *J. Chromatogr. A* 1217 (2010) 1075–1082, doi:10.1016/j.chroma.2009.07.003.
- [11] Z. Pataj, I. Ilisz, R. Berkecz, A. Misicka, D. Tymecka, F. Fülöp, D.W. Armstrong, A. Péter, Comparison of performance of Chirobiotic T, T2 and TAG columns in the separation of β^2 - and β^3 -homooamino acids, *J. Sep. Sci.* 31 (2008) 3688–3697, doi:10.1002/jssc.200800388.
- [12] Z. Pataj, R. Berkecz, I. Ilisz, A. Misicka, D. Tymecka, F. Fülöp, D.W. Armstrong, A. Péter, High-performance liquid chromatographic chiral separation of β^2 -homooamino acids, *Chirality* 21 (2009) 787–798, doi:10.1002/chir.20670.
- [13] I. Ilisz, N. Grecsó, A. Aranyi, P. Suchotin, D. Tymecka, B. Wilenska, A. Misicka, F. Fülöp, W. Lindner, A. Péter, Enantioseparation of β^2 -amino acids on cinchona alkaloid-based zwitterionic chiral stationary phases. Structural and temperature effects, *J. Chromatogr. A* 1334 (2014) 44–54, doi:10.1016/j.chroma.2014.01.075.
- [14] I. Ilisz, N. Grecsó, A. Misicka, D. Tymecka, I. Lázár, W. Lindner, A. Péter, Comparison of the separation performances of cinchona alkaloid-based zwitterionic stationary phases in the enantioseparation of β^2 - and β^3 -amino acids, *Molecules* 20 (2014) 70–87, doi:10.3390/molecules2010070.
- [15] G. Hellinghausen, D. Roy, J.T. Lee, Y. Wang, C.A. Weatherly, D.A. Lopez, K.A. Nguyen, J.D. Armstrong, D.W. Armstrong, Effective methodologies for enantiomer separations of 150 pharmacology and toxicology related 1°, 2° and 3° amines with core-shell chiral stationary phases, *J. Pharm. Biomed. Anal.* 155 (2018) 70–81, doi:10.1016/j.jpba.2018.03.032.
- [16] D.C. Patel, Z.S. Breitbach, M.F. Wahab, C.L. Barhate, D.W. Armstrong, Gone in seconds: Praxis, performance, and peculiarities of ultrafast chiral liquid chromatography with superficially porous particles, *Anal. Chem.* 87 (2015) 9137–9148, doi:10.1021/acs.analchem.5b00715.
- [17] R.M. Wimalasinghe, Z.S. Breitbach, J.T. Lee, D.W. Armstrong, Separation of peptides on superficially porous particle-based macrocyclic glycopeptide liquid chromatography stationary phases: consideration of fast separations, *Anal. Bioanal. Chem.* 409 (2017) 2437–2447, doi:10.1007/s00216-017-0190-4.
- [18] G. Kučerová, J. Vozka, K. Kalíková, R. Geryk, D. Plecítá, T. Pajpanova, E. Tesařová, Enantioselective separation of unusual amino acids by high performance liquid chromatography, *Sep. Purif. Technol.* 119 (2013) 123–128, doi:10.1016/j.seppur.2013.09.010.
- [19] D. Roy, D.W. Armstrong, Fast super/subcritical fluid chromatographic enantioseparations on superficially porous particles bonded with broad selectivity chiral selectors relative to fully porous particles, *J. Chromatogr. A* 360339 (2019) 1605, doi:10.1016/j.chroma.2019.06.060.
- [20] D. Folprechtová, O. Kozlov, D.W. Armstrong, M.G. Schmid, K. Kalíková, E. Tesařová, Enantioselective potential of teicoplanin- and vancomycin-based superficially porous particles-packed columns for supercritical fluid chromatography, *J. Chromatogr. A* 460867 (2020) 1612, doi:10.1016/j.chroma.2019.460867.
- [21] C.L. Barhate, M.F. Wahab, Z.S. Breitbach, D.S. Bell, D.W. Armstrong, High efficiency, narrow particle size distribution, sub-2 μ m based macrocyclic glycopeptide chiral stationary phases in HPLC and SFC, *Anal. Chim. Acta* 898 (2015) 128–137, doi:10.1016/j.aca.2015.09.048.
- [22] O.H. Ismail, A. Cioqli, C. Villani, M. De Martino, M. Pierini, A. Cavazzini, D.S. Bell, F. Gasparri, Ultra-fast high-efficiency enantioseparations by means of a teicoplanin-based chiral stationary phase made on sub-2 μ m totally porous silica particles of narrow size distribution, *J. Chromatogr. A* 1427 (2016) 55–68, doi:10.1016/j.chroma.2015.11.071.
- [23] O.H. Ismail, M. Antonelli, A. Cioqli, M. De Martino, M. Catani, C. Villani, A. Cavazzini, M. Ye, D.S. Bell, F. Gasparri, Direct analysis of chiral active pharmaceutical ingredients and their counter ions by ultra-high performance liquid chromatography with macrocyclic glycopeptide-based chiral stationary phases, *J. Chromatogr. A* 1576 (2018) 42–50, doi:10.1016/j.chroma.2018.09.029.
- [24] D. Roy, M.F. Wahab, T.A. Berger, D.W. Armstrong, Ramifications and insights on the role of water in chiral sub/supercritical fluid chromatography, *Anal. Chem.* 91 (2019) 14672–14680, doi:10.1021/acs.analchem.9b03908.
- [25] D.C. Patel, Z.S. Breitbach, J.J. Yu, K.A. Nguyen, D.W. Armstrong, Quinine bonded to superficially porous particles for high-efficiency and ultrafast liquid and supercritical fluid chromatography, *Anal. Chim. Acta* 963 (2017) 164–174, doi:10.1016/j.aca.2017.02.005.
- [26] D.C. Patel, M.F. Wahab, T.C. O'Haver, D.W. Armstrong, Separations at the speed of sensors, *Anal. Chem.* 90 (2018) 3349–3356, doi:10.1021/acs.analchem.7b04944.
- [27] S. Du, Y. Wang, C.A. Weatherly, K. Holden, D.W. Armstrong, Variations of L- and D-amino acid levels in the brain of wild-type and mutant mice lacking D-amino acid oxidase activity, *Anal. Bioanal. Chem.* 410 (2017) 2971–2979, doi:10.1007/s00216-018-0979-9.
- [28] K. Schmitt, U. Woitode, M. Kohout, T. Zhang, W. Lindner, M. Lämmerhofer, Comparison of small size fully porous particles and superficially porous particles of chiral anion-exchange type stationary phases in ultra-high performance liquid chromatography: effect of particle and pore size on chromatographic efficiency and kinetic performance, *J. Chromatogr. A* 1569 (2018) 149–159, doi:10.1016/j.chroma.2018.07.056.
- [29] U. Woitode, S. Neubauer, W. Lindner, S. Buckenmaier, M. Lämmerhofer, Enantioselective multiple heart cut two-dimensional ultra-high-performance liquid chromatography method with a core-shell chiral stationary phase in the second dimension for analysis of all proteinogenic amino acids in a single run, *J. Chromatogr. A* 1562 (2018) 69–77, doi:10.1016/j.chroma.2018.05.062.
- [30] U. Woitode, R.J. Reischl, S. Buckenmaier, W. Lindner, M. Lämmerhofer, Imaging peptide and protein chirality via amino acid analysis by chiral \times chiral two-dimensional correlation liquid chromatography, *Anal. Chem.* 90 (2018) 7963–7971, doi:10.1021/acs.analchem.8b00676.
- [31] W. Kopaciewicz, M.A. Rounds, J. Fausnaugh, F.E. Regnier, Retention model for high-performance ion-exchange chromatography, *J. Chromatogr. A* 266 (1983) 3–21, doi:10.1016/S0021-9673(01)90875-1.
- [32] C.V. Hoffmann, M. Lämmerhofer, W. Lindner, Novel strong cation-exchange type chiral stationary phase for the enantiomer separation of chiral amines by high-performance liquid chromatography, *J. Chromatogr. A* 1161 (2007) 242–251, doi:10.1016/j.chroma.2007.05.092.
- [33] T. Orosz, N. Grecsó, G. Lajkó, Z. Szakonyi, F. Fülöp, D.W. Armstrong, I. Ilisz, A. Péter, Liquid chromatographic enantioseparation of carbocyclic β -amino acids possessing limonene skeleton on macrocyclic glycopeptide-based chiral stationary phases, *J. Pharm. Biomed. Anal.* 145 (2017) 119–126, doi:10.1016/j.jpba.2017.06.010.
- [34] A.Y. Meyer, Molecular mechanics and molecular shape. Part 4. Size, shape, and steric parameters, *J. Chem. Soc. Perkin Trans. 2* (1986) 1567, doi:10.1039/p29860001567.
- [35] A. Berthod, X. Chen, J.P. Kullman, D.W. Armstrong, F. Gasparri, I. D'Acquarica, C. Villani, A. Carotti, Role of the carbohydrate moieties in liquid recognition on teicoplanin- based LC stationary phases, *Anal. Chem.* 72 (2000) 1767–1780 doi:10.1021/ac991004 t.
- [36] J.C. Giddings, Dynamics of chromatography, Part 1: Principles and theory, Marcel Dekker, Inc. 1965.
- [37] I. Halász, R. Endeke, J. Asshauer, Ultimate limits in high-pressure liquid chromatography, *J. Chromatogr. A* 112 (1975) 37–60, doi:10.1016/S0021-9673(00)99941-2.

- [38] F. Gritti, M. Martin, G. Guiochon, Influence of viscous friction heating on the efficiency of columns operated under very high pressures, *Anal. Chem.* 81 (2009) 3365–3384, doi:[10.1021/ac802632x](https://doi.org/10.1021/ac802632x).
- [39] A. de Villiers, H. Lauer, R. Szucs, S. Goodall, P. Sandra, Influence of frictional heating on temperature gradients in ultra-high-pressure liquid chromatography on 2.1 mm I.D. columns, *J. Chromatogr. A* 1113 (2006) 84–91, doi:[10.1016/j.chroma.2006.01.120](https://doi.org/10.1016/j.chroma.2006.01.120).
- [40] B. Koppenhoefer, E. Bayer, Chiral recognition in the resolution of enantiomers by GLC, *Chromatographia* 19 (1984) 123–130, doi:[10.1007/BF02687727](https://doi.org/10.1007/BF02687727).
- [41] R.E. Boelm, D.E. Martire, D.W. Armstrong, Theoretical considerations concerning the separation of enantiomeric solutes by liquid chromatography, *Anal. Chem.* 60 (1988) 522–528, doi:[10.1021/ac00157a006](https://doi.org/10.1021/ac00157a006).
- [42] S. Allenmark, V. Schurig, Chromatography on chiral stationary phases, *J. Mater. Chem.* 7 (1997) 1955–1963, doi:[10.1039/a702403g](https://doi.org/10.1039/a702403g).
- [43] T. Fornstedt, P. Sajonz, G. Guiochon, Thermodynamic study of an unusual chiral separation, *J. Am. Chem. Soc.* 119 (1997) 1254–1264, doi:[10.1021/ja9631458](https://doi.org/10.1021/ja9631458).
- [44] G. Götmar, T. Fornstedt, G. Guiochon, Apparent and true enantioselectivity in enantioseparations, *Chirality* 12 (2000) 558–564, doi:[10.1002/1520-636X\(2000\)12:7<558::AID-CHIR2>3.0.CO;2-2](https://doi.org/10.1002/1520-636X(2000)12:7<558::AID-CHIR2>3.0.CO;2-2).
- [45] A. Sepsey, É. Horváth, M. Catani, A. Felinger, The correctness of van 't Hoff plots in chiral and achiral chromatography, *J. Chromatogr. A* 1611 (2020) 6–8, doi:[10.1016/j.chroma.2019.460594](https://doi.org/10.1016/j.chroma.2019.460594).
- [46] L.D. Asnin, M.V. Stepanova, Van't Hoff analysis in chiral chromatography, *J. Sep. Sci.* 41 (2018) 1319–1337, doi:[10.1002/jssc.201701264](https://doi.org/10.1002/jssc.201701264).
- [47] E.N. Reshetova, M.V. Kopchenova, S.E. Vozisov, A.N. Vasyanin, L.D. Asnin, Enantioselective retention mechanisms of dipeptides on antibiotic-based chiral stationary phases: Leucyl-leucine, glycyl-leucine, and leucyl-glycine as case studies, *J. Chromatogr. A* 1602 (2019) 368–377, doi:[10.1016/j.chroma.2019.06.025](https://doi.org/10.1016/j.chroma.2019.06.025).
- [48] L.D. Asnin, M.V. Kopchenova, S.E. Vozisov, M.A. Klochkova, Y.A. Klimova, Enantioselective retention mechanisms of dipeptides on antibiotic-based chiral stationary phases. II. Effect of the methanol content in the mobile phase, *J. Chromatogr. A* 1626 (2020) 461371, doi:[10.1016/j.chroma.2020.461371](https://doi.org/10.1016/j.chroma.2020.461371).



Contents lists available at ScienceDirect

Journal of Pharmaceutical and Biomedical Analysis

journal homepage: www.journals.elsevier.com/journal-of-pharmaceutical-and-biomedical-analysis

Macrocyclic glycopeptides- and derivatized cyclofructan-based chiral stationary phases for the enantioseparation of fluorinated β -phenylalanine analogs

Dániel Tanács^a, Róbert Berkecz^a, Sayeh Shahmohammadi^b, Enikő Forró^b,
Daniel W. Armstrong^c, Antal Péter^a, István Ilisz^{a,*}

^a Institute of Pharmaceutical Analysis, Interdisciplinary Excellence Centre, University of Szeged, Somogyi u. 4, H-6720 Szeged, Hungary

^b Institute of Pharmaceutical Chemistry, University of Szeged, Eötvös u. 6, H-6720 Szeged, Hungary

^c Department of Chemistry and Biochemistry, University of Texas at Arlington, Arlington, TX 76019-0065, USA

ARTICLE INFO

Keywords:

Superficially porous particles
Enantioselective separation
Macrocyclic glycopeptide-based chiral stationary phases
Cyclofructan-6-based chiral stationary phases
Fluorinated β -phenylalanines

ABSTRACT

The enantioseparation of five fluorinated β -phenylalanine analogs together with the nonfluorinated α - and β -phenylalanines has been investigated utilizing chiral stationary phases. The employed chiral selectors include macrocyclic antibiotics, such as vancomycin, teicoplanin, and teicoplanin aglycone, isopropyl carbamate functionalized cyclofructan-6, and *Cinchona* alkaloid-based *tert*-butyl carbamate quinine, all covalently bonded to 2.7 μ m superficially porous silica particles. The applied conditions included reversed-phase and polar-ionic modes where the vancomycin-, and the cyclofructan-6-based core-shell particles proved to offer suitable efficiency. Under reversed-phase conditions typical hydrophobic chromatographic behavior was observed, especially in the H₂O/MeOH system. The improved selectivity with increasing MeOH content observed in polar ionic mode suggests that H-bonding may not play a major role in the chiral recognition. The stoichiometric displacement model was probed to gather information on the ionic interactions. The ion-exchange process was found to affect retention, but it has no essential contribution to chiral recognition. Without paying special attention to the optimization of the system volume of the UHPLC instrument plate heights varying in the range of 10–50 μ m were obtained. In all cases, retention and selectivity decreased with increasing temperature, and enthalpy-driven enantioselectivity was observed. Elution sequences were determined in all cases.

1. Introduction

Enantiomerically pure β -aryl-substituted β -amino acids are important compounds from both biological and chemical aspects and are widely investigated in drug research [1]. Some are used in the synthesis of novel antibiotics [2] and analgesic endomorphin-1 analog tetrapeptides [3]. Owing to the significantly different characteristics of the C–F bond, replacing one or more hydrogen atoms in a compound by fluorine, a considerable difference in biological activity can be expected. Due to their importance in the design and synthesis of potential pharmaceutical drugs fluorinated amino acids have gained increasing attention [4]. For example (±)-eflornithine is used for the treatment of trypanosomiasis [5] and facial hirsutism in women [6]. To be able to determine enantiomeric purities and to optimize the synthetic routes using fluorinated precursor molecules, i.e. chiral synthons, enantioselective separation

assays must be developed.

The various possibilities for direct stereoselective analyses of chiral molecules, including amino acids, have been reviewed in many papers and book chapters [7,8]. Despite the vast literature chiral analysis, examples of liquid chromatography-based enantioselective separations of fluorinated amino acids are limited. In the early 2000s, ligand-exchange micellar capillary chromatography was applied for the enantioseparation of fluorine-substituted phenylalanine analogs [9], while stereoisomers of nonproteogenic polyfluoroamino acids and peptides were resolved on Chiralcel OD-H [10]. For the enantioseparation of five -NHBoc and -CO₂Et protected fluorinated cyclic β^3 -amino acid analogs and their nonfluorinated counterparts polysaccharide-based chiral stationary phases (CSPs) were applied [11]. Very recently *Cinchona* alkaloid-based zwitterionic CSPs have been successfully utilized for the enantioseparation of fluorinated β -phenylalanine derivatives [12].

* Correspondence to: Institute of Pharmaceutical Analysis, University of Szeged, Somogyi B. u. 4, H-6720 Szeged, Hungary.
E-mail address: ilisz.istvan@szte.hu (I. Ilisz).

<https://doi.org/10.1016/j.jpba.2022.114912>

Received 5 April 2022; Received in revised form 20 June 2022; Accepted 23 June 2022

Available online 26 June 2022

0731-7085/© 2022 The Authors. Published by Elsevier B.V. This is an open access article under the CC BY license (<http://creativecommons.org/licenses/by/4.0/>).

In SFC due to the lower eluent viscosity columns with smaller particle sizes have become more widespread [13–15]. However, today numerous liquid phase enantioselective separations are being carried out on traditional HPLC systems, utilizing typically chiral columns of fully porous particles (FPPs) of 5 μm . Thanks to the efficient functionalization of the selector molecules and the development of silica technology, a new generation of chiral columns based on core-shell particles (superficially porous particles, SPPs) and sub-2 μm FPPs opened a promising perspective in “chiral” liquid chromatography. Due to the intensive work of different research groups the most frequently applied chiral selectors were bonded to SPPs or FPPs resulting in very effective CSPs. Armstrong et al. [16] and Gasparrini et al. [17] used macrocyclic glycopeptides (teicoplanin, teicoplanin aglycone, vancomycin) for immobilization, while functionalized cyclofructans were linked to SPP and FPP support by Armstrong et al. [16,18]. Functionalized polysaccharides on SPP and FPP support were first applied by Chankvetadze et al. [19], while *Cinchona* alkaloid-based mono- and zwitterionic CSPs applying SPPs and FPPs was developed by Armstrong et al. [20] and Lämmerhofer et al. [21], respectively. It is worth noting that in addition to the above citations, some very recent review papers have summarized these new results [22–24].

The aims of this work are to explore the chromatographic behavior of fluorine-containing compounds of pharmaceutical relevance and to characterize the CSPs from both a kinetic and thermodynamic point of view. Another goal of this study was to develop methods using high-efficiency core-shell particles for liquid chromatography-based enantioselective separation of five fluorinated β -phenylalanine analogs and the nonfluorinated α - and β -phenylalanines. Applying both reversed-

phase (RP) and polar-ionic (PI) mobile phase systems permitted evaluation of the effects of bulk solvent composition, the nature, and concentration of various mobile phase components in the reversed-phase mode (RPM). This study focuses on general tendencies resulting from the structural peculiarities of the pharmacologically interesting fluorinated analytes, in the context of their enantioseparation on different core-shell particle-based CSPs. Evaluation of van Deemter plots provided a basis for the kinetic behavior while a separate thermodynamic characterization is also an integral part of this study. Knowing the absolute configuration of all the studied enantiomers their elution sequences also were determined.

2. Materials and methods

2.1. Chemicals and materials

Structures of the studied analytes are shown in Fig. 1. (S)- and (R)-phenylalanine (1) was purchased from Sigma-Aldrich (St Louis, MO, USA). Racemic amino acid 2 was prepared through ring cleavage of racemic 4-phenylazetidin-2-one with 18% HCl [25], while 3–7 were synthesized through condensation of the corresponding aldehydes with malonic acid in the presence of NH_4OAc in EtOH [26]. CAL-B (*Candida antarctica* lipase B)-catalyzed ring cleavage of 4-phenylazetidin-2-one resulted in phenyl-substituted β -amino acid (S)-2 with excellent *ee* ($\geq 99\%$) [25]. Enantiomeric fluorophenyl-substituted β -amino acids (S)-3–7 (*ee* $\geq 99\%$) were prepared through lipase PSIM (*Burkholderia cepacia*)-catalyzed hydrolysis of the corresponding racemic β -amino carboxylic ester hydrochlorides [26].

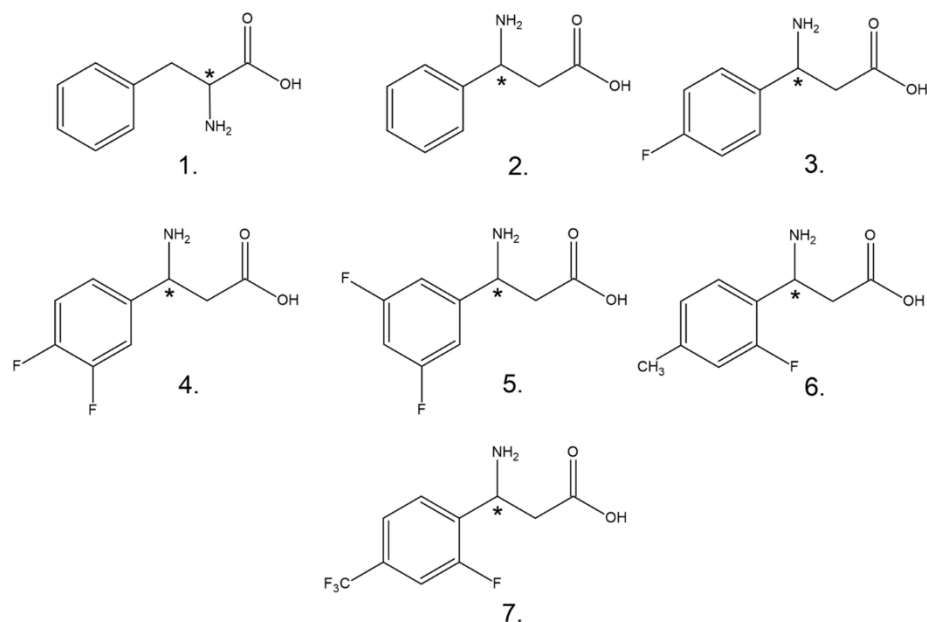


Fig. 1. Structure of analytes, 1, phenylalanine; 2, 3-amino-3-phenylpropanoic acid; 3, 3-amino-3-(4-fluorophenyl)propanoic acid; 4, 3-amino-3-(3,4-difluorophenyl)propanoic acid; 5, 3-amino-3-(3,5-difluorophenyl)propanoic acid; 6, 3-amino-3-(2-fluoro-4-methylphenyl)propanoic acid; 7, 3-amino-3-[2-fluoro-4-(trifluoromethyl)phenyl]propanoic acid.

Methanol (MeOH), acetonitrile (MeCN), and water of LC-MS grade, NH_3 dissolved in MeOH, triethylamine (TEA), formic acid (FA), glacial acetic acid (AcOH), and ammonium acetate (NH_4OAc) of analytical reagent grade were from VWR International (Radnor, PA, USA).

2.2. Apparatus and chromatography

The applied Waters® ACQUITY UPLC® H-Class PLUS UHPLC System with Empower 3 software (Waters Incorporation, Milford, MA, USA) consisted of a quaternary solvent manager, sample manager FTN-H, column manager, PDA detector, and QDa mass spectrometer detector.

Chiral selectors, used in this study are attached covalently to 2.7 μm silica-based SPPs. The core diameter and shell thickness of the SPPs were 1.7 μm and 0.5 μm , respectively. All columns have 100×3.0 mm i.d. or 100×2.1 mm i.d. dimensions (abbreviations for i.d. dimensions are:

3.0 and 2.1, respectively). Selectors of macrocyclic glycopeptide-based columns are vancomycin (VancoShell, V-3.0, and V-2.1), teicoplanin (TeicoShell, T-3.0 and T-2.1), teicoplanin aglycone (TagShell, Tag-3.0, and Tag-2.1). Isopropyl carbamate functionalized cyclofructan-6 (CF6-P-3.0 and CF6-P-2.1) and *Cinchona* alkaloid-based *tert*-butyl carbamate quinine (Q-Shell, Q-3.0) were also employed. All columns were obtained from AZYP (LLC, Arlington, TX, USA).

Stock solutions of analytes (1.0 mg mL^{-1}) were prepared in MeOH and diluted with the mobile phase. The hold-up time (t_0) of the columns was determined by 0.1% AcOH dissolved in MeOH and detected at 210 or 256 nm. The flow rate was set at 0.3 mL min^{-1} , which provided suitable efficiency for both column dimensions, and the column temperature at 20°C (if not otherwise stated).

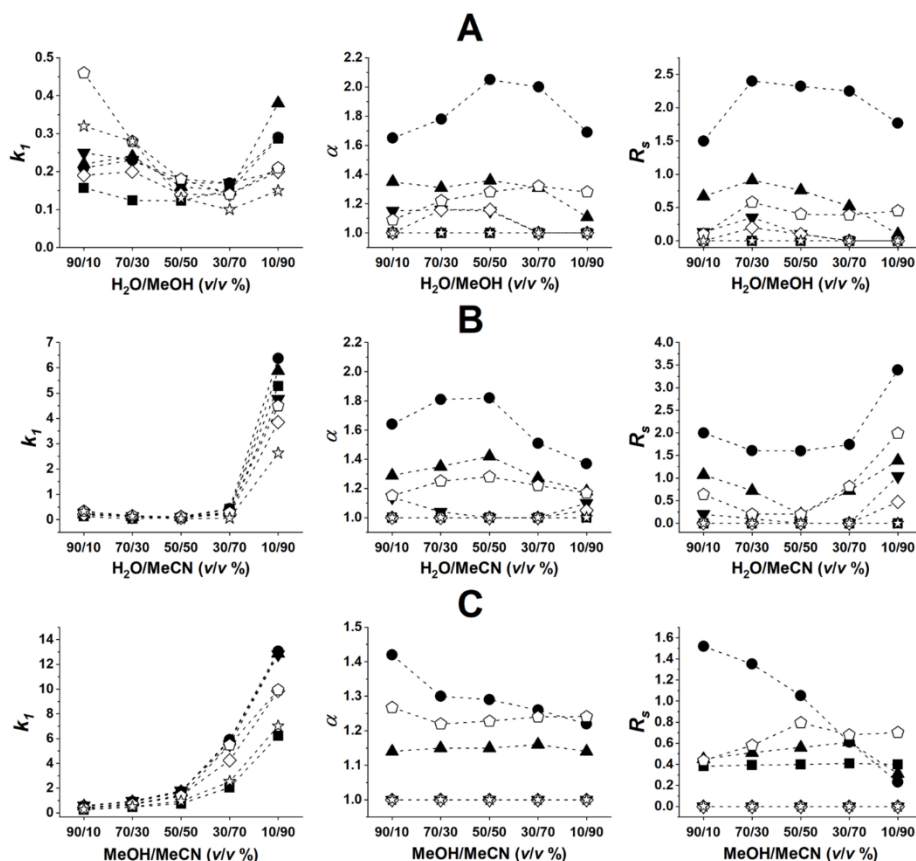


Fig. 2. Effect of bulk solvent composition on retention factor of first eluting enantiomer (k_1), separation factor (α), and resolution (R_s) on VancoShell CSP. Chromatographic conditions: column, VancoShell (V-3.0); mobile phase, A, $\text{H}_2\text{O}/\text{MeOH}$, 90/10–10/90 (v/v) containing 0.1% TEAA, B, $\text{H}_2\text{O}/\text{MeCN}$, 90/10–10/90 (v/v) containing 0.1% TEAA, C, MeOH/MeCN , 90/10–10/90 (v/v) containing 0.1% TEAA; detection, 215 nm; flow rate, 0.3 mL min^{-1} ; temperature, 20°C ; symbols, analyte 1, ■; 2, ●; 3, ▲; 4, ◻; 5, ○; 6, ◻; and 7, ☆.

3. Results and discussion

3.1. Separation of phenylalanine analogs on macrocyclic glycopeptide-based CSPs

For the separation of amino acids, amines, and organic acids, macrocyclic glycopeptide-based CSPs can be applied in different chromatographic modes, however, the best performances are usually achieved in polar ionic mode (PIM) and RPM. Among macrocyclic antibiotics, teicoplanin and teicoplanin aglycone-based CSPs are most frequently used for the enantioseparation of α - and β -amino acids [23]. Preliminary experiments revealed unexpectedly that despite the variation of mobile phase composition the teicoplanin-based T-3.0 CSP did not exhibit significant enantioselectivity either in RPM or PIM (data not shown). Under the same conditions, the teicoplanin aglycone-based Tag-3.0 CSP exhibited some separation ability for a few fluorinated β -phenylalanines (*vide infra*), while the vancomycin-based V-3.0 CSP provided the best results. Fig. 2 and Table S1 provide data for the separations achieved with V-3.0 CSP using RP mobile phase systems of H₂O/MeOH (90/10–10/90 v/v) (Fig. 2 A) or H₂O/MeCN (90/10–10/90 v/v) (Fig. 2B), all containing 0.1%(v/v) TEAA. The retention factor of the first eluting enantiomer (k_1) exhibited curve minima with increasing MeOH or MeCN content in both eluent systems. With increasing water content, typical hydrophobic chromatographic behavior, especially in the H₂O/MeOH system was observed. The increased retentions observed at higher MeOH or MeCN content can be explained by the decreased solvation shell of the ionized analytes and selector as well as the decreased solubility of these analytes in organic solvents. Interestingly, at high MeCN content, an order of magnitude higher k_1 values were observed compared to MeOH. The solvation (solubility) of ionized analytes in polar but aprotic MeCN is less favored, resulting in increased retention. The lowest k_1 values were obtained between 50% and 70%(v/v) MeOH or MeCN content of the RP mobile phase. Typically, selectivity peaked at 30–50%(v/v) organic content in the mobile phase, then decreased. Resolution values in the H₂O/MeOH system displayed similar α value trends in that they displayed maxima. In the H₂O/MeCN system, R_S values exhibited minimum curves with the highest R_S values registered at the highest MeCN content.

In PIM a mixture of MeOH (possessing polar and protic properties) and MeCN (as polar but aprotic solvent) together with acid and base additives are generally used. In PIM the MeOH/MeCN ratio was varied from 90/10–10/90 (v/v), and all mobile phases contained 0.1%(v/v) TEAA. As a result of the increase of MeCN content in the mobile phase, a significant increase in retention factors was obtained for all analytes (Fig. 2 C). At high MeCN content, the solvation of polar amino acids in the aprotic solvent decreases markedly resulting in high retentions, while the increasing ratio of protic MeOH favors the solvation of polar amino acids, *i.e.*, retention decreases. The stronger interaction with the CSP was not associated with enhanced enantioselectivity; α and R_S generally were greater at higher MeOH contents, especially for analyte 2. The improved selectivity with increasing MeOH content suggests that H-bonding may not play a major role in these enantioseparations.

As mentioned earlier, in the case of the teicoplanin aglycone-based CSP (Tag-3.0) moderate enantioselectivity could be achieved for some analytes. Applying the same eluent systems as for V-3.0, analytes 1, 6, and 7 could at least partially be enantioseparated (Fig. S1). The trends in the change of k_1 , α , and R_S values are similar to those observed on the V-3.0 column. Interestingly, the two CSPs with different structures exhibited complementary properties to the enantioselective recognition of α - and β -phenylalanine. Namely, α -phenylalanine could be effectively enantioseparated with Tag-3.0, but not with V-3.0, while β -phenylalanine with V-3.0, but not with Tag-3.0. Based on this observation the importance of steric contributions in the chiral recognition process is probable.

3.2. Evaluation of the stoichiometric displacement model

Both vancomycin- and teicoplanin aglycone-based selectors contain carboxyl and primary amino groups available for the ionic interactions with the amino or carboxyl group of the analyte. If ionic interactions have a determining role in the chiral recognition process it is supposed that the chromatographic ion-exchange mechanism can be described by the stoichiometric displacement model [27]. The model predicts a linear relationship between the logarithm of the retention factor and the logarithm of the counter-ion concentration for the retention behavior based on ion-pairing and ion-exchange mechanisms,

$$\log k = \log K_Z - Z \log c_{\text{counter-ion}} \quad (1)$$

where Z is the effective charge (ratio of the charge number of the analytes and the counter-ions), while K_Z describes the ion-exchange equilibrium. To check on the role of ionic interactions in the retention mechanism, the effects of counter-ion concentration on the chromatographic properties were examined on both V-3.0 and Tag-3.0 CSPs, applying optimized H₂O/MeOH, H₂O/MeCN, and MeOH/MeCN mobile phase conditions. In these experiments, the concentration of TEAA was varied in the range of 0.90–14.35 mM ensuring slightly acidic conditions, *i.e.*, the carboxyl group on both selector and select could be present in deprotonated form, while the primary amino groups could be protonated. According to the data summarized in Fig. S2 with increased counter-ion concentration reduced retention is obtained. The linear fittings (plotting $\log k$ against $\log c_{\text{counter-ion}}$) could be done with $R^2 > 0.98$ in all cases, where the slopes varied between -0.10 and -0.25 in the case of V-3.0, and between -0.01 and -0.11 in the case of Tag-3.0 column. It is worth mentioning that on both CSPs, practically equal slopes were calculated for each enantiomer, *i.e.*, no significant difference could be observed in the enantioselectivities with varying counter-ion concentration (data not shown). Based on these findings it can be stated that in the studied chromatographic systems the ion-exchange process affects retention, but has no vital role in chiral recognition.

3.3. Separation of β -phenylalanine analogs on cyclofructane-6-based CSP

Cyclofructans (CFs) belong to the macrocyclic oligosaccharide family and are composed of 6 or more β -2,1 linked D-fructofuranose subunits [28]. It is important to note that the so-called CF6, containing six fructofuranose units does not have a central hydrophobic cavity, accordingly the formation of a hydrophobic inclusion complex (like in the case of cyclodextrins) is not possible. Their central core exhibits a similar structure as the 18-crown-6 crown ether, which is the reason why the chromatographic behavior resembles that of the crown ethers. Unlike the case of synthetic crown ethers, the amine group of the analyte does not have to be protonated and enantioselective interactions can occur in organic solvents and supercritical CO₂ rather than aqueous solvents [29].

Enantioseparations on cyclofructan-based CSPs generally are carried out in normal-phase mode and PIM [22]. Taking the solubility of amino acids into consideration, separations were carried out in the PIM using MeOH/MeCN as a bulk solvent in the presence of TFA and TEA as acid and base additives. Since the primary amino group and its interaction with core cyclofructan O-atoms play an important role in the enantioselective recognition mechanism, first the effects of the concentration of acid, and the acid to base ratio were investigated. Fig. 3 A depicts the effects of the TFA/TEA ratio in the MeOH/MeCN 10/90 (v/v) mobile phase for the selected analytes 1, 2, 3, and 7. As can be seen in Fig. 3 A, k_1 slightly decreases with an increase in the TFA/TEA ratio, while α and R_S vary only slightly, but are usually somewhat better at ca. TFA:TEA 3:2 ratio. Keeping the TFA/TEA ratio at 3:2 their amount was varied between 0.15/0.10 (v/v%)–0.60/0.40 (v/v%) (Fig. 3B). With increasing TFA/TEA concentration k_1 slightly decreases, α does not change significantly, while R_S showed its maximum value at TFA:TEA 0.15:0.10 (v/v%) or

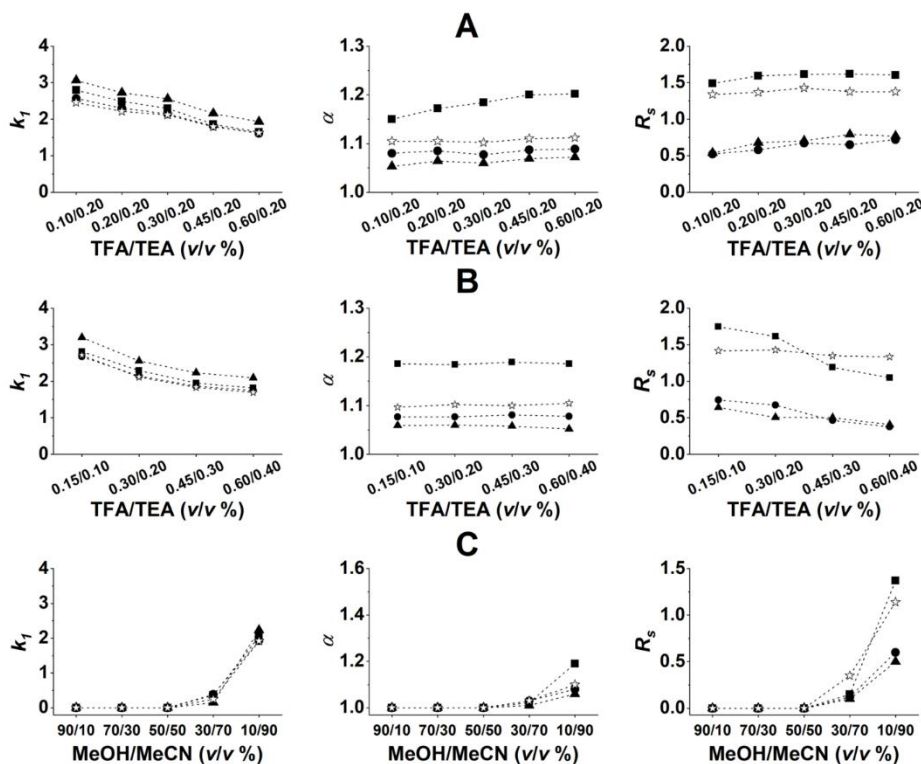


Fig. 3. Effect of A, TFA/TEA ratio, B, TFA/TEA concentration and C, MeOH/MeCN bulk solvent composition on retention factor of first eluting enantiomer (k_1), separation factor (α), and resolution (R_s) of analytes 1, 2, 3, and 7 on LarihcShell-P CSP. Chromatographic conditions: column, LarihcShell-P (CF6-P-3.0); mobile phase, MeOH/MeCN, 10/90 (v/v) containing TFA/TEA in concentration of A, 0.10/0.20, 0.20/0.20, 0.30/0.20, 0.45/0.20 and 0.60/0.20 (v/v%), B, 0.15/0.10, 0.30/0.20, 0.45/0.30 and 0.60/0.40 (v/v%) and C, MeOH/MeCN, 90/10–10/90 (v/v) containing 0.3% TFA and 0.2% TEA; detection, 215 nm; flow rate, 0.3 ml min⁻¹; temperature, 20 °C; symbols, analyte 1, ■; 2, ●; 3, ▲; 4, ▼; 5, ◊; 6, ○; and 7, ☆.

0.30:0.20 (v/v%) concentration. TFA has a strong ion-pairing character and the trifluoroacetate-anion may interact with the protonated amino group of the amino acids. Therefore, less protonated amino groups are available for the interaction with O-atoms of the CF-6 ring, and retentions slightly decrease.

In the PIM the effect of bulk solvent composition was studied in a MeOH/MeCN 90/10–10/90 (v/v) mobile phase containing 0.3%(v/v) TFA and 0.2%(v/v) TEA. According to the data illustrated in Fig. 3 C, analytes were considerably retained only when the MeCN content exceeded 70%(v/v). The high concentration of aprotic MeCN hinders solvation of polar amino acids in the mobile phase leading to increased retention. As concerns α and R_s values, they behave differently than in the case of V-3.0 CSP (Fig. 3 C vs. Fig. 2 C). The improved selectivity with increasing MeCN content suggests that stereoselective hydrogen bonding interactions between amino acids and isopropyl carbamate moiety of the selector take part in chiral recognition.

Functionalized *Cinchona* alkaloids (quinine and quinidine) are frequently applied for the chiral recognition of amino acid enantiomers [30–32]. For a set of experiments a CSP of *tert*-butylcarbamate quinine

immobilized on SPP support (Q-Shell, Q-3.0) was tested. A weak-anion exchange process between the protonated quinuclidine moiety of the chiral selector and the free carboxyl group of the analyte was assumed to take place. Contrary to our expectations, the Q-3.0 CSP did not exhibit considerable enantiorecognition ability applying *aq*.NH₄OAc/MeOH mobile phase systems. Variation of H₂O/MeOH bulk solvent composition between 90/10–10/90 (v/v) containing 100 mM NH₄OAc revealed that k_1 increases significantly with increasing water content, but chiral recognition could not be achieved except for analytes 2 and 3 for which a partial separation was registered (data not shown).

As concerns elution sequences on macrocyclic glycopeptide phases $S < R$ was observed. However, on cyclofructan-6- and *Cinchona* alkaloid-based CSPs, the opposite, $R < S$ elution order was observed. Selected chromatograms for the chiral separation of enantiomers of the studied analytes are depicted in Fig. 4. Also, it should be noted that baseline enantiomeric separation of all these analytes can be achieved by lowering the temperature.

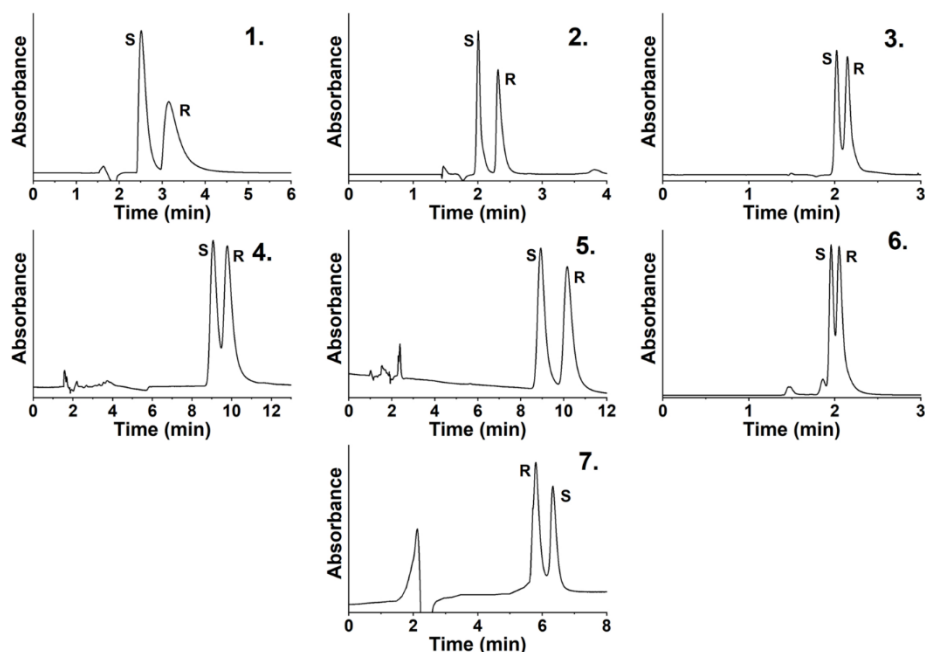


Fig. 4. Selected chromatograms Chromatographic conditions: column, for analyte 1, TagShell (Tag-3.0), for 2–6, VancoShell (V-3.0), and for 7, LarihcShell-P (CF6-P-3.0); mobile phase, for analyte 1 and 6, H₂O/MeOH/TEAA, 10/90/0.1 (v/v/v), for 2 and 3, H₂O/MeOH/TEAA 70/30/0.1 (v/v/v), for 4 and 5, H₂O/MeCN/TEAA, 10/90/0.1 (v/v/v), and for 7, MeOH/MeCN 10/90 (v/v) containing 0.3 mM TFA and 0.2 mM TEA; detection, 215 nm; flow rate, 0.3 ml min⁻¹; temperature, 20 °C.

3.4. van Deemter analysis

For the determination of van Deemter plots, mobile phases ensuring best separations and relatively low backpressures were selected. CSPs of

both column dimensions (i.d. 3.0 and 2.1 mm) were studied to gain information about column kinetics.

In the case of VancoShell CSP a mobile phase of H₂O/MeCN 30/70 (v/v) containing 0.1% TEAA (for analytes 2, 3, and 6) was selected.

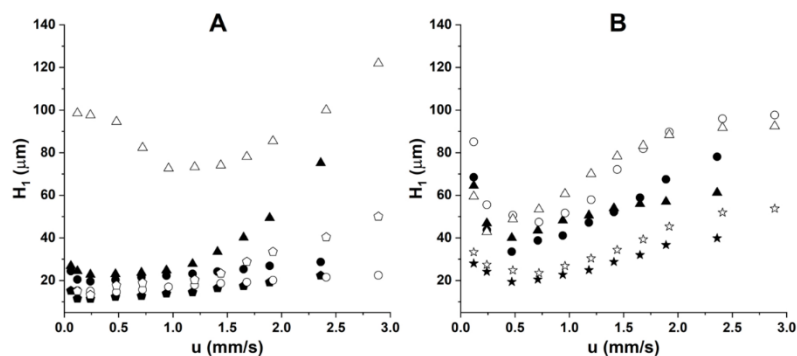


Fig. 5. van Deemter plots on VancoShell (A) and LarihcShell (B) CSPs, Chromatographic conditions: columns, A, VancoShell, V-3.0 and V-2.1, and B, LarihcShell-P, CF6-P-3.0 and CF6-P-2.1; mobile phase, A, H₂O/MeCN (30/70 v/v) containing 0.1% TEAA and B, MeOH/MeCN (10/90 v/v) containing 0.3 mM FA and 0.2 mM TEA; flow rate, 0.025–2.0 ml min⁻¹; detection, 256 nm; temperature, 20 °C; symbols, A, analyte 2, 3 and 6 on column V-3.0, ●, ▲, ●, respectively, and on column V-2.1, ○, △, □, respectively, and B, symbols, analyte 2, 3, and 7 on column CF6-P-3.0, ●, ▲, ★, respectively, and on column CF6-P-2.1, ○, △, ☆, respectively.

On V-3.0 and V-2.1 CSPs the curves for the first eluting enantiomer show a slight minimum for all studied analytes at ~ 0.2 – 0.3 mm sec⁻¹ linear flow rate, however, this minimum for analyte 3 on V-2.1 CSP was shifted to ~ 1.0 – 1.2 mm sec⁻¹ (Fig. 5A). Interestingly, for analyte 2 the H-u plot on the V-2.1 column runs below the plot determined for V-3.0. It is worth noting that for analyte 3, the H value for the first eluting enantiomer drastically increases with higher flow rates.

Van Deemter plots for analytes 2, 3, and 7 on LarihcShell-P CSPs were determined by using a mobile phase of MeOH/MeCN 10/90 (v/v) containing 0.3%(v/v) FA and 0.2%(v/v) TEA. On both CF6-P-3.0 and CF6-P-2.1 CSPs in the PIM, the curves for the first eluting enantiomer show characteristic minima at ~ 0.5 mm sec⁻¹ linear flow rate (Fig. 5B). The H minima on CF6-P-3.0 and CF6-P-2.1 generally was higher than on V-3.0 and V-2.1 CSPs.

It should be mentioned that 2.1 mm i.d. columns were usually less efficient than the 3.0 mm ones for both types of selectors. This might be explained that column packing for the 2.1 mm is not ideal, compared to the 3.0 mm, however, wall effects may also contribute to worse efficiencies registered with the 2.1 mm columns. In this study we have not paid special attention to physically optimizing the UHPLC instrument for the measurements with the core-shell particle-based columns. The obtained plate heights (H_{min}) generally varied in the range of 10–50 μ m. Comparing these results with the literature, it is clear that H_{min} very strongly depends on the nature of analytes, and similar examples can be found for other macrocyclic glycopeptide-based SPP CSPs [33,34]. The system volume of the UHPLC instrument was not optimized and lowering the extra-column effects may lead to a reduced H_{min} to some extent.

3.5. Thermodynamic characterization

In chiral separations, temperature effects on retention and selectivity can be evaluated using the van't Hoff equation in the form of

$$\ln \alpha = -\frac{\Delta(\Delta H^\circ)}{RT} + \frac{\Delta(\Delta S^\circ)}{R} \quad (2)$$

here α is the selectivity factor, $\Delta(\Delta H^\circ)$ and $\Delta(\Delta S^\circ)$ are the differences in standard enthalpy and standard entropy, R is the universal gas constant, T is the temperature in degrees Kelvin. Utilizing Eq. 2, the problems related to the determination of the phase ratio can be excluded, however, the obtained thermodynamic parameters will still contain both enantioselective and nonselective contributions as discussed by Asnin

and Stepanova [35].

The effects of temperature on chromatographic parameters were studied for analytes 2–6 on V-3.0 (analytes 1 and 7 exhibited no separation on V-3.0) in the temperature range 5–50 °C. As discussed above, both in the RPM and PIM, retention and enantioselectivity depend on mobile phase composition. To explore how the changes in eluent composition affect the thermodynamic temperature dependence, studies were carried out with different mobile phase compositions. In RPM H₂O/MeOH 70/30 and 10/90 (v/v), and H₂O/MeCN 70/30 and 10/90 (v/v), while in PIM MeOH/MeCN 70/30 and 30/70 (v/v), all containing 0.1%(v/v) TEAA eluents were employed. Data presented in Table S2 reveal, that in all cases retention and selectivity decrease with increasing temperature. Resolution in most cases decreased with increasing temperature, but in a few cases, a maximum curve was registered for R_S with increasing temperature.

When calculating thermodynamic parameters (based on Eq. 2) except for analyte 6, all of the plots of $\ln \alpha$ vs. $1/T$ could be fitted with straight lines with good correlation coefficients ($R^2 > 0.97$). According to the data in Table 1 the $\Delta(\Delta H^\circ)$ and $\Delta(\Delta S^\circ)$ exhibit negative values in all cases. The negative $\Delta(\Delta H^\circ)$ and $\Delta(\Delta S^\circ)$ values mean a stronger complex formation between the selector and the second eluted enantiomer, while the negative entropy was less favorable for enantioseparation. At a given mobile phase composition, the non-fluorinated analog (2) possesses the most negative $\Delta(\Delta H^\circ)$ and $\Delta(\Delta S^\circ)$ values. Analyte 6, which contains an electron-withdrawing (F-atom) and an electron-donating moiety (methyl group), in most cases, exhibited different behavior. As Fig. 6 illustrates the $\ln \alpha$ vs. $1/T$ plots could only be fitted with exponential curves, suggesting different overall binding situations in the limited temperature ranges. Based on the data presented in Table 1, it can be stated that under RP conditions the $\Delta(\Delta H^\circ)$ and $\Delta(\Delta S^\circ)$ values are considerably affected by the eluent composition. In both eluent systems markedly more negative $\Delta(\Delta H^\circ)$ and $\Delta(\Delta S^\circ)$ values were obtained in eluents with higher H₂O content. Unfortunately, in PIM no enantioselectivity could be achieved for analytes 4 and 5, while in the case of analyte 6 a distinct behavior was observed, as mentioned above. The rather limited data show more negative $\Delta(\Delta H^\circ)$ and $\Delta(\Delta S^\circ)$ values with higher MeCN content, as we described in the case of Cinchona alkaloid-based CSPs [12].

On CF6-P-3.0 CSP the effect of temperature on the enantioseparation was studied with a mobile phase of MeOH/MeCN 10/90 (v/v) containing 0.3%(v/v) TFA and 0.2%(v/v) TEA (Table 2 and Table S3). The analytes behave similarly that in the case of V-3.0 CSP, i.e., k_t , α , and R_S

Table 1
Effects of eluent composition on the thermodynamic parameters of analytes 2–6 on VancoShell (V-3.0) CSP.

Analyte	Temp. range (°C)	$-\Delta(\Delta H^\circ)$ (kJ mol ⁻¹)	$-\Delta(\Delta S^\circ)$ (J mol ⁻¹ K ⁻¹)	$-\Delta(\Delta G^\circ)_{298\text{ K}}$ (kJ mol ⁻¹)	T_{iso} (°C)	Q					
A, Mobile phase H ₂ O/MeOH (v/v)											
		70/30	10/90	70/30	10/90	70/30	10/90	70/30	10/90		
2	5-50	5.69	4.26	14.64	10.04	1.33	1.26	115.6	150.8	1.30	1.42
3	5-50	3.23	3.04	8.80	8.28	0.60	0.57	93.4	94.1	1.23	1.23
4	5-40	1.72	–	4.67	–	0.33	–	95.0	–	1.24	–
5	5-30	2.28	–	6.55	–	0.32	–	74.5	–	1.17	–
B, Mobile phase H ₂ O/MeCN (v/v)											
		70/30	10/90	70/30	10/90	70/30	10/90	70/30	10/90	70/30	10/90
2	5-50	7.16	4.62	19.62	13.12	1.31	0.70	91.8	78.7	1.22	1.18
3	5-50	3.79	2.33	10.50	6.58	0.66	0.37	88.3	90.99	1.21	1.119
4	5-50	3.94*	1.19	12.85*	3.28	0.11*	0.21	33.33*	88.28	1.03*	1.21
5	5-50	–	0.80	–	2.27	–	0.12	–	79.56	–	1.18
C, Mobile phase MeOH/MeCN (v/v)											
		70/30	30/70	70/30	30/70	70/30	30/70	70/30	30/70	70/30	30/70
2	10-50	2.54	2.56	6.64	6.81	0.61	0.51	117.6	100.6	1.31	1.25
3	5-50	1.39	1.53	3.66	4.02	0.30	0.33	107.5	106.8	1.28	1.28

Chromatographic conditions: column, VancoShell (V-3.0); mobile phase, A, H₂O/MeOH 70/30 (v/v) and H₂O/MeOH 10/90 (v/v); B, H₂O/MeCN 70/30 (v/v) and H₂O/MeCN 10/90 (v/v); C, MeOH/MeCN 70/30 (v/v) and MeOH/MeCN 30/70 (v/v) all containing 0.1% TEAA; detection, 215 nm; $\ln \alpha$ vs. $1/T$ curves; T_{iso} , temperature where the enantioselectivity cancels; Q = $\Delta(\Delta H^\circ)/298 \times \Delta(\Delta S^\circ)$

^a temperature range: 5–25 °C

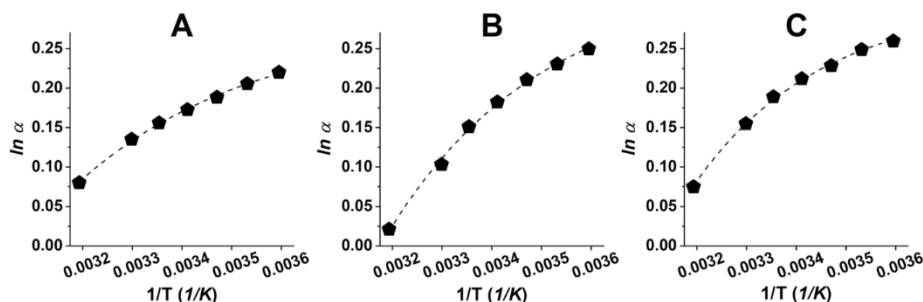


Fig. 6. $\ln \alpha$ vs. $1/T$ curves for analyte 6 on VancoShell CSP, Chromatographic conditions: column, VancoShell V-3.0; mobile phase, A, $\text{H}_2\text{O}/\text{MeOH}/\text{TEAA}$, 70/30/0.1 (v/v/v), B, $\text{H}_2\text{O}/\text{MeCN}$, 70/30 (v/v/v) C, MeOH/MeCN , 30/70/0.1 (v/v/v); detection, 215 nm; flow rate, 0.3 ml min⁻¹; temperature, 5–50 °C; symbol analyte 6, ●.

Table 2
Thermodynamic parameters determined on LarichShell-P (CF6-P-3.0) CSP.

Compound	$-\Delta(\Delta H^\circ)$ (kJ mol ⁻¹)	$-\Delta(\Delta S^\circ)$ (J mol ⁻¹ K ⁻¹)	$-\Delta(\Delta G^\circ)_{298\text{ K}}$ (kJ mol ⁻¹)	T_{iso} (°C)	Q
1	2.62	7.51	0.38	75.8	1.17
2	1.60	4.82	0.16	58.6	1.11
3	1.26	3.78	0.13	60.7	1.12
4	1.41	4.34	0.12	51.5	1.04
5	1.49	4.25	0.22	77.5	1.18
6	0.91	2.37	0.20	108.6	1.28
7	0.60	1.25	0.23	207.0	1.61

Chromatographic conditions: column, LarichShell-P (CF6-P-3.0); mobile phase, MeOH/MeCN 10/90 (v/v) containing 0.3%(v/v) FA and 0.2%(v/v) TEA; detection, 215 nm; temperature range, 5–50 °C; $\ln \alpha$ vs. $1/T$ curves; T_{iso} , temperature where the enantioselectivity cancels; $Q = \Delta(\Delta H^\circ)/298 \times \Delta(\Delta S^\circ)$; temperature range, 5–50 °C

decrease with increasing temperature. Concerning the thermodynamic parameters values were similar in magnitude to those obtained in PIM with V-3.0 CSP. On CF6-P-3.0 CSP α - and β -phenylalanine exhibited the most negative $\Delta(\Delta H^\circ)$ and $\Delta(\Delta S^\circ)$ suggesting that the fluoro substitution reduced the differences experienced by the enantiomers in the process of chiral recognition.

To reveal the contribution of the enthalpy and entropy terms to the enantioseparation $Q = \Delta(\Delta H^\circ)/[T \times \Delta(\Delta S^\circ)]$; $T = 298\text{ K}$ values were also calculated. According to the data in Tables 1 and 2 all the enantio-recognition processes were enthalpically driven, $Q > 1.0$ indicating the relatively higher contribution of enthalpy to the free energy. For the separation of enantiomers.

an interesting consequence is that there is a temperature, the so-called "isoeutropic" temperature (T_{iso}), where the two enantiomers coelute since entropy and enthalpy changes compensate each other. In this study, in all cases T_{iso} was outside the studied temperature range (Tables 1 and 2).

4. Conclusions

Applying teicoplanin-, teicoplanin aglycone-, vancomycin-, *tert*-butylcarbamate quinine-, and cyclofructan-6-based CSPs under RP and PI conditions, the vancomycin- and the cyclofructan-6-based CSPs were found to exhibit sufficient effectiveness in the enantiomeric separation of α -phenylalanine, β -phenylalanine and its fluorinated analogs. Baseline separation could be achieved with vancomycin-based CSP for four analytes, with cyclofructan-6-based CSP for two analytes, while with teicoplanin aglycone-based CSP for one analyte. In the case of vancomycin-based CSP, the hydrophobic chromatographic behavior

observed with increasing water content is explained by the decreased solvation shell of the ionized analytes and selector. The high increase in retention factors obtained for all analytes with increased MeCN content in PIM was due to the decreased solubility of the polar analytes. Utilizing the stoichiometric displacement model for a description of a possible ion-exchange mechanism, long-range ionic interactions were found to play a negligible role in the chiral recognition process in the case of vancomycin- and teicoplanin aglycone-based selectors. The cyclofructan-6-based CSP offers a markedly different recognition mechanism, which led to baseline separation for the studied analytes in the PIM and a reversal in the enantiomeric elution order. Under PIM conditions, with increasing MeCN content, improved selectivity was observed, suggesting that hydrogen bonding interactions may play a role in the enantio-recognition in the case of cyclofructan-6-based CSP.

The thermodynamic characterization carried out under RP conditions in the case of vancomycin-based CSP revealed that changes in the eluent composition markedly affected the differences in standard enthalpy and standard entropy, without significantly affecting the enthalpy and entropy contributions in the enantioseparation process. Analyses of van Deemter plots in both PIM and RPM confirmed a typical shape with a plate height minima and a flat C-term dependence in most cases. The kinetic characterization provided evidence that the 3.0 i.d. columns outperform the 2.1 mm columns, probably due to wall effects. In this study data were handled without corrections for the extra-column volume of the instrument. The advantageous features of core-shell particles, namely offering the possibility of high-speed enantioseparations and reduced solvent consumption compared to 5- μm particle-based "traditional" columns are worth exploiting.

Declaration of Competing Interest

The authors declare that they have no known competing financial interests or personal relationships that could have appeared to influence the work reported in this paper.

Data availability

Data will be made available on request.

Acknowledgments

This work was supported by National Research, Development and Innovation Office-NKFI through projects K137607 and K129049. Project no. TKP2021-EGA-32 has been implemented with the support provided by the Ministry of Innovation and Technology of Hungary from the National Research, Development and Innovation Fund, financed

under the TKP2021-EGA funding scheme.

Appendix A. Supporting information

Supplementary data associated with this article can be found in the online version at doi:10.1016/j.jpba.2022.114912.

References

- [1] E. Juaristi, V.A. Soloshonok. *Enantioselective Synthesis of β -Amino Acids*, second ed, Wiley, 2005.
- [2] M. Jin, M.A. Fischbach, J. Clardy, A biosynthetic gene cluster for the acetyl-CoA carboxylase inhibitor andrimid, *J. Am. Chem. Soc.* 128 (2006) 10660–10661, <https://doi.org/10.1021/ja063194c>.
- [3] G. Cardillo, L. Gentilucci, P. Melchiorre, S. Spampinato, Synthesis and binding activity of endomorphin-1 analogues containing β -amino acids, *Bioorg. Med. Chem. Lett.* 10 (2000) 2755–2758, [https://doi.org/10.1016/S0960-894X\(00\)00562-X](https://doi.org/10.1016/S0960-894X(00)00562-X).
- [4] J. Han, A.M. Remete, L.S. Dobson, L. Kiss, K. Izawa, H. Moriwaki, V.A. Soloshonok, D. O'Hagan, Next generation organofluorine containing blockbuster drugs, *J. Fluor. Chem.* 239 (2020), 109639, <https://doi.org/10.1016/j.jfluchem.2020.109639>.
- [5] J. Pepin, C. Guern, F. Milord, P.J. Schechter, Difluoromethylornithine for arseno-resistant trypanosoma brucei gambiense sleeping sickness, *Lancet* 330 (1987) 1431–1433, [https://doi.org/10.1016/S0140-6736\(87\)91131-7](https://doi.org/10.1016/S0140-6736(87)91131-7).
- [6] J.E. Wolf, D. Shander, F. Huber, J. Jackson, C.-S. Lin, B.M. Mathes, K. Schrode, Randomized, double-blind clinical evaluation of the efficacy and safety of topical eflornithine HCl 13.9% cream in the treatment of women with facial hair, *Int. J. Dermatol.* 46 (2007) 94–98, <https://doi.org/10.1111/j.1365-4632.2006.03079.x>.
- [7] I. Ilisz, A. Péter, W. Lindner, State-of-the-art enantioseparations of natural and unnatural amino acids by high-performance liquid chromatography, *TrAC Trends Anal. Chem.* 81 (2016) 11–22, <https://doi.org/10.1016/j.trac.2016.01.016>.
- [8] G.K.E. Scriba, *Chiral Separations*, Springer New York, New York, NY, 2019, <https://doi.org/10.1007/978-1-4939-9438-0>.
- [9] J.M. Lin, T. Hobo, Inspection of the reversal of enantiomer migration order in ligand exchange micellar electrokinetic capillary chromatography, *Biomed. Chromatogr.* 15 (2001) 207–211, <https://doi.org/10.1002/BMC.63>.
- [10] T. Tono, A. Nishikawa, T. Yajima, H. Nagano, K. Mikami, Fluorous substituent-based enantiomer and diastereomer separation: orthogonal use of HPLC columns for the synthesis of nonproteinogenic polyfluoro amino acids and peptides, *Eur. J. Org. Chem.* 2008 (2008) 1331–1335, <https://doi.org/10.1002/ejoc.200701052>.
- [11] G. Lajkó, T. Orosz, L. Kiss, E. Forró, F. Fülöp, A. Péter, I. Ilisz, High-performance liquid chromatographic enantioseparation of fluorinated cyclic β -amino acid derivatives on polysaccharide-based chiral stationary phases. Comparison with nonfluorinated counterparts, *Biomed. Chromatogr.* 30 (2016) 1441–1448, <https://doi.org/10.1002/bmc.3702>.
- [12] G. Némethi, R. Berkecz, S. Shahmohammadi, E. Forró, W. Lindner, A. Péter, I. Ilisz, Enantioselective high-performance liquid chromatographic separation of fluorinated β -phenylalanine derivatives utilizing Cinchona alkaloid-based ion-exchanger chiral stationary phases, *J. Chromatogr. A* (2022), 462974, <https://doi.org/10.1016/j.chroma.2022.462974>.
- [13] C.L. Barhate, I.A. Joyce, A.A. Makarov, K. Zawatzky, F. Bernardoni, W.A. Schafer, D.W. Armstrong, C.J. Welch, E.L. Regalado, Ultrafast chiral separations for high throughput enantiopurity analysis, *Chem. Commun.* 53 (2017) 509–512, <https://doi.org/10.1039/C6CC08512A>.
- [14] G.L. Losacco, H. Wang, I.A. Haidar Ahmad, J. Dasilva, A.A. Makarov, I. Mangion, F. Gasparri, M. Lämmerhofer, D.W. Armstrong, E.L. Regalado, Enantioselective UHPLC screening combined with in silico modeling for streamlined development of ultrafast enantiopurity assays, *Anal. Chem.* 94 (2022) 1804–1812, <https://doi.org/10.1021/acs.analchem.1c04585>.
- [15] C. West, Recent trends in chiral supercritical fluid chromatography, *TrAC Trends Anal. Chem.* 120 (2019), 115648, <https://doi.org/10.1016/j.trac.2019.115648>.
- [16] D.C. Patel, Z.S. Breitbach, M.F. Wahab, C.L. Barhate, D.W. Armstrong, Gone in seconds: praxis, performance, and peculiarities of ultrafast chiral liquid chromatography with superficially porous particles, *Anal. Chem.* 87 (2015) 9137–9148, <https://doi.org/10.1021/acs.analchem.5b00715>.
- [17] O.H. Ismail, M. Antonelli, A. Ciochi, M. De Martino, M. Catani, C. Villani, A. Cavazzini, M. Ye, D.S. Bell, F. Gasparri, Direct analysis of chiral active pharmaceutical ingredients and their counterparts by ultra high performance liquid chromatography with macrocyclic glycopeptide-based chiral stationary phases, *J. Chromatogr. A* 1576 (2018) 42–50, <https://doi.org/10.1016/j.chroma.2018.09.029>.
- [18] J. Yu, M. Wey, S.K. Firooz, D.W. Armstrong, Ionizable cyclofructan 6-based stationary phases for hydrophilic interaction liquid chromatography using superficially porous particles, 2021 849, *Chromatographia* 84 (2021) 821–832, <https://doi.org/10.1007/s10337-021-04063-6>.
- [19] K. Lomsadze, G. Jibuti, T. Farkas, B. Chankvetadze, Comparative high-performance liquid chromatography enantioseparations on polysaccharide based chiral stationary phases prepared by coating totally porous and core-shell silica particles, *J. Chromatogr. A* 1234 (2012) 50–55, <https://doi.org/10.1016/j.chroma.2012.01.084>.
- [20] D.C. Patel, Z.S. Breitbach, J.J. Yu, K.A. Nguyen, D.W. Armstrong, Quinine bonded to superficially porous particles for high-efficiency and ultrafast liquid and supercritical fluid chromatography, *Anal. Chim. Acta* 963 (2017) 164–174, <https://doi.org/10.1016/j.aca.2017.02.005>.
- [21] K. Schmitt, U. Woiwode, M. Kohout, T. Zhang, W. Lindner, M. Lämmerhofer, Comparison of small size fully porous particles and superficially porous particles of chiral anion-exchange type stationary phases in ultra-high performance liquid chromatography: effect of particle and pore size on chromatographic efficiency and kinetic, *J. Chromatogr. A* 1569 (2018) 149–159, <https://doi.org/10.1016/j.chroma.2018.07.056>.
- [22] R. Berkecz, G. Némethi, A. Péter, I. Ilisz, Liquid chromatographic enantioseparations utilizing chiral stationary phases based on crown ethers and cyclofructans, *Molecules* 26 (2021) 4648, <https://doi.org/10.3390/molecules26154648>.
- [23] R. Berkecz, D. Tanács, A. Péter, I. Ilisz, Enantioselective liquid chromatographic separations using macrocyclic glycopeptide-based chiral selectors, *Molecules* 26 (2021) 3380, <https://doi.org/10.3390/molecules26113380>.
- [24] A. Cavazzini, G. Nádai, F. Dondi, F. Gasparri, A. Ciochi, C. Villani, Study of mechanisms of chiral discrimination of amino acids and their derivatives on a teicoplanin-based chiral stationary phase, *J. Chromatogr. A* 1031 (2004) 143–158, <https://doi.org/10.1016/j.chroma.2003.10.090>.
- [25] E. Forró, T. Pál, G. Tasnádi, F. Fülöp, A new route to enantiopure β -aryl-substituted β -amino acids and 4-aryl-substituted β -lactams through lipase-catalyzed enantioselective ring cleavage of β -lactams, *Adv. Synth. Catal.* 348 (2006) 917–923, <https://doi.org/10.1002/asc.200505434>.
- [26] S. Shahmohammadi, F. Fülöp, E. Forró, Efficient synthesis of new fluorinated β -amino acid enantiomers through lipase-catalyzed hydrolysis, *Molecules* 25 (2020) 5990, <https://doi.org/10.3390/molecules25245990>.
- [27] W. Kopaciewicz, M.A. Rounds, J. Fausnaugh, F.E. Regnier, Retention model for high-performance ion-exchange chromatography, *J. Chromatogr. A* 266 (1983) 3–21, [https://doi.org/10.1016/S0021-9673\(01\)90875-1](https://doi.org/10.1016/S0021-9673(01)90875-1).
- [28] P. Sun, C. Wang, Z.S. Breitbach, Y. Zhang, D.W. Armstrong, Development of new HPLC chiral stationary phases based on native and derivatized cyclofructans, *Anal. Chem.* 81 (2009) 10215–10226, https://doi.org/10.1021/AC902257A/SUPPL_FILE/AC902257A_SI_001.PDF.
- [29] D. Roy, D.W. Armstrong, Fast super/subcritical fluid chromatographic enantioseparations on superficially porous particles bonded with broad selectivity chiral selectors relative to fully porous particles, *J. Chromatogr. A* 1605 (2019), 360339, <https://doi.org/10.1016/j.chroma.2019.06.069>.
- [30] T. Orosz, E. Forró, F. Fülöp, W. Lindner, I. Ilisz, A. Péter, Effects of N-methylation and amidation of cyclic β -amino acids on enantioselectivity and retention characteristics using Cinchona alkaloid- and sulfonic acid-based chiral zwitterionic stationary phases, *J. Chromatogr. A* 1535 (2018) 72–79, <https://doi.org/10.1016/j.chroma.2017.12.070>.
- [31] N. Grecsó, E. Forró, F. Fülöp, A. Péter, I. Ilisz, W. Lindner, Combinatorial effects of the configuration of the cationic and the anionic chiral subunits of four zwitterionic chiral stationary phases leading to reversal of elution order of cyclic β -amino acid enantiomers as ampholytic model compounds, *J. Chromatogr. A* 1467 (2016) 178–187, <https://doi.org/10.1016/j.chroma.2016.05.041>.
- [32] I. Ilisz, A. Bajtai, W. Lindner, A. Péter, Liquid chromatographic enantiomer separations applying chiral ion-exchangers based on Cinchona alkaloids, *J. Pharm. Biomed. Anal.* 159 (2018) 127–152, <https://doi.org/10.1016/j.jpba.2018.06.045>.
- [33] D. Tanács, R. Berkecz, A. Misicka, D. Tymecka, F. Fülöp, D.W. Armstrong, I. Ilisz, A. Péter, Enantioseparation of β -amino acids by liquid chromatography using core-shell chiral stationary phases based on teicoplanin and teicoplanin aglycone, *J. Chromatogr. A* 1653 (2021), 462383, <https://doi.org/10.1016/j.chroma.2021.462383>.
- [34] D. Polprechtová, K. Kalíková, K. Kadkhodaei, C. Reiterer, D.W. Armstrong, E. Teslová, M.G. Schmid, Enantioseparation performance of superficially porous particle vancomycin-based chiral stationary phases in supercritical fluid chromatography and high performance liquid chromatography; applicability for psychoactive substances, *J. Chromatogr. A* 1637 (2021), <https://doi.org/10.1016/j.chroma.2020.461846>.
- [35] I.D. Asnin, M.V. Stepanova, Van't Hoff analysis in chiral chromatography, *J. Sep. Sci.* 41 (2018) 1319–1337, <https://doi.org/10.1002/jssc.201701264>.



Contents lists available at ScienceDirect

Journal of Chromatography A

journal homepage: www.elsevier.com/locate/chroma

Enantioseparation of α -substituted proline analogs with macrocyclic glycopeptide-based chiral stationary phases immobilized on superficially porous particles of silica applying liquid chromatography with ultraviolet and mass spectrometric detection

Dániel Tanács^a, Róbert Berkecz^a, Daniel W. Armstrong^b, Antal Péter^a, István Ilisz^{a,*}

^a Institute of Pharmaceutical Analysis, University of Szeged, H-6720 Szeged, Somogyi utca 4, Hungary

^b Department of Chemistry and Biochemistry, University of Texas at Arlington, Arlington, TX 76019-0065, United States of America

ARTICLE INFO

Article history:

Received 22 February 2023

Revised 5 April 2023

Accepted 14 April 2023

Available online 14 April 2023

Keywords:

Liquid chromatography, Superficially porous particles, Enantioseparation of α -substituted proline analogs, Macrocyclic glycopeptide-based selectors, Thermodynamic and kinetic evaluation

ABSTRACT

In this study, the liquid chromatography-based direct enantioseparation of the stereoisomers of α -substituted proline analogs has been investigated utilizing chiral stationary phases with UV and/or mass spectrometric (MS) detection. Macrocyclic antibiotics, such as vancomycin, teicoplanin, modified teicoplanin, and teicoplanin aglycone, all covalently immobilized to 2.7 μ m superficially porous silica particles have been applied as stationary phases. Mobile phases utilizing mixtures of methanol and acetonitrile with different additives (polar-ionic mode) were optimized during method development. Best separations were achieved with mobile phases of 100% MeOH containing either 20 mM acetic acid or 20 mM triethylammonium acetate. Special attention was given to the applicability of MS-compatible mobile phases. Acetic acid was found to be advantageous as a mobile phase additive for MS detection.

Enantioselective chromatographic behaviors are interpreted based on the explored correlations between the analytes' structural features and those of the applied chiral stationary phases. For the thermodynamic characterization, separations were studied in the temperature range of 5–50 °C. Generally, retention and selectivity decreased with increasing temperature, and in most cases, enthalpy-driven enantioselectivity was observed, but entropic contributions also were present. Unexpectedly, unusual shapes for the van Deemter curves were registered in the kinetic evaluations. General trends could be observed in the enantiomeric elution orders: $S < R$ on VancoShell and NicoShell, and opposite $R < S$ on TeicoShell and TagShell columns.

© 2023 The Author(s). Published by Elsevier B.V.

This is an open access article under the CC BY license (<http://creativecommons.org/licenses/by/4.0/>)

1. Introduction

One of the most abundant biological macromolecules in all living cells is proteins, an important class of natural compounds with diverse biological functions. Many possess pharmacological activity, e.g., hormones, enzyme inhibitors, receptor ligands, antibiotics, neurotransmitters, etc. Lower molecular weight peptides, e.g., peptidomimetics and peptide-based therapeutics, are compounds of high importance in drug discovery research [1]. However, peptide therapies can be problematic when limited by poor absorption, proteolytic instability, undesirable side effects, and rapid elimination from the body. Generally, the all *L*-stereochemistry of the peptide's constituent amino acids can accentuate such

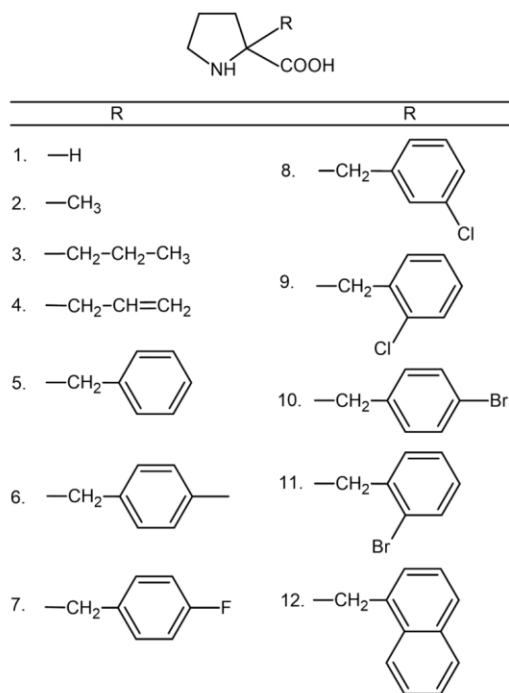
problems [1,2]. Chemical modifications of peptides, e.g., the substitution of an *L*-amino acid by the corresponding *D*-amino acid during peptide synthesis or incorporation of sterically constrained amino acids, are convenient options to enhance metabolic stability and modify pharmacological activity [3–5]. Among protein amino acids, proline is an attractive target moiety. It contains an α -imino group in a five-membered ring. When incorporated into peptides or peptidomimetics, the unique ring structure may develop special properties, such as conformational rigidity and enhanced chemical stability. Moreover, proline within a peptide chain may lead to the appearance of *cis/trans* isomerization [6,7] and induces strong type-II β -turns [8]. The biological importance of proline, especially the role of *D*-proline and its metabolism in living organisms, has recently been reviewed in several scientific papers and book chapters [9–13].

Since, in all living systems, the biological activity of chiral compounds strongly depends on their steric arrangement, identifying

* Corresponding author at: Institute of Pharmaceutical Analysis, University of Szeged, Somogyi B. u. 4, H-6720 Szeged, Hungary.
E-mail address: ilisz.istvan@szte.hu (I. Ilisz).

<https://doi.org/10.1016/j.chroma.2023.463997>

0021-9673/© 2023 The Author(s). Published by Elsevier B.V. This is an open access article under the CC BY license (<http://creativecommons.org/licenses/by/4.0/>)

Fig. 1. Structure of α -substituted proline analogs.

the absolute configuration of the chiral building blocks is required. Many scientific papers deal with separating amino acid stereoisomers and determining their location and configuration in the peptide sequence. In most analytical procedures, the stereochemistry of proteinic amino acids, after peptide hydrolysis, is determined by applying chiral or non-chiral derivatization before chromatographic separation [14–20]. It is worth noting that chiral stationary phases (CSPs) applied with subsequent mass spectrometric (MS) detection (e.g., HPLC-MS/MS) offer the advantage of enantiomeric separation and determination without any derivatization process thus, the pitfalls of the derivatization process (e.g., incomplete derivatization, racemization, kinetic resolution, etc.) can be avoided [19]. However, developing MS-compatible mobile phases is still challenging in “chiral chromatography”.

Despite the unique structural features of proline, relatively few papers have focused on the enantiomeric separation of its α -substituted analogs. Chiral analysis of hydroxyproline [20] and different α -substituted proline analogs [21,22] was performed on its *N*-derivatized form. The present paper focuses on the direct enantioseparation of the free form of highly constrained α -substituted proline analogs possessing either alkyl or aromatic side chains. The structures of the studied analytes are shown in Fig. 1.

Developing columns packed with highly efficient particles is one of the most challenging areas in “chiral chromatography”. The advantageous features of CSPs based on superficially porous silica particles have already been proved [23–25]. In this study liquid chromatographic analyses were carried out with macrocyclic

glycopeptide-based selectors such as vancomycin (VancoShell), teicoplanin (TeicoShell), teicoplanin aglycone (TagShell), and functionalized teicoplanin (NicoShell), all covalently bonded to 2.7 μ m high-efficiency superficially porous particles (SPPs).

Experiments were performed in the polar-ionic mode (PIM) utilizing columns with 3.0 and 2.1 mm internal diameters (i.d.). Effects of the nature and concentration of the mobile phase components, acid, and salt additives under various conditions were studied. Due to the lack of a chromophore in α -substituted proline analogs possessing alkyl side chains, optimizing conditions for chiral separation with MS detection was necessary. Since the configurations of all samples are known, the elution sequences were determined in all cases.

2. Materials and methods

2.1. Chemicals and reagents

(*R*)- and (*S*)-proline were purchased from Sigma-Aldrich (Steinheim, Germany). Racemic and enantiopure α -substituted proline analogs were obtained from BioQuadrant Inc. (Montreal, Quebec, Canada). Methanol (MeOH), acetonitrile (MeCN), and water of LC-MS grade, triethylamine (TEA), formic acid (FA), glacial acetic acid (AcOH), triethylammonium acetate (TEAA), trifluoroacetic acid (TFA), ammonium acetate (NH₄OAc), and ammonium formate (NH₄HCOO) of analytical reagent grade were from VWR International (Radnor, PA, USA).

2.2. Apparatus

The applied Waters® ACQUITY UPLC® H-Class PLUS UHPLC System (Waters Incorporation, Milford, MA, USA) consisted of a quaternary solvent manager, sample manager FTN-H, column manager, photodiode array (PDA) detector, and MS (QDa) detector. The QDa detector parameters were set: positive ion mode, probe temperature, 600 °C, capillary voltage, 1.5 V, cone voltage, 20 V. The UHPLC system was controlled with Empower 3 software.

Chiral selectors employed in this study are attached covalently to 2.7 μm silica-based SPPs. The core diameter and shell thickness of the SPPs were 1.7 μm and 0.5 μm , respectively. All columns have 100 \times 3.0 mm i.d. or 100 \times 2.1 mm i.d. dimensions. (Abbreviations for dimensions are: 3.0 mm i.d. and 2.1 mm i.d., respectively). Selectors of the macrocyclic glycopeptide-based columns are vancomycin (VancoShell, V-3.0, and V-2.1), teicoplanin (TeicoShell, T-3.0, and T-2.1), teicoplanin aglycone (TagShell, TAG-3.0, and TAG-2.1) and modified teicoplanin (NicoShell, N-3.0). All columns were obtained from AZYP LLC (Arlington, TX, USA).

Analyte stock solutions (1.0 mg mL⁻¹) were prepared in MeOH and diluted with the mobile phase. The columns' hold-up time (t_0) was determined with 0.1% AcOH dissolved in MeOH and detected at 210 or 256 nm. The flow rate and the column temperature were set at 0.3 mL min⁻¹ and 20 °C, respectively, if not otherwise stated.

3. Results and discussion

The investigated α -substituted proline analogs can be divided into two sub-groups: (i) those that contain an aliphatic moiety (2–4) with different chain lengths and (ii) those possessing an aromatic moiety (5–12) differing in nature and position of substituents on the aromatic ring. All these different structural features may affect the molecular characteristics (e.g., size and polarity of the solute), thus influencing the selector–analyte interactions.

For the preliminary investigations, six analytes were selected: proline (1), analytes 2 and 4 from α -substituted proline analogs possessing aliphatic side chains, and analytes 5, 6, and 10 from molecules possessing an aromatic moiety. Thus, all the critical structural features were represented, and the effects of different mobile phase additives, their concentration, the bulk solvent composition of the mobile phase, and the geometric size of the columns could be explored.

3.1. Effect of nature of mobile phase additives

Chiral separation of amino acids on macrocyclic glycopeptide-based CSPs can be performed in different chromatographic modes. The best performances are usually achieved in PIM with MeOH/MeCN as a bulk solvent in the presence of TEAA or in reversed-phase mode (RPM), applying MeOH or MeCN with aqueous TEAA [26–29]. In preliminary experiments, the teicoplanin-based T-3.0 column exhibited only moderate enantioselectivity by the variation of mobile phase composition either in RPM or PIM (data not shown). Under the same conditions, the teicoplanin aglycone-based TAG-3.0 CSP and the vancomycin-based V-3.0 CSP provided better results. Mobile phase additives may significantly affect enantioselectivity, therefore, the nature of different additives was first studied on V-3.0 and TAG-3.0 CSPs applying a mobile phase composition of MeOH/MeCN 80/20 (v/v) containing 20 mM additives. As examples of the observed effects, chromatograms obtained with analyte 5 are presented in Figure S1 in the Supplementary Materials. Based on these results, taking the peak shape, retention, resolution, and detection mode into account, applying TFA was less advantageous. The effects of FA, TEAA, NH₄HCOO, and NH₄OAc were found to strongly depend on the bulk

solvent composition of the mobile phase, the nature of the analyte, and the selector. From a chromatographic point of view, TEAA is a good choice, however, due to its ion suppression effect in the case of MS detection, applying AcOH as an additive is more advantageous. Based on these results, TEAA (with UV detection) or AcOH (with MS detection) was applied as a mobile phase additive in all further experiments.

3.2. Mobile phase selection

To study the influence of MeOH/MeCN ratio on the PIM enantioseparation, mobile phases composed of 100/0 – 20/80 (v/v) MeOH/MeCN containing 20 mM AcOH were employed, and the chromatographic properties of the preselected analytes (1, 2, 4, 5, 6, and 10) were recorded on V-3.0, TAG-3.0, and N-3.0 CSPs. Effective separations could not be observed on the N-3.0 column. Fig. 2 shows the results obtained with the V-3.0 and TAG-3.0 columns. On both columns, k_1 increases with increasing MeCN content; however, the increase in retention factor is most prominent at or above a 60/40 (v/v) MeOH/MeCN ratio. The change of mobile phase polarity can explain the retention behavior observed. The solvation of the polar amino acids decreases with increasing MeCN content (i.e., with increasing apolarity), leading to higher retentions, while increasing MeOH content results in a more polar mobile phase and better solvation, accompanied by decreased retentions. Additionally, all amino acids are less soluble in MeCN.

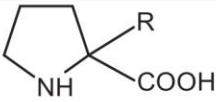
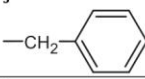
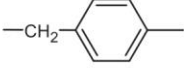
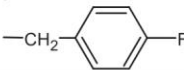
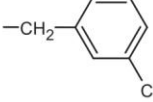
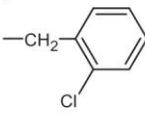
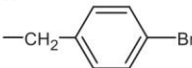
By examining the α and R_S values, it can be seen that they decrease (or are unchanged when there is no enantioseparation) with increasing MeCN content (Fig. 2). This indicates that the increased retentive interactions between the analyte and the selector with increasing MeCN content are not enantioselective. The highest α and R_S values were obtained at 100% MeOH concentration. Interestingly, comparing the two CSPs, k_1 values were higher on the TAG-3.0 column, while higher α and R_S values were registered on the V-3.0 column. It should be noted that under the applied conditions, enantiomers of 2 and 4 on the V-3.0 CSP, plus enantiomers of 1 on the TAG-3.0 CSP, could not be enantioresolved (Fig. 2).

For the purpose of comparison, the effect of the MeOH/MeCN ratio on chiral recognition of analytes 4, 5, 6, and 10 was studied by applying 20 mM TEAA instead of 20 mM AcOH with PDA detection. (Enantioseparation of 1 and 2 due to the lack of chromophore moiety could not be monitored with PDA detection). Results, depicted in Figure S2, indicate that the general trends observed in the change of k_1 , α , and R_S values as a function of MeOH/MeCN ratio are very similar to the ones observed in the presence of AcOH (Fig. 2), i.e., k_1 increases, while α and R_S decrease with increasing MeCN content. Interestingly, retention was much less in the presence of TEAA than in the case of AcOH, while selectivity and resolution were comparable. Contrary to the results obtained with AcOH, the N-3.0 CSP exhibited some separation ability for compounds 4, 5, 6, and 10 in the presence of TEAA (Fig. S2). Comparing the results obtained with the two additives, it can be concluded that the applicability of a mobile phase additive is usually a compromise between detection capability and chromatographic separation properties.

3.3. Structure-retention (selectivity) relationships

The sterically demanding structures of the macrocyclic glycopeptide-based CSPs and constrained α -substituted proline analogs (Fig. 1) influence the retention and the chiral recognition in several ways. Table 1 and Table S1 report the k_1 , α , and R_S values observed on V-3.0, T-3.0, TAG-3.0, and N-3.0 CSPs with the most effective two mobile phases applied, i.e., 100% MeOH containing either 20 mM AcOH or 20 mM TEAA. Investigation of the structure of the chiral selector in both applied eluent systems

Table 1Chromatographic data for the separation of α -substituted proline analogs on macrocyclic glycopeptide-based chiral stationary phases in the presence of AcOH as mobile phase additive.

Analyte (R)	Column	k_f	α	R_s	<i>e.e.o.</i>
					
1 —H	V-3.0 T-3.0 TAG-3.0 N-3.0	1.04 7.56 9.74 0.64	1.27 1.00 1.00 1.00	1.26 0.00 0.00 0.00	$R < S$ — — —
2 —CH ₃	V-3.0 T-3.0 TAG-3.0 N-3.0	0.57 8.15 9.19 0.38	1.00 1.46 1.41 1.00	0.00 1.65 2.52 0.00	— $S < R$ $S < R$ —
3 —CH ₂ —CH ₂ —CH ₃	V-3.0 T-3.0 TAG-3.0 N-3.0	0.31 7.64 2.54 0.25	1.00 1.00 2.32 1.00	0.00 0.00 1.90 0.00	— — $S < R$ —
4 —CH ₂ —CH=CH ₂	V-3.0 T-3.0 TAG-3.0 N-3.0	0.37 4.59 4.56 0.16	1.00 1.31 1.07 1.62	0.00 1.62 0.21 0.92	— $R < S$ $R < S$ $S < R$
5 	V-3.0 T-3.0 TAG-3.0 N-3.0	0.51 1.93 2.24 0.26	3.03 1.08 1.53 1.71	3.62 ~ 0.10 1.90 1.67	$S < R$ $R < S$ $R < S$ $S < R$
6 	V-3.0 T-3.0 TAG-3.0 N-3.0	0.40 1.88 2.31 0.15	2.96 1.13 1.67 1.98	3.68 0.71 2.16 1.96	$S < R$ $R < S$ $R < S$ $S < R$
7 	V-3.0 T-3.0 TAG-3.0 N-3.0	0.52 1.74 2.04 0.29	1.52 1.10 1.34 1.50	1.49 0.15 1.22 1.32	$S < R$ $R < S$ $R < S$ $S < R$
8 	V-3.0 T-3.0 TAG-3.0 N-3.0	0.55 1.49 2.10 0.30	2.34 1.13 1.18 1.59	3.36 0.18 0.60 1.80	$S < R$ $R < S$ $R < S$ $S < R$
9 	V-3.0 T-3.0 TAG-3.0 N-3.0	0.48 1.70 3.49 0.28	1.52 1.00 1.17 1.43	0.96 0.00 0.55 0.89	$S < R$ — $R < S$ $S < R$
10 	V-3.0 T-3.0 TAG-3.0 N-3.0	0.74 1.69 2.66 0.37	1.54 1.14 1.36 1.44	1.66 0.40 1.28 1.37	$S < R$ $R < S$ $R < S$ $S < R$

(continued on next page)

Table 1 (continued)

Analyte (R)	Column	k_1	α	R_s	e.e.o.
11 	V-3.0	0.59	1.33	0.80	$S < R$
	T-3.0	2.68	1.00	0.00	–
	TAG-3.0	4.22	1.24	0.85	$R < S$
	N-3.0	0.29	1.60	1.22	$S < R$
12 	V-3.0	0.77	2.31	2.87	$S < R$
	T-3.0	2.89	1.00	0.00	–
	TAG-3.0	5.18	1.42	1.39	$R < S$
	N-3.0	0.38	1.56	1.62	$S < R$

Chromatographic conditions: columns, VancoShell (V-3.0), TeicoShell (T-3.0), TagShell (TAG-3.0) and NicoShell (N-3.0); mobile phase, 100% MeOH containing 20 mM AcOH; flow rate, 0.3 ml min⁻¹; detection, MS; e.e.o., enantiomeric elution order.

showed that on V-3.0 and N-3.0 CSPs, the interactions between selector and selectand are particularly weak, resulting in very low retention factors (Tables 1 and S1). Despite the short retention times, the differences in interactions between the two enantiomers with the chiral selector are significant enough to result in baseline

separation in several cases, especially for analytes possessing aromatic side chains. The TEAA-containing mobile phase system proved less effective for the enantioseparation of α -substituted proline analogs, especially in the case of N-3.0 CSP (Table 1 vs. Table S1).

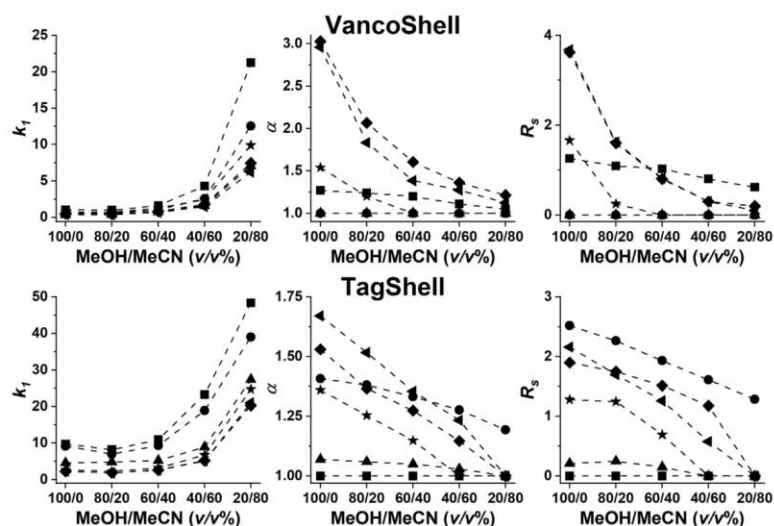


Fig. 2. Effect of MeCN content on the chromatographic parameters of analytes 1, 2, 4, 5, 6, and 10. Chromatographic conditions: columns, VancoShell (V-3.0) and TagShell (TAG-3.0); mobile phase, MeOH/MeCN 100/0, 80/20, 60/40, 40/60 and 20/80 (v/v) all containing 20.0 mM AcOH; flow rate, 0.3 ml min⁻¹; detection, MS; symbols, for analyte 1 ■, for 2 ●, for 4 ▲, for 5 ◆, for 6 ◀, and for 10 ★.

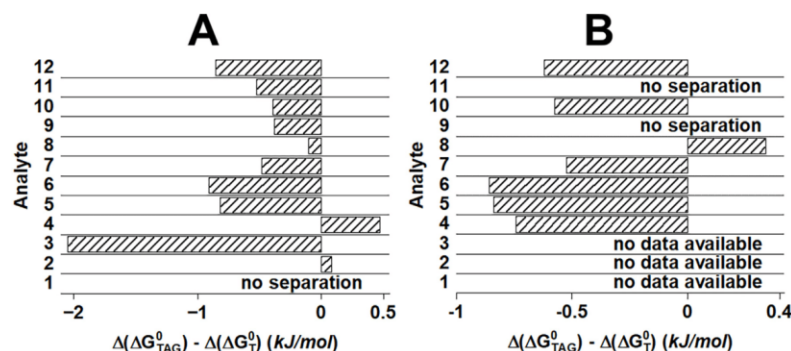


Fig. 3. Enantioselective energy differences between the aglycone and the native teicoplanin CSPs. Chromatographic conditions: column, TeicoShell (T-3.0) and TagShell (TAG-3.0); mobile phase, A, 100% MeOH containing 20.0 mM AcOH, B, 100% MeOH containing 20.0 mM TEAA; flow rate, 0.3 ml min⁻¹; detection, PDA, 215 nm.

Interestingly, all analytes exhibit much higher retention in both mobile phase systems on T-3.0 and TAG-3.0 CSPs. However, these stronger interactions usually do not contribute to improved enantioselectivities. Higher α and R_S only in the case of analytes 2, 3, and 4 were observed in the AcOH-containing eluent (Table 1). Comparing retention behaviors of the studied analytes on the teicoplanin-based CSPs reveals that stronger interactions are formed with TAG-3.0 than with T-3.0. Generally, the improved interactions resulted in higher α and R_S values. These two CSPs differ in the presence (or absence) of three saccharide units which may intervene in the chiral recognition process in at least three distinct ways [30]. They may (i) sterically hinder the access of the molecules to binding sites on the aglycone basket; (ii) block the two phenol hydroxyl groups on the aglycone where two sugar units are attached; (iii) and block the alcohol moiety on the aglycone where the third sugar unit is linked. To quantify the effect of the three saccharide moieties in chiral recognition, the differences in enantioselective free energies obtained on TAG-3.0 and T-3.0 [$\Delta(\Delta G^0_{TAG}) - \Delta(\Delta G^0_T)$] were calculated. A negative number means that the separation of enantiomers of a specific analyte is more effective on TAG-3.0, while a positive number indicates better enantioselectivity on T-3.0. Data in Fig. 3 show that enantioseparations, in most cases, were more effective on TAG-3.0, indicating that the sugar units hinder the stereoselective interactions between the selector and the selectand. Exceptions were analytes 2 and 4 in AcOH-containing eluent and analyte 8 in TEAA-containing eluent, where slightly higher selectivities were registered on T-3.0 CSP. Of the studied macrocyclic glycopeptide-based CSPs the V-3.0 and TAG-3.0 CSPs proved to be the most effective for the enantioseparation of α -substituted proline analogs. One possible reason may be that vancomycin structurally resembles teicoplanin aglycone. While teicoplanin contains three saccharide units, vancomycin possesses only one, and as discussed above, enantioseparation is more advantageous in the absence of sugar moieties for the studied proline analogs.

The nature of the proline substitute (Fig. 1) also has a profound effect on chiral recognition and must be explored. Based on the obtained results (Table 1), it can be seen that for the V-3.0 CSP employing AcOH-containing mobile phases, retention is significantly reduced by a substituent in the α position. Only a slight difference can be seen in the chromatographic behaviors comparing the aliphatic and aromatic substituents; the presence of the aromatic moiety may induce π - π interactions in the basket of the selector, ideally leading to higher selectivity and retention.

On both T-3.0 and TAG-3.0 CSPs, compounds with aliphatic substituents (2–4) were more strongly retained than compounds with aromatic substituents (5–12). In other words, substituting the H atom with an aromatic ring substantially reduced the retention. Despite the strong retention, no enantioselectivity was observed in the case of proline. Interestingly, the methyl substitution had no substantial effect on the retention but resulted in a very efficient chiral recognition (compound 2 vs. 1). To explain the observed changes in enantioselectivities, a strong steric effect is assumed, and the importance of molecular geometry (i.e., the shape and size of the molecule) is likely in the case of the teicoplanin-based selectors, even in the absence of saccharide substituents.

The effect of the nature and position of the substituent on the aromatic ring (5 vs. 6, 7, and 10; 8 vs. 9 and 10 vs. 11) can be explored in both eluent systems on the two most effective CSPs V-3.0 and TAG-3.0. The electron-donating methyl substitution on the benzyl ring (5 vs. 6) does not markedly change the chromatographic properties. In contrast, substitution with an electron-withdrawing atom (5 vs. 7 and 10) resulted in more significant variations of the chromatographic values, however, these variations depend on the applied conditions (i.e., on the mobile phase and the CSP).

The position of the halogen atom in 8 vs. 9, and 10 vs. 11 was found to affect chiral recognition markedly. Both the chlorine (8 and 9) and the bromine (10 and 11) placed in *ortho* position led to significantly longer retentions but reduced, or in most cases eliminated enantioselectivity on both V-3.0 and TAG-3.0 CSPs in both eluent systems. The halogen substitution of the aromatic ring in an *ortho* position may sterically hinder effective chiral recognition in the case of the studied α -substituted proline analogs.

All the studied analytes are available in racemic and enantiomerically pure forms, thus the enantiomeric elution order was determined in all cases. A general trend could be observed: on V-3.0 and N-3.0 CSPs where the elution order was $S < R$. However, on the T-3.0 and TAG-3.0 CSPs, it was opposite: $R < S$ (Table 1 and Table S1 and Fig. 4).

Selected chromatograms for the enantioseparation of the α -substituted proline analogs are depicted in Fig. 4.

3.4. Thermodynamic characterization

Optimizing column temperature to achieve more efficient enantioseparations is worthwhile [31–33]. In addition to gaining shorter analysis time and/or higher resolution, temperature effects on

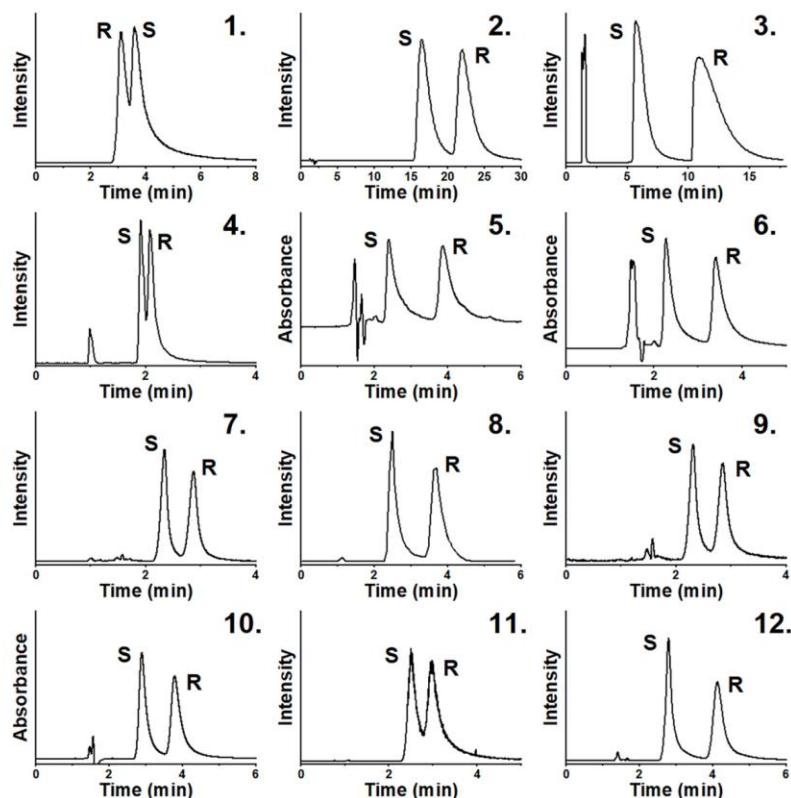


Fig. 4. Selected chromatograms of analytes 1–12. Chromatographic conditions: columns, for analytes 1, 5–10 and 12 VancosShell (V-3.0), for 2 and 3 TagShell (TAG-3.0), and for 4 and 11 NicosShell (N-3.0); mobile phase, for analytes 1–4, 7–9, 11, and 12 100% MeOH containing 20.0 mM AcOH, for analytes 5, 6, and 10 100% MeOH containing 20.0 mM TEAA; flow rate, 0.3 ml min⁻¹; temperature, for analytes 1–6, 8 and 12, 20 °C, for 7 and 9–11, 5.0 °C.

chromatographic parameters may provide information about the mechanism of chiral recognition. Enantioselectivity is related to the difference in free energy changes of adsorption of the enantiomers [$\Delta(\Delta G^\circ)$], and the van't Hoff equation (plotting $R \ln \alpha$ vs. $1/T$) is frequently applied to determine thermodynamic parameters,

$$\ln \alpha = -\frac{\Delta(\Delta H^\circ)}{RT} + \frac{\Delta(\Delta S^\circ)}{R} \quad (1)$$

where α is the selectivity factor, $\Delta(\Delta H^\circ)$ and $\Delta(\Delta S^\circ)$ are the differences in standard enthalpy and standard entropy, R is the universal gas constant, and T is the temperature in degrees Kelvin. Applying Eq. (1), the problems related to the determination of the phase ratio can be excluded, however, contributions of enantioselective and non-selective sites to the free energy cannot be distinguished [34].

The effects of temperature on the chromatographic parameters for all the analytes were studied on V-3.0 and TAG-3.0 CSPs over the temperature range of 5–50 °C. Experimental data on both columns with a mobile phase of 100% MeOH containing 20 mM AcOH are presented in Table S2.

In all cases, the k values on V-3.0 and TAG-3.0 CSPs decreased with increasing temperature. As expected, α and R_S decreased with increasing temperature, except for 4 on the TAG-3.0 column, where α slightly increased with increasing temperature in the temperature range of 10–50 °C. For analytes possessing an aliphatic side chain (2–4), some improvement in R_S could be registered with increasing temperature on TAG-3.0 CSP, probably due to the favorable kinetic effects observed at higher temperatures.

The differences in the changes in standard enthalpy and entropy [$-\Delta(\Delta H^\circ)$ and $-\Delta(\Delta S^\circ)$] calculated from the $\ln \alpha$ vs. $1/T$ curves are presented in Table 2. The $\Delta(\Delta H^\circ)$ values on V-3.0 CSP ranged from -10.80 to -2.43 kJ mol⁻¹, and on TAG-3.0 CSP from -6.45 to $+1.15$ kJ mol⁻¹. Comparing the $\Delta(\Delta G^\circ)$ values determined for the two CSPs, more efficient bindings are found on the V-3.0 CSP, as reflected by the more negative $\Delta(\Delta G^\circ)$ values. The trends in the change in $\Delta(\Delta H^\circ)$ and $\Delta(\Delta S^\circ)$ were similar. The relative contribution to the free energy of adsorption can be characterized by the calculation of the enthalpy/entropy ratio, $Q = \Delta(\Delta H^\circ)/[298 \times \Delta(\Delta S^\circ)]$. As indicated in Table 2, the enantio-

Table 2
Thermodynamic parameters, $-\Delta(\Delta H^\circ)$, $-\Delta(\Delta S^\circ)$, $-\Delta(\Delta G^\circ)$, correlation coefficient (R^2), T_{iso} and Q values of analytes **1–12** on **VancoShell (V-3.0)** CSP.

Compound	$-\Delta(\Delta H^\circ)$ (kJ mol ⁻¹)	$-\Delta(\Delta S^\circ)$ (J mol ⁻¹ K ⁻¹)	$-\Delta(\Delta G^\circ)$ 298 K (kJ mol ⁻¹)	Corr. coeff. R^2	T_{iso} (°C)	Q
V-3.0						
1	2.43	6.29	0.56	0.992	112.5	1.29
2			no separation			
3			no separation			
4			no separation			
5	9.89	24.71	2.52	0.995	127.2	1.34
6	10.80	27.91	2.48	0.992	113.8	1.30
7	4.21	10.97	0.94	0.989	110.4	1.29
8	8.60	22.31	1.95	0.993	112.3	1.29
9	6.14	17.65	0.88	0.970	74.8	1.17
10	5.19	14.22	0.95	0.992	92.1	1.23
11	5.36	15.86	0.63	0.985	64.6	1.13
12	8.92	23.64	1.87	0.991	104.2	1.27
TAG-3.0						
1			no separation			
2	2.15	4.69	0.75	0.993	184.2	1.53
3	4.00	6.70	2.00	0.996	323.4	2.00
4	-1.15	-4.46	0.16	0.994	-15.4	0.86
5	5.65	15.74	0.96	0.998	86.0	1.21
6	6.45	17.68	1.18	0.999	91.5	1.22
7	3.80	10.50	0.67	0.998	89.1	1.22
8	4.32	13.35	0.34	0.999	50.2	1.09
9	2.93	8.81	0.31	0.999	60.1	1.12
10	4.05	11.28	0.68	0.999	85.4	1.20
11	3.06	8.76	0.45	0.993	76.1	1.17
12	4.35	12.03	0.77	0.991	86.7	1.21

Chromatographic conditions: columns, VancoShell (V-3.0) and TagShell (TAG-3.0); mobile phase, MeOH containing 20 mM AcOH; detection, MS-QDa; R^2 , correlation coefficient of van't Hoff plots, $\ln \alpha$ vs. $1/T$ curves; T_{iso} , temperature, where the enantioselectivity cancels; $Q = \Delta(\Delta H^\circ)/298 \times \Delta(\Delta S^\circ)$; temperature range, 5–50 °C.

elective discriminations are enthalpically-driven ($Q > 1$), except for analyte **4** on **TAG-3.0** CSP, which is probably related to the unique structural features of the allyl-group in the α -position of proline. (Analytes **2–4** on **V-3.0**, while **1** on **TAG-3.0** was not separable under the conditions applied in the thermodynamic study.)

Based on the $\Delta(\Delta H^\circ)$ and $\Delta(\Delta S^\circ)$ values, correlations between the structure of the analyte and the thermodynamic parameters can be explored. Compared to analyte **5**, analyte **6**, containing an electron-donating methyl group, possesses more negative $\Delta(\Delta H^\circ)$ and $\Delta(\Delta S^\circ)$ values. In contrast, analytes **7** and **10** containing electron-withdrawing atoms (F or Br atom at the same position) possess less negative $\Delta(\Delta H^\circ)$ and $\Delta(\Delta S^\circ)$ values. This is also true for analytes **8**, **9**, and **11** possessing Cl or Br substituents on the aromatic ring. The electron density of the aromatic moiety seems to be correlated to the energetics of sorption. The comparison of the thermodynamic parameters of **7** vs. **10** further supports this assumption; in the case of analyte **7**, the presence of the F atom results in lower electron density on the aromatic moiety compared to analyte **10**, resulting in less negative $\Delta(\Delta H^\circ)$ and $\Delta(\Delta S^\circ)$ values.

Comparing the thermodynamic parameters of **8** vs. **9** and **10** vs. **11** may shed light on the possible effects of the halogen atom's position on the aromatic ring. The less negative $\Delta(\Delta G^\circ)$ values determined for the analytes possessing the halogen atom in the *ortho* position clearly show a less favorable binding to the selector.

The thermodynamic analysis can also be applied to calculate the "isoelutotropic" temperature (T_{iso}), at which the entropy and enthalpy changes compensate each other, and the enantiomers coelute [34,35]. Applying temperatures higher than T_{iso} , the enantiomeric elution order should be reversed. As shown in Table 2, T_{iso} was out of the applied temperature range for most of the stud-

ied analytes, while for analyte **5**, it was around 50 °C. However, due to the column's limitations, higher temperatures could not be applied to prove the reversal in the enantiomeric elution order.

3.5. Kinetic studies

The kinetics of the selector-selectand interactions are commonly studied by preparing plate height (H) vs. linear velocity (u) curves (van Deemter plots) [25,36–39]. To gather data for the characterization of column efficiencies, experiments were performed with analytes **1**, **2**, **4**, **5**, **6**, and **10** applying a mobile phase composition of MeOH/MeCN 80/20 (v/v) containing 20 mM AcOH on VancoShell and TagShell columns, possessing 3.0 and 2.1 mm internal diameters. (As mentioned earlier, best performances were obtained with pure MeOH. However, to avoid high back-pressures at higher flow rates, the mixture of MeOH and MeCN was applied in the kinetic study, resulting in a significantly lower viscosity eluent.) The flow rate was varied between 0.1–1.0 ml min⁻¹ (0.24–2.36 mm sec⁻¹) on the column with a 3.0 mm i.d. and 0.05–0.5 ml min⁻¹ (0.24–2.41 mm sec⁻¹) on the column with a 2.1 mm i.d. (data are depicted in Fig. 5).

Interestingly, under the applied conditions, the shape of van Deemter curves for the first eluting enantiomer is unusual; no H minima vs. linear velocity can be identified for the analytes studied. Consequently, the curves do not fit the classical van Deemter equation ($H = A + B/u + Cu$), as reported in some cases [25,39]. At higher flow rates in a few cases (e.g., analytes **1** and **2** on VancoShell columns), lower H values are obtained, caused probably by improved stationary phase mass transfer processes triggered by frictional heating. It is important to highlight that the H - u plots

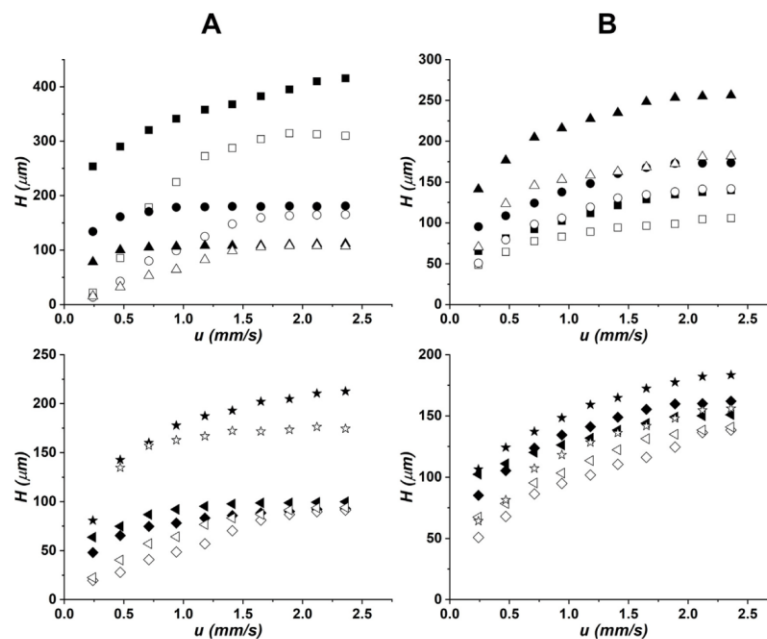


Fig. 5. van Deemter plots for analytes 1, 2, 4, 5, 6, and 10 on macrocyclic glycopeptide-based CSPs. Chromatographic conditions: columns, A, VancosShell (V-3.0; full symbols) and VancosShell (V-2.1; empty symbols); B, TagShell (TAG-3.0; full symbols) and TagShell (TAG-2.1; empty symbols); mobile phase, MeOH/MeCN (80/20 v/v) containing 20 mM AcOH; flow rate, 0.05 – 1.0 ml min⁻¹; detection, MS; temperature, 20 °C; symbols for analyte 1, ■ and □; 2, ● and ○; 4, ▲ and △; 5, ◆ and ◇; 6, ◀ and ▶; 10, ★ and ✱.

measured on 2.1 mm i.d. columns run below those obtained with the same column type with a larger 3.0 mm i.d. for all the studied analytes. This finding partly contradicts our previous results. Applying the same core-shell particle-based columns earlier, the narrow bore columns (2.1 mm i.d.) in most cases possessed decreased efficiency compared to their counterparts with 3.0 mm i.d. [40,41]. However, the narrow bore columns offered more efficient kinetics in some cases (e.g., for β^2 -amino acids with aromatic side chains and certain fluorinated phenylalanine analogs) [40,41]. All these findings draw attention to an important fact; the kinetic performance of a column depends not only on the geometric size and the mobile phase composition, as described often in the literature, but also on the nature of analytes. It should be noted here that data were handled without corrections for the extra-column volume of the instrument. Physically modifying the UHPLC (i.e., reducing the extra-column effects) would probably result in lower plate heights.

4. Conclusions

In this study, macrocyclic glycopeptide-based chiral stationary phases immobilized on superficially porous particles of silica were successfully applied for the direct enantiomeric separation of α -substituted proline analogs. The most effective CSPs were the vancomycin- and the teicoplanin aglycone-based ones, used in the polar-ionic mode. Effects of mobile phase additives (acids and

salts) were found to strongly depend on the applied conditions, the nature of the analyte, and the chiral selector. Depending on the applied detection type (MS or UV), best performances were obtained using 100% MeOH with 20 mM acetic acid or 20 mM triethylammonium acetate.

Details of the chiral recognition mechanism could be explored by comparing the chromatographic and the thermodynamic parameters of the structurally strongly related α -substituted proline analogs. Regarding the structure of the teicoplanin-based selectors, the sugar units were found to hinder the enantioselective interactions in most cases. Regarding the structure of the analytes, the electron density of the aromatic moiety was found to be correlated to the energetics of sorption. The position of the halogen substituent affects chiral recognition; the *ortho* position resulted in a less favorable binding to the chiral selector.

Interestingly, the kinetic study revealed a different shape for the van Deemter plots than usual, i.e., no *H* minima were recorded for the studied analytes. Further, at higher flow rates, the efficiencies began to improve somewhat, most likely due to frictional heating improving stationary phase mass transfer. Contrary to the results usually obtained, a more efficient kinetic performance of columns with 2.1 mm i.d. was found.

Declaration of Competing Interest

The authors declare no conflict of interest.

CRediT authorship contribution statement

Dániel Tanács: Investigation, Writing – original draft, Visualization. **Róbert Berkecz:** Conceptualization, Writing – original draft, Writing – review & editing. **Daniel W. Armstrong:** Conceptualization, Writing – original draft, Writing – review & editing. **Antal Péter:** Conceptualization, Writing – original draft, Writing – review & editing. **István Ilisz:** Conceptualization, Writing – original draft, Writing – review & editing, Supervision, Project administration, Funding acquisition.

Data availability

Data will be made available on request.

Acknowledgments

This work was supported by National Research, Development and Innovation Office-NKFI through project K137607. Project no. TKP2021-EGA-32 has been implemented with the support provided by the Ministry of Innovation and Technology of Hungary from the National Research, Development and Innovation Fund, financed under the TKP2021-EGA funding scheme. The work was also supported by the ÚNKP-22-3-SZTE-162 New National Excellence Program of the Ministry for Culture and Innovation from the source of the National Research, Development and Innovation Fund. The authors express their acknowledgments to Prof. D. Tourwé (Vrije Universiteit Brussels, Brussel, Belgium) for the generous gift of proline analogs.

Supplementary materials

Figure S1. Effect of mobile phase additives on chromatographic behavior of analyte **5**. Chromatographic conditions: columns, VancosShell (V-3.0) and TagShell (TAG-3.0); mobile phase, MeOH/MeCN 80/20 (v/v) containing 20 mM additives; additives, FA, TFA, AcOH, TEAA, NH₄HCO₃, NH₄OAc; flow rate, 0.3 ml min⁻¹; detection, PDA, 215 nm

Figure S2. Effect of MeCN content on chromatographic parameters of analytes **4**, **5**, **6**, and **10**. Chromatographic conditions: columns, VancosShell (V-3.0), TagShell (TAG-3.0) and NicoShell (N-3.0); mobile phase, MeOH/MeCN 100/0, 75/25, 50/50 and 25/75 (v/v) all containing 20.0 mM TEAA; flow rate, 0.3 ml min⁻¹; detection, PDA, 215 nm; symbols for analyte **4**, ▲; **5**, ◆; **6**, ◀ and **10**, ★

Supplementary material associated with this article can be found, in the online version, at [doi:10.1016/j.chroma.2023.463997](https://doi.org/10.1016/j.chroma.2023.463997).

References

- [1] T. Uhlig, T. Kyrianiou, F.G. Martinelli, C.A. Oppici, D. Heilgers, D. Hills, X.R. Calvo, P. Verhaert, The emergence of peptides in the pharmaceutical business: from exploration to exploitation, *EuPA Open Proteom* 4 (2014) 58–69, [doi:10.1016/j.euprot.2014.05.003](https://doi.org/10.1016/j.euprot.2014.05.003).
- [2] C. López-Otin, L.M. Matrisian, Emerging roles of proteases in tumour suppression, *Nat. Rev. Cancer* 7 (2007) 800–808, [doi:10.1038/nrc2228](https://doi.org/10.1038/nrc2228).
- [3] M.C. Manning, K. Patel, R.T. Borchardt, Stability of protein pharmaceuticals, *Pharm. Res. An Off. J. Am. Assoc. Pharm. Sci.* 6 (1989) 903–918, [doi:10.1023/A:1015929109894](https://doi.org/10.1023/A:1015929109894).
- [4] K.A. Witt, T.J. Gillespie, J.D. Huber, R.D. Egleton, T.P. Davis, Peptide drug modifications to enhance bioavailability and blood-brain barrier permeability, *Peptides* 22 (2001) 2329–2343, [doi:10.1016/S0196-9781\(01\)00537-X](https://doi.org/10.1016/S0196-9781(01)00537-X).
- [5] S. Ritztmann, M. Collins, Racemization of aspartic acid in human proteins, *Ageing Res. Rev.* 1 (2002) 43–59, [doi:10.1016/S0047-6374\(01\)00363-3](https://doi.org/10.1016/S0047-6374(01)00363-3).
- [6] A. Yaron, F. Naider, S. Scharpe, Proline-dependent structural and biological properties of peptides and proteins, *Crit. Rev. Biochem. Mol. Biol.* 28 (1993) 31–81, [doi:10.1080/10409239309082572](https://doi.org/10.1080/10409239309082572).
- [7] J. Jacob, H. Duclouier, D.S. Cafiso, The role of proline and glycine in determining the backbone flexibility of a channel-forming peptide, *Biophys. J.* 76 (1999) 1367–1376, [doi:10.1016/S0006-3495\(99\)77298-X](https://doi.org/10.1016/S0006-3495(99)77298-X).
- [8] J.A. Robinson, The design, synthesis and conformation of some new β -hairpin mimetics: novel reagents for drug and vaccine discovery, *Synlett* 2000 (2000) 429–441, [doi:10.1055/s-2000-6770](https://doi.org/10.1055/s-2000-6770).
- [9] L. Szabados, A. Savouré, Proline: a multifunctional amino acid, *Trends Plant Sci* 15 (2010) 89–97, [doi:10.1016/j.tplants.2009.11.009](https://doi.org/10.1016/j.tplants.2009.11.009).
- [10] J.J. Tanner, S.-M. Fendt, D.F. Becker, The proline cycle as a potential cancer therapy target, *Biochemistry* 57 (2018) 3433–3444, [doi:10.1021/acs.biochem.8b00215](https://doi.org/10.1021/acs.biochem.8b00215).
- [11] J.M. Phang, Proline metabolism in cell regulation and cancer biology: recent advances and hypotheses, *Antioxid. Redox Signal.* 30 (2019) 635–649, [doi:10.1089/ars.2017.7350](https://doi.org/10.1089/ars.2017.7350).
- [12] M. Endicott, M. Jones, J. Hull, Amino acid metabolism as a therapeutic target in cancer: a review, *Amino Acids* 53 (2021) 1169–1179, [doi:10.1007/s00726-021-03052-1](https://doi.org/10.1007/s00726-021-03052-1).
- [13] T. Miyamoto, H. Homma, D-Amino acid metabolism in bacteria, *J. Biochem.* 170 (2021) 5–13, [doi:10.1093/jb/mvab043](https://doi.org/10.1093/jb/mvab043).
- [14] A. Rocco, Z. Aturki, S. Fanali, Chiral separations in food analysis, *TrAC Trends Anal. Chem.* 52 (2013) 206–225, [doi:10.1016/j.trac.2013.05.022](https://doi.org/10.1016/j.trac.2013.05.022).
- [15] A. Furusho, R. Koga, T. Akita, M. Mita, T. Kimura, K. Hamase, Three-dimensional high-performance liquid chromatographic determination of Asn, Ser, Ala, and Pro enantiomers in the plasma of patients with chronic kidney disease, *Anal. Chem.* 91 (2019) 11569–11575, [doi:10.1021/acs.analchem.9b01615](https://doi.org/10.1021/acs.analchem.9b01615).
- [16] C. Ishii, T. Akita, M. Mita, T. Ide, K. Hamase, Development of an online two-dimensional high-performance liquid chromatographic system in combination with tandem mass spectrometric detection for enantiomeric analysis of free amino acids in human physiological fluid, *J. Chromatogr. A* 1570 (2018) 91–98, [doi:10.1016/j.chroma.2018.07.076](https://doi.org/10.1016/j.chroma.2018.07.076).
- [17] J.P. Violi, D.P. Bishop, M.P. Padula, J.R. Steele, K.J. Rodgers, Considerations for amino acid analysis by liquid chromatography-tandem mass spectrometry: a tutorial review, *TrAC Trends Anal. Chem.* 131 (2020) 116018, [doi:10.1016/j.trac.2020.116018](https://doi.org/10.1016/j.trac.2020.116018).
- [18] G.L. Marcone, E. Rosini, E. Crespi, L. Pollegioni, D-amino acids in foods, *Appl. Microbiol. Biotechnol.* 104 (2020) 555–574, [doi:10.1007/s00253-019-10264-9](https://doi.org/10.1007/s00253-019-10264-9).
- [19] C. Carezzi, S. Sacchi, M. Abbondi, L. Pollegioni, Direct chromatographic methods for enantioresolution of amino acids: recent developments, *Amino Acids* 52 (2020) 849–862, [doi:10.1007/s00726-020-02873-w](https://doi.org/10.1007/s00726-020-02873-w).
- [20] H. Zahradnicková, S. Opekar, L. Řimnáčová, P. Šimek, M. Moos, Chiral secondary amino acids, their importance, and methods of analysis, *Amino Acids* 54 (2022) 687–719, [doi:10.1007/s00726-022-03136-6](https://doi.org/10.1007/s00726-022-03136-6).
- [21] A. Péter, E. Vékcs, A. Árki, D. Tourwé, W. Lindner, Direct high-performance liquid chromatographic enantioseparation of α -substituted proline analogues on a quinine-derived chiral anion-exchanger stationary phase, *J. Sep. Sci.* 26 (2003) 1125–1132, [doi:10.1002/jssc.200301524](https://doi.org/10.1002/jssc.200301524).
- [22] A. Péter, G. Tórk, E. Vékcs, J. Van Betsbrugge, D. Tourwé, HPLC separation of enantiomers of α -substituted proline analogues by the application of (S)-N-(4-nitrophenoxycarbonyl)phenylalanine methoxycarbonyl ester as chiral derivatizing agent, *J. Liq. Chromatogr. Relat. Technol.* 27 (2004) 17–29, [doi:10.1081/JLC-120027083](https://doi.org/10.1081/JLC-120027083).
- [23] O.H. Ismail, S. Felletti, C. De Luca, L. Pasti, N. Marchetti, V. Costa, F. Gasparini, A. Cavazzini, M. Catani, The way to ultrafast, high-throughput enantioseparations of bioactive compounds in liquid and supercritical fluid chromatography, *Molecules* 23 (2018) 1–12, [doi:10.3390/molecules23102709](https://doi.org/10.3390/molecules23102709).
- [24] N. Khundadze, S. Pantisualia, C. Fanali, T. Farkas, B. Chankvetadze, On our way to sub-second separations of enantiomers in high-performance liquid chromatography, *J. Chromatogr. A* 1572 (2018) 37–43, [doi:10.1016/j.chroma.2018.08.027](https://doi.org/10.1016/j.chroma.2018.08.027).
- [25] D.C. Patel, Z.S. Breitbach, M.F. Wahab, C.L. Barhate, D.W. Armstrong, Gone in seconds: praxis, performance, and peculiarities of ultrafast chiral liquid chromatography with superficially porous particles, *Anal. Chem.* 87 (2015) 9137–9148, [doi:10.1021/acs.analchem.5b00715](https://doi.org/10.1021/acs.analchem.5b00715).
- [26] I. Ilisz, A. Péter, W. Lindner, State-of-the-art enantioseparations of natural and unnatural amino acids by high-performance liquid chromatography, *TrAC Trends Anal. Chem.* 81 (2016) 11–22, [doi:10.1016/j.trac.2016.01.016](https://doi.org/10.1016/j.trac.2016.01.016).
- [27] I. Ilisz, Z. Pataj, A. Aranyi, A. Péter, High-performance liquid chromatography of biologically important, small epimeric peptides and their L, D-amino acid content, *Mini-Reviews Med. Chem.* 10 (2010) 287–298, [doi:10.2174/138955710791330981](https://doi.org/10.2174/138955710791330981).
- [28] R. Berkecz, D. Tanács, A. Péter, I. Ilisz, Enantioselective liquid chromatographic separations using macrocyclic glycopeptide-based chiral selectors, *Molecules* 26 (2021) 3380, [doi:10.3390/molecules26113380](https://doi.org/10.3390/molecules26113380).
- [29] T.J. Ward, K.D. Ward, Chiral separations: a review of current topics and trends, *Anal. Chem.* 84 (2012) 626–635, [doi:10.1021/ac202892w](https://doi.org/10.1021/ac202892w).
- [30] A. Berthod, X. Chen, J.P. Kullman, D.W. Armstrong, F. Gasparini, I. D'Acquaric, C. Villani, A. Carotti, Role of the carbohydrate moieties in chiral recognition on teicoplanin-based LC stationary phases, *Anal. Chem.* 72 (2000) 1767–1780, [doi:10.1021/ac991004t](https://doi.org/10.1021/ac991004t).
- [31] S. Allenmark, V. Schurig, Chromatography on chiral stationary phases, *J. Mater. Chem.* 7 (1997) 1955–1963, [doi:10.1039/a702403g](https://doi.org/10.1039/a702403g).
- [32] T. Fornstedt, P. Sajonz, G. Guiochon, Thermodynamic study of an unusual chiral separation. Propanolol enantiomers on an immobilized cellulase, *J. Am. Chem. Soc.* 119 (1997) 1254–1264, [doi:10.1021/ja9631458](https://doi.org/10.1021/ja9631458).
- [33] G. Göttmar, T. Fornstedt, G. Guiochon, Apparent and true enantioselectivity in enantioseparations, *Chirality* 12 (2000) 558–564, [doi:10.1002/1520-636X\(2000\)12:7<558::AID-CHIR2>3.0.CO;2-2](https://doi.org/10.1002/1520-636X(2000)12:7<558::AID-CHIR2>3.0.CO;2-2).
- [34] L.D. Asnin, M.V. Stepanova, Van't Hoff analysis in chiral chromatography, *J. Sep. Sci.* 41 (2018) 1319–1337, [doi:10.1002/jssc.201701264](https://doi.org/10.1002/jssc.201701264).
- [35] A. Berthod, W. Li, D.W. Armstrong, Multiple enantioselective retention mechanisms on derivatized cyclodextrin gas chromatographic chiral stationary phases, *Anal. Chem.* 64 (1992) 873–879, [doi:10.1021/ac00032a009](https://doi.org/10.1021/ac00032a009).

- [36] I.D. Asnin, A.A. Boteva, O.P. Krasnykh, M.V. Stepanova, I. Ali, Unusual van Deemter plots of optical isomers on a chiral brush-type liquid chromatography column, *J. Chromatogr. A* 1592 (2019) 112–121, doi:[10.1016/j.chroma.2019.01.048](https://doi.org/10.1016/j.chroma.2019.01.048).
- [37] S. Felletti, C. De Luca, G. Lievore, T. Chenet, B. Chankvetadze, T. Farkas, A. Cavazzini, M. Catani, Shedding light on mechanisms leading to convex-upward van Deemter curves on a cellulose tris(4-chloro-3-methylphenylcarbamate)-based chiral stationary phase, *J. Chromatogr. A* 1630 (2020), doi:[10.1016/j.chroma.2020.461532](https://doi.org/10.1016/j.chroma.2020.461532).
- [38] D. Folprechtová, K. Kalíková, K. Kadkhodaei, C. Reiterer, D.W. Armstrong, E. Tesařová, M.G. Schmid, Enantioseparation performance of superficially porous particle vancomycin-based chiral stationary phases in supercritical fluid chromatography and high performance liquid chromatography: applicability for psychoactive substances, *J. Chromatogr. A* 1637 (2021), doi:[10.1016/j.chroma.2020.461846](https://doi.org/10.1016/j.chroma.2020.461846).
- [39] S. Aslani, M.F. Wahab, M.E. Kenari, A. Berthod, D.W. Armstrong, An examination of the effects of water on normal phase enantioseparations, *Anal. Chim. Acta* 1200 (2022) 339608, doi:[10.1016/j.aca.2022.339608](https://doi.org/10.1016/j.aca.2022.339608).
- [40] D. Tanács, R. Berkecz, A. Misicka, D. Tymecka, F. Fülöp, D.W. Armstrong, I. Ilisz, A. Péter, Enantioseparation of β -amino acids by liquid chromatography using core-shell chiral stationary phases based on teicoplanin and teicoplanin aglycone, *J. Chromatogr. A* 1653 (2021) 462383, doi:[10.1016/j.chroma.2021.462383](https://doi.org/10.1016/j.chroma.2021.462383).
- [41] D. Tanács, R. Berkecz, S. Shahmohammadi, E. Forró, D.W. Armstrong, A. Péter, I. Ilisz, Macrocyclic glycopeptides- and derivatized cyclofructan-based chiral stationary phases for the enantioseparation of fluorinated β -phenylalanine analogs, *J. Pharm. Biomed. Anal.* 219 (2022) 114912, doi:[10.1016/j.jpba.2022.114912](https://doi.org/10.1016/j.jpba.2022.114912).